Nonlinear Output feedback Design for

Autonomous Underwater Vehicle :

Port Controlled Hamiltonian Approach

BY

Muhammad Fuady Emzir

A Thesis Presented to the

DEANSHIP OF GRADUATE STUDIES

KING FAHD UNIVERSITY OF PETROLEUM & MINERALS

DHAHRAN, SAUDI ARABIA

In Partial Fulfillment of the
Requirements for the Degree of

MASTER OF SCIENCE

In

System Engineering

June 2012

Nonlinear Output Feedback Design for Autonomous Underwater Vehicle : Port Controlled Hamiltonian Approach

Master Thesis

Submitted for the Partial Fulfillment of the Requirements for the Degree of
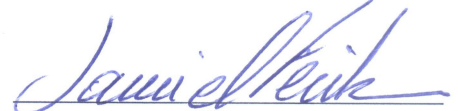
Master of Science

Department of System Engineering
College of Computer Science and Engineering
King Fahd University of Petroleum and Minerals

June 25, 2012

KING FAHD UNIVERSITY OF PETROLEUM & MINERALS
DHAHRAN 31261, SAUDI ARABIA
DEANSHIP OF GRADUATE STUDIES

This thesis, written by **Muhammad Fuady Emzir** under the direction of his thesis advisor and approved by his thesis committee, has been presented to and accepted by the Dean of Graduate Studies, in partial fulfilment of the requirements for the degree of **Master of Science in System Engineering**.

<u>**Thesis Committee**</u>

Dr. Sami El Ferik (Advisor)

Dr. Fouad Al-Sunni (Member)

Dr. M. El Shafei (Member)

Dr. Fouad Al-Sunni
Department Chairman

Dr. Salam Zummo
Dean of Graduate Studies

26/6/12

Date

To

My Father and Mother, My beloved wife, Riska, My beloved son and daughter
Afiifah and Muhammad

Preface

This thesis is submitted to King Fahd University of Petroleum and Minerals (KFUPM) for partial fulfilment of the requirements for the degree of Master of Science.

Acknowledgements

Contents

List of Tables

List of Figures

Abstract

The development of output feedback controller design for AUV is considered in this thesis. The development is carried out in PCH framework. Firstly, the AUV dynamics are transformed into PCH formulation. Then the feedback controllers based on dissipation of the closed loop system are designed. The $\mathcal{L}_2$ disturbance attenuation controller and its adaptive scheme are then elaborated. Necessary and sufficient conditions to guaranty stability are stated. Robustness of the controller to parameter uncertainties is studied by assuming uncertainties in both inertia and damping matrices. The general design approach is applied to develop a PCH-based control design for AUV for trajectory tracking and $\mathcal{L}_2$ disturbance attenuation. The simulation shows that the designed controller is robust with respect to uncertainty in inertia and damping matrices respectively. The $\mathcal{L}_2$ disturbance attenuation controller and its adaptive scheme are able to attenuate the exogenous disturbance effect.

In addition, the thesis also presents an extension of PCH based controller design to the underactuated case. An absence of some actuating forces create inability to track the position and attitude at the same time. The development of underactuated controller design for AUV is developed as an extension of fully actuated controller design. Necessary and sufficient conditions to guaranty stability for the underactuated condition are developed. Simulation results show the ability of the proposed design to drive the underactuated AUV in three dimensions trajectory.

In the last part of the thesis, two observer designs are developed. The first one is based on PCH error passivation and the second is based on Lyapunov design. The separation principle is presented to complete the stability proof. The PCH observers are designed for AUV equipped with both Inertial Navigation System (INS) sensor and depth sensor. The simulation results show that the controller-observer arrangement is able to track the desired trajectory with some small drift on the horizontal inertial position. The Lyapunov-based observer is designed for AUV equipped with beacon inertial measurement. Uniform Global Exponential Stability (UGES) is achieved for this observer. These stability results are stronger when compared to similar results in the literature. Finally, using the cascaded-system theory, we are able to establish the stability conditions for AUV controller-observer closed-loop system.

Arabic Abstract

ويعتبر تطوير ردود الفعل الناتج عن تصميم وحدة تحكم AUV في هذه الأطروحة. ويتم تطوير في إطار PCH. أولا، يتم تحويل ديناميات AUV في صياغة PCH.

ثم تم تصميم وحدات التحكم ردود الفعل على أساس تبديد للنظام الدائرة المغلقة. ووضع بعد ذلك تخفيف اضطراب $\mathcal{L}_2$ تحكم ومخطط لها على التكيف. وذكر الشروط الضرورية والكافية لكفالة الاستقرار. تدرس قوة من وحدة تحكم لعدم اليقين المعلمة بافتراض عدم اليقين في كل من الجمود والمصفوفات التخميد. يتم تطبيق نهج التصميم العام لوضع تصميم سيطرة PCH ومقره لتتبع مسار AUV و $\mathcal{L}_2$ تخفيف الاضطرابات. وتبين المحاكاة أن وحدة تحكم تصميم قوي فيما يتعلق عدم اليقين في الجمود والمصفوفات التخميد على التوالي. توهين اضطراب $\mathcal{L}_2$ تحكم ومخطط لها على التكيف هي قادرة على التخفيف من تأثير الاضطرابات الخارجية.

بالإضافة إلى ذلك، يقدم أطروحة أيضا امتدادا للتصميم PCH تحكم يستند إلى حالة underactuated. عدم وجود بعض القوى المشغلات خلق عدم القدرة على متابعة الموقف والموقف في الوقت نفسه. تم تطوير تطوير تصميم للتحكم underactuated AUV امتدادا للتصميم تحكم دفعتها تماما. يتم وضع الشروط اللازمة والكافية لضمان لاستقرار حالة underactuated. نتائج المحاكاة تظهر قدرة التصميم المقترح لدفع underactuated AUV في مسار الأبعاد الثلاثة.

في الجزء الأخير من الرسالة، وضعت تصاميم المراقب اثنين. ويستند أول واحد في التخميل خطأ PCH ويقوم الثاني على تصميم يابونوف. ويرد مبدأ فصل لاستكمال إثبات الاستقرار. وقد صممت هذه المراقبين PCH ل AUV مجهزة على حد سواء استشعار دائرة الهجرة والتجنيس واستشعار عمق. نتائج المحاكاة تبين أن الترتيب تحكم-مراقب هي قادرة على تتبع مسار المطلوب مع بعض الانجراف صغيرة على موقف بالقصور الذاتي أفقي. تم تصميم المراقب يابونوف ومقرها لاوط مجهزة قياس منارة بالقصور الذاتي. ويتحقق الاستقرار موحدة أسي العالمية UGES لهذا المراقب. هذه النتائج استقرار في لبنان أقوى بالمقارنة مع نتائج مماثلة في الأدب. أخيرا، وذلك باستخدام نظرية تتالي نظام، ونحن قادرون على تهيئة الظروف لاستقرار النظام AUV حلقة مغلقة وحدة التحكم، المراقب.

Chapter 1

Introduction

The world of autonomous vehicle has seen a remarkable development over the last decades. The idea of having a self-driven device that can perform various tasks without human intervention is appealing from both industrial and theoretical point of view. This thesis considers *nonlinear output feedback control* of an Autonomous Underwater Vehicle (AUV). In this work, we propose nonlinear control algorithms that can be implemented in a real AUV system.

1.1 Motivation

The unmanned vehicles, either remotely operated or autonomous, eliminate the need for human physical presence and hence reduce the accidental risk and save life. Remotely operated unmanned vehicles rely on remote operator station to control and navigate the vehicle. Autonomous vehicles are independent of human operator. These vehicles rely on the built-in machine intelligence and the

on-board embedded control system. The design of the control system represents challenging problems in the development of autonomous unmanned vehicles, due to the high-dimensional sensory data, the computation-intensive processing and the real-time execution constraints. The problem is even more complex for underwater autonomous unmanned vehicles due to power and communication limitations imposed by the working environment.

An AUV is an unmanned untethered underwater vehicle that carries its own power source and relies on an on-board computer and built-in machine intelligence to execute a mission consisting of a series of preprogrammed instructions (potentially) modifiable on-line by data or information gathered by the vehicle sensors. An AUV can be launched from simpler, smaller ships (compared to Remotely Operated Vehicles (ROV)), or even docks or piers, since there is no umbilical cable. This also enables AUV operation at significant distance from a support ship or platform. The operational cost is further reduced since a human operator is not needed.

On the other hand, the absence of a human operator dictates that AUV operations are limited by the vehicle control system, the computing and sensing capabilities. The lack of an umbilical cable limits the AUV to its own power source, thus reducing feasible missions durations. As a result of these limitations, power, navigation and mission management are three technologies which are considered critical for the future use of AUV. Indeed, advances in these technologies are necessary for AUV designers to meet objectives such as flexible communication, efficient solution to temporal planning and resource allocation, information integration and recognition in the process of multi-sensor operation, planning for a given task and adaptation to system and environmental changes.

During the last decades, AUV applications became increasingly popular for commercial use in the ocean industry and scientific research communities around the world. Oil companies for example nowadays have put more efforts to move the surface oil drilling platforms to seabed. In order to extract more oil and gas from the reservoirs, the oil installations are placed closer to the sources. Several different installations are placed on sea bed and they are connected to onshore facilities with pipelines. This entails an increased demand for subsea equipment that can carry out surveillance and maintenance work as seabed installations are in periodical need of surveillance and repair work. As the use of deep ocean divers is no longer an option, it follows that this work must be caried out automatically by AUV, or by ROV. Another application of AUV is the scanning and inspection of pipe lines. One of the most essential tasks in this operation and also for surveillance of seabed installations is accurate positioning.

AUV dynamic equations are often easily described using the Euler-Lagrange equation, using six Degrees of Freedom (DOF) velocity equation in body fixed axes. It is well known that Euler-Lagrange dynamic equations can be highly nonlinear and particularly for AUV, some parameters like squared drag and Coriolis are proportional to the squared vehicle velocity. These facts present a challenge in control design and in estimation since the traditional methods for linear systems might be very difficult to apply and the results might be far from satisfactory.

Many nonlinear control design for nonlinear Euler Lagrange system, particularly for AUV have been proposed. For instance, there have been sliding mode, feedback linearization and passivity-based control. The main obstacle stems from the fact that, all these techniques require the knowledge of inertial position, angle and velocity, which generally are not being all measured.

Among these three, the most difficult to obtain is the inertial position. This happens since, in under water, the attenuation of radio wave in the sea water is very high and hence the use of Global Positioning Systems (GPS) based navigation is impossible. Therefore, determination of the position in three dimensions with sufficient accuracy and update rate is still one of the biggest challenges in the development of underwater vehicle technology. Position measurements are usually obtained by means of acoustic systems. The accuracy of these measurements, however, is generally not to the sub meter level required for inspection. The data collection has also a low data rate, high data loss and sometimes very high measurement noise. In addition, for some operation conditions, the use of beacon based measurement is not possible, i.e. like exploration under ice covered surfaces, or a wide operational area.

In recent years, we have witnessed an impressive evolution in the sonar technology which has resulted in implementable solutions for high accuracy online relative positioning systems for underwater vehicles[85]. For this to be possible, the distance between the vehicle and the target is limited. Unfortunately, in many cases, for instance when scanning a pipeline, the scanned data would have limited value without a clear understanding of its location in the global frame. This brings us back to the challenges pertaining to the poor quality of acoustic measurements[85].

Motivated by such challenges, we will investigate, in this thesis, the possibility of using only strap down Inertial Navigation System (INS) measurement with help of the nonlinear model of AUV to get an estimation of the inertial position. INS offers high data rate and a considerably low noise measurement. The only drawback is that the INS is an autonomous system that is not corrected by veloc-

ity or position measurement and the position measurement are taken from two fold integration of the acceleration measurement which makes INS inertial position error goes unbounded. In this thesis, we shall investigate how the nonlinear model can help to reduce the growth or, if possible, eliminate the position error of INS measurement.

In addition to that, we consider the problem of underactuated AUV. Several control designs of fully actuated AUV have been reported in the literature. While the reported design schemes seem to be straight forward and simple, yet, they assume that the vehicle has complete actuation force to move in six degrees of freedom. In real implementation, like several other mechanical devices, many AUV types have less actuation force than the total degrees of freedom. An AUV with actuation forces less than the total degrees of freedom is called *underactuated* AUV. The presence of this restriction may lead to poor position tracking which may lead to instability.

All theoretical developments was carried based on dissipativity theorems. Among the emerging techniques that appeared in the last decade was the Interconnection and Damping Assignment (IDA) - Port Controlled Hamiltonian (PCH). PCH is a generalization of the Euler-Lagrange systems written in a pair of canonical equations. In recent years, PCH has been developed and well investigated, see [76, 74, 97]. The Hamiltonian function, as originally defined in classical mechanics, acts as the total energy the system has at a certain time. At present, there are two research fields in PCH. The first is on application of energy based Lyapunov function method, either in control design, observer design, or both and the second is on the realization of general nonlinear systems in PCH, see [99, 16, 62]. There are numerous applications of the PCH, such as, applications in power sys-

tems, [90, 91, 98], multiple generator power systems with steam valve [57], nuclear reactor [18, 19], mechatronic actuator modelling[41] and dynamic positioning of ship [70]. The work on PCH based control design of underwater vehicle has been considered also in [7], where they considered the problem of stabilization of classes of relative equilibria for underactuated underwater vehicle using Kirchoff's equations representation and neglecting hydrodynamic drag and dissipative forces. In our work, we will present the PCH realization of AUV considering hydrodynamic and dissipative forces, where the dynamic equation of AUV is based on [24], which is based on Quasi Euler Lagrange Equation (QELE). This dynamic equation is considered more realistic because it considers the restoring force and hydrodynamic drag.

To summarize, our approach uses the framework of PCH in which the AUV dynamics are transformed into PCH. Based on this transformed model, the controller design, including the underactuated conditions, observer design and separation principle are developed.

1.2 Problem Formulations and Objectives

In our developments of nonlinear output feedback of AUV using PCH approach, the following tasks are completed.

1. The representation of the AUV dynamics in PCH form.

2. The design of an initial stabilization controller based on dissipativity formalism.

3. The design of a robust $\mathcal{L}_2$ control.

4. The design of an adaptive robust $\mathcal{L}_2$ control.

5. The design of an underactuated controller.

6. The design of an observer.

7. Analysis of stability of the observer-based controller design.

1.3   Thesis Organization

The thesis is organized as follows

Chapter 2 summarizes the previous developments in nonlinear observer, model-based control and output feedback design of AUV.

Chapter 3 contains the preliminaries materials to understand the topics of the thesis. It contains the AUV kinematics, dynamics, properties and assumptions used throughout the thesis. In addition, preliminary background in normed space, stability and dissipativity theorem, as well as the AUV model properties are presented.

Chapter 4 presents the main developments of this thesis. This chapter summarizes the previous results of IDA-PCH technique. It also contains the procedure to transform the AUV dynamics into PCH. The $\mathcal{L}_2$ disturbance attenuation in the general framework of PCH systems is then developed which constitutes an extension of the previous work in the literature. Subsequently, the adaptive scheme of $\mathcal{L}_2$ disturbance attenuation is presented. The proposed technique is then applied for the AUV systems and the stability analysis of the closed loop system and the robustness against the exogenous dis-

turbances and parameter uncertainty are studied. The simulation results demonstrating the performance of the controller are presented in the last section of the chapter.

Chapter 5 proposes a design methodology to construct nonlinear trajectory tracking control in both two and three dimensions for underactuated AUV. Although the design is implemented for AUV that has four degrees of freedom actuation forces, generally, it can be implemented as well for the one that has only three degrees of freedom, i.e. surge, pitch and sway actuation forces only. In addition, we present the stability analysis and robustness of the proposed underactuated trajectory tracking control design. The simulation results are presented to demonstrate the performance of the controller, as well as the comparison between the proposed controller design and the underactuated AUV controller design available in literature.

Chapter 6 contains the development of a nonlinear observer design for a class of PCH systems. The separation principle is presented for the class of PCH system. The nonlinear observer design is then applied to AUV for INS based sensory measurement suite. This chapter also contains an alternative observer design covering the case where the inertial position and angle measurement are available. The proposed AUV observer is closely related to the one proposed in [83]. The separation principle for the particular case of AUV is presented as well. Finally, the simulation results are presented in the last section of the chapter.

Chapter 7 presents a general conclusion and possible extension of the present work.

Chapter 2

Preliminaries

2.1 Introduction

This chapter covers the control design and system analysis backgrounds necessary for all theoretical developments and simulation in this thesis. In section 2.2 we give an introduction on rigid body kinematics. Autonomous Underwater Vehicle (AUV) dynamics are covered in section 2.3. Normed space, function space, nonlinear stability analysis and dissipativity theorem are covered in sections 2.5, 2.6 and 2.7 respectively. The last section presents the AUV model properties that is used in the simulations .

2.2 Vehicle Kinematics

In order to describe the motion of an AUV in Six Degrees of Freedom (DOF), generalized coordinates are required to represent the position of center gravity

and the attitude of the vehicle in space. These six different motion components are defined as, *surge, sway, heave, yaw, pitch, roll*. Hence, the general motion of an AUV in 6 DOF can be described by the following vectors

$$
\boldsymbol{\eta} = \begin{bmatrix} \boldsymbol{\eta}_1^\top, \boldsymbol{\eta}_2^\top \end{bmatrix}^\top \qquad \boldsymbol{\eta}_1 = [x, y, z]^\top \qquad \boldsymbol{\eta}_2 = [\phi, \theta, \psi]^\top
$$

$$
\boldsymbol{\nu} = \begin{bmatrix} \boldsymbol{\nu}_1^\top, \boldsymbol{\nu}_2^\top \end{bmatrix}^\top \qquad \boldsymbol{\nu}_1 = [u, v, w]^\top \qquad \boldsymbol{\nu}_2 = [p, q, r]^\top
$$

$$
\boldsymbol{\tau} = \begin{bmatrix} \boldsymbol{\tau}_1^\top, \boldsymbol{\tau}_2^\top \end{bmatrix}^\top \qquad \boldsymbol{\tau}_1 = [X, Y, Z]^\top \qquad \boldsymbol{\tau}_2 = [K, L, M]^\top \qquad (2.1)
$$

Where $\boldsymbol{\eta}$ denotes the position and attitude vector in the earth fixed frame, $\boldsymbol{\nu}$ denotes the body fixed linear and angular velocity vector and $\boldsymbol{\tau}$ is used to describe the forces and moments acting on the vehicle in the body fixed frame. If the available measurements are relative to the body fixed frame, using the Euler-Rotation theorem, we can transform the measurements to the earth fixed position. The earth fixed coordinate is obtained by integration of the earth-fixed transformed linear velocity, which is given by

$$
\dot{\boldsymbol{\eta}}_1 = \mathbf{J}_1(\boldsymbol{\eta}_2)\boldsymbol{\nu}_1 \qquad (2.2)
$$

where $\mathbf{J}_1(\boldsymbol{\eta}_2)$ is a translational rotation transformation matrix which is a function of the Euler angles, roll ϕ, pitch θ and yaw ψ, given by

$$
\mathbf{J}_1(\boldsymbol{\eta}_2) = \begin{bmatrix} c\psi c\theta & -s\psi c\phi + c\psi s\theta s\phi & s\psi s\phi + c\psi c\phi s\theta \\ s\psi c\theta & c\psi c\phi + s\phi s\theta s\psi & -c\psi s\phi + s\psi c\phi s\theta \\ -s\theta & c\theta s\phi & c\phi c\theta \end{bmatrix} \qquad (2.3)
$$

The body fixed angular velocity vector $\boldsymbol{\nu}_2$ and the Earth fixed angular velocity

10

(Euler rate) vector $\boldsymbol{\eta}_2$ are related through a rotation transformation matrix $\mathbf{J}_2(\boldsymbol{\eta}_2)$ according to

$$\dot{\boldsymbol{\eta}}_2 = \mathbf{J}_2(\boldsymbol{\eta}_2)\boldsymbol{\nu}_2 \tag{2.4}$$

where $\mathbf{J}_2(\boldsymbol{\eta}_2)$ is given by

$$\mathbf{J}_2(\boldsymbol{\eta}_2) = \begin{bmatrix} 1 & s\phi t\theta & c\phi t\theta \\ 0 & c\phi & -s\phi \\ 0 & \dfrac{c\phi}{c\theta} & \dfrac{c\phi}{c\theta} \end{bmatrix} \tag{2.5}$$

Where, $c(.) = \cos$, $s(.) = \sin$ and $t(.) = \tan$.

2.3 AUV Dynamics

Dynamics of underwater vehicles including hydrodynamic parameter uncertainties are highly nonlinear, coupled and time varying. Several models for AUV dynamics are available in the literatures [24]. From mechanical analysis point of view, the derivation of AUV equation motions can be done using both Newton's approach (free body diagram), or Lagrange approach. Both modelling approaches lead to the same equation of motion using body fixed velocities expression given by

$$\mathbf{M}\dot{\boldsymbol{\nu}} + \mathbf{C}(\boldsymbol{\nu})\boldsymbol{\nu} + \mathbf{D}(\boldsymbol{\nu})\boldsymbol{\nu} + g(\boldsymbol{\eta}) = \boldsymbol{\tau} \tag{2.6}$$

where

$$\mathbf{M} \in \mathbb{R}^{6 \times 6} = \text{Inertia matrix including added mass.}$$

$$\mathbf{C}(\boldsymbol{\nu}) \in \mathbb{R}^{6 \times 6} = \text{Matrix of Coriolis and centripetal term}$$

$$\text{including added mass.}$$

$$\mathbf{D}(\boldsymbol{\nu}) \in \mathbb{R}^{6 \times 6} = \text{Damping matrix}$$

$$g(\boldsymbol{\eta}) \in \mathbb{R}^{6} = \text{Vector of gravitational forces and moments.}$$

$$\boldsymbol{\tau} \in \mathbb{R}^{6} = \text{Control Inputs.}$$

The inertia matrix, M is the sum of the rigid body inertia matrix $\mathbf{M}_{RB}$ and the hydrodynamic virtual inertia (added mass) $\mathbf{M}_{A}$. As the vehicle moves underwater, additional forces and moment coefficients have to be added to account for the effective mass of the fluid surrounding the vehicle. These coefficients are referred to as added (virtual) mass and includes added moments of inertia and cross coupling terms such as force coefficients which are generated due to the linear and angular accelerations.

The added mass concept is usually misunderstood to be finite amount of water surrounding the vehicle, such that the vehicle and the fluid represent a new system with larger mass than the mass of the original system. However, as pointed in [24], this is not true, since vehicle motion will force the whole fluid to oscillate with different fluid particles amplitudes in phase with the harmonic motion of the vehicle. The added mass should be considered as the total of pressure induced forces and moments due to a forced harmonic motion of the body which is proportional to the acceleration of the body. For completely immersed vehicle, the added mass coefficients can be reasonably assumed symmetric and frequency

independent[24]. For some special shapes, the added mass can be obtained analytically, see [24] for more details.

Based on the kinetic energy of the fluid,$\mathbf{T}_A = \frac{1}{2}\boldsymbol{\nu}\mathbf{M}_A\boldsymbol{\nu}^\top$, the added mass forces and moments can be derived using Kirchhoff's equations [88]. Then, the added mass forces and moments can be seen as the sum of the hydrodynamic inertia forces and moments $\mathbf{M}_A$ and the hydrodynamic Coriolis and centripetal forces and moments $\mathbf{C}$.

Definition 2.1 (Rigid Body Inertia). [24] The rigid body inertia matrix $\mathbf{M}_{RB}$ parameter is unique and satisfies

$$\mathbf{M}_{RB} = \mathbf{M}_{RB}^\top; \; \dot{\mathbf{M}}_{RB} = 0 \tag{2.7}$$

where

$$\mathbf{M}_{RB} = \begin{bmatrix} m\mathbf{I}_{3\times3} & -m\mathbf{S}(r_g) \\ m\mathbf{S}(r_g) & \mathbf{I}_0 \end{bmatrix} \tag{2.8}$$

Here $\mathbf{I}_{3\times3}$ is the identity matrix, $\mathbf{I}_0 = \mathbf{I}_0^\top > 0$ is the inertia tensor with respect to the body fixed frame origin and $\mathbf{S}(r_g) \in SS(3)$ is 3×3 Skew Symmetric Matrix given by

$$\mathbf{S}(\lambda) = \begin{bmatrix} 0 & -\lambda_3 & \lambda_2 \\ \lambda_3 & 0 & -\lambda_1 \\ -\lambda_2 & \lambda_1 & 0 \end{bmatrix} \tag{2.9}$$

Definition 2.2 (Coriolis and Centripetal Matrix). [24] Let $\mathbf{M} > 0$ be a 6×6 inertia matrix defined by

$$\mathbf{M} = \begin{bmatrix} \mathbf{M}_{11} & \mathbf{M}_{12} \\ \mathbf{M}_{21} & \mathbf{M}_{22} \end{bmatrix} \tag{2.10}$$

13

The Coriolis and centripetal matrix is given by

$$
\mathbf{C}(\boldsymbol{\nu}) = \begin{bmatrix} \mathbf{0}_{3\times3} & -\mathbf{S}(\mathbf{M}_{11}\boldsymbol{\nu}_1 + \mathbf{M}_{12}\boldsymbol{\nu}_2) \\ -\mathbf{S}(\mathbf{M}_{11}\boldsymbol{\nu}_1 + \mathbf{M}_{12}\boldsymbol{\nu}_2) & -\mathbf{S}(\mathbf{M}_{21}\boldsymbol{\nu}_1 + \mathbf{M}_{22}\boldsymbol{\nu}_2) \end{bmatrix}
\tag{2.11}
$$

Definition 2.3 (Added Mass). $\mathbf{M}_A$ is a 6×6 added mass inertia matrix defined as

$$
\mathbf{M}_A \triangleq \begin{bmatrix} X_{\dot{u}} & X_{\dot{v}} & X_{\dot{w}} & X_{\dot{p}} & X_{\dot{q}} & X_{\dot{r}} \\ Y_{\dot{u}} & Y_{\dot{v}} & Y_{\dot{w}} & Y_{\dot{p}} & Y_{\dot{q}} & Y_{\dot{r}} \\ Z_{\dot{u}} & Z_{\dot{v}} & Z_{\dot{w}} & Z_{\dot{p}} & Z_{\dot{q}} & Z_{\dot{r}} \\ K_{\dot{u}} & K_{\dot{v}} & K_{\dot{w}} & K_{\dot{p}} & K_{\dot{q}} & K_{\dot{r}} \\ M_{\dot{u}} & M_{\dot{v}} & M_{\dot{w}} & M_{\dot{p}} & M_{\dot{q}} & M_{\dot{r}} \\ N_{\dot{u}} & N_{\dot{v}} & N_{\dot{w}} & N_{\dot{p}} & N_{\dot{q}} & N_{\dot{r}} \end{bmatrix}
\tag{2.12}
$$

where X, Y, Z, K, M, N are linear forces and torques applied to the vehicle. For instance, the hydrodynamic added mass force Y_A along the y-axis due to an acceleration $\dot{u}$ in the x direction is written as

$$
Y_A = Y_{\dot{u}}\dot{u}, \text{ where } Y_{\dot{u}} \triangleq \frac{\partial Y}{\partial \dot{u}}
\tag{2.13}
$$

In an ideal fluid, the hydrodynamics damping matrix, $\mathbf{D}$, is real, non-symmetrical and strictly positive. With rough assumptions such as a symmetric vehicle and non-coupled motion, $\mathbf{D}$ can be simplified to a diagonal matrix $\mathbf{D}(\boldsymbol{\nu}) = \text{diag}(d_{1,i} + d_{2,i}|\nu_i|), i = 1, \cdots 6$ where d_1 is a linear damping coefficient and d_2 is a quadratic (drag) damping coefficient. In the hydrodynamic terminology, the gravitational and buoyant forces $g(\boldsymbol{\eta})$ are called restoring forces. The gravitational forces act through the center of gravity while the buoyant forces act through the center of

14

buoyancy. Environmental disturbances due to waves, wind and ocean currents and their mathematical expressions are discussed in details in [24].

All the above hydrodynamics parameters can be analytically expressed under some ideal hypothesis [71] includes: the fluid has constant and uniform density, it is incompressible, inviscid, irrotational, unbounded and of infinite extent except for the body itself. As mentioned in [4], the first hypothesis may not be always fulfilled as when navigating at sea near a river's mouth, due to local salinity changes, but it can be considered valid in the most common missions of Remotely Operated Vehicles (ROV) that operate in a very limited area. On the contrary, the fluid may always be assumed incompressible with a very high degree of accuracy. If the vehicle under question is open-frame with no sharp edges or lifting surfaces and operates at slow speeds, the null viscosity and irrotational hypothesis may be considered valid, while the last one regarding unboundedness may be critical when navigating near the sea bottom, the sea surface or near any other separating surface, but it is commonly supposed to be satisfied in standard operating conditions. The resulting motion equation are coupled and nonlinear. Coupling is due to off-diagonal added mass and drag components. However at low speed operations, these components can be neglected which will give an uncoupled model. This approximation relies on the following :

- the off-diagonal elements of the added mass matrix of a rigid body having three symmetry planes are identically null,

- the off-diagonal elements of such positive definite matrix are much smaller than their diagonal counterparts (see [24], p. 37) and

- the hydrodynamic damping coupling is negligible at low speed.

15

However, for AUV operated at high speed, off diagonal added mass and drag component cannot be neglected.

2.4 Properties and Assumptions

In this section we present several properties and assumptions that will be used in the next chapter. First, we recall again the AUV equation of motion mentioned before

$$\dot{\boldsymbol{\eta}} = \mathbf{J}(\boldsymbol{\eta}_2)\boldsymbol{\nu} \tag{2.14}$$

$$\mathbf{M}\dot{\boldsymbol{\nu}} + \mathbf{C}(\boldsymbol{\nu})\boldsymbol{\nu} + \mathbf{D}(\boldsymbol{\nu})\boldsymbol{\nu} + g(\boldsymbol{\eta}_2) = \boldsymbol{\tau} + \mathbf{J}(\boldsymbol{\eta}_2)^{-1}\mathbf{b} \tag{2.15}$$

$$\dot{\mathbf{b}} = -\mathbf{T}^{-1}\mathbf{b} + \mathbf{Bn} \tag{2.16}$$

$$\mathbf{y} = \boldsymbol{\eta} + \boldsymbol{v}_n \tag{2.17}$$

Notes, we have added the bias $\mathbf{b}$ into the equations. Biases will contain all unmodelled disturbance and noise coming from the surrounding environment. As mentioned in [28], biases are assumed to be slowly time varying and can be modeled by first order Markov chain. $\mathbf{T}$ is a constant diagonal positive definite matrix and $\mathbf{B}$ is a diagonal magnitude scaling of the noise $\mathbf{n}$. The plant dynamics then are transformed into inertial frame coordinates

$$\mathbf{M}^*(\boldsymbol{\eta})\dot{\boldsymbol{\nu}}_e + \mathbf{C}^*(\boldsymbol{\nu},\boldsymbol{\eta})\boldsymbol{\nu}_e + \mathbf{D}^*(\boldsymbol{\nu},\boldsymbol{\eta})\boldsymbol{\nu}_e + g^*(\boldsymbol{\eta}_2) = \mathbf{J}(\boldsymbol{\eta}_2)^{-\top}\boldsymbol{\tau} + \mathbf{b} \tag{2.18}$$

where $(\cdot)^{\top}$ stands for matrix transpose and

$$\mathbf{M}^*(\boldsymbol{\eta}) \triangleq \mathbf{J}(\boldsymbol{\eta}_2)^{-\top}\mathbf{M}\mathbf{J}(\boldsymbol{\eta}_2)^{-1}$$

$$\mathbf{C}^*(\boldsymbol{\nu}, \boldsymbol{\eta}) \triangleq \mathbf{J}(\boldsymbol{\eta}_2)^{-\top}\left[\mathbf{C}(\boldsymbol{\nu}) - \mathbf{M}\mathbf{J}(\boldsymbol{\eta}_2)^{-1}\dot{\mathbf{J}}(\boldsymbol{\eta}_2)\right]\mathbf{J}(\boldsymbol{\eta}_2)^{-1}$$

$$\mathbf{D}^*(\boldsymbol{\eta}) \triangleq \mathbf{J}(\boldsymbol{\eta}_2)^{-\top}\mathbf{D}(\boldsymbol{\nu})\mathbf{J}(\boldsymbol{\eta}_2)^{-1}$$

$$g^*(\boldsymbol{\eta}_2) \triangleq \mathbf{J}(\boldsymbol{\eta}_2)^{-\top}g(\boldsymbol{\eta}_2)$$

$$\boldsymbol{\nu}_e \triangleq \mathbf{J}(\boldsymbol{\eta}_2)\boldsymbol{\nu}$$

The following properties and assumptions are assumed to be valid for the AUV type of interest, [83],[28]

Assumption 2.1. The operating conditions of the AUV that are strictly inside the following region

$$-\pi/2 < \theta_{\min} \le \theta \le \theta_{\max} < \pi/2$$

$$-\pi/2 < \phi_{\min} \le \phi \le \phi_{\max} < \pi/2$$

Property 2.1. The matrix $(\dot{\mathbf{M}}^* - 2\mathbf{C}^*)$ is skew symmetric, i.e.

$$\mathbf{x}^{\top}\left[\dot{\mathbf{M}}^* - 2\mathbf{C}^*\right]\mathbf{x} = 0, \ \forall \mathbf{x} \in \mathbb{R}^n$$

In body fixed frame the Coriolis and centripetal matrix is skew symmetric as well, i.e.,

$$\mathbf{x}^{\top}\mathbf{C}(\boldsymbol{\nu})\mathbf{x} = 0, \ \forall \mathbf{x} \in \mathbb{R}^n$$

Property 2.2. The Coriolis and centripetal matrix is linearly dependent on $\boldsymbol{\nu}$, i.e.

for all $\boldsymbol{\eta}, \mathbf{x}, \mathbf{y}, \mathbf{z} \in \mathbb{R}^6$, the following expression is true

$$\mathbf{C}^*(\mathbf{x} + \alpha\mathbf{y}, \boldsymbol{\eta})\mathbf{z} = \mathbf{C}^*(\mathbf{x}, \boldsymbol{\eta})\mathbf{z} + \alpha\mathbf{C}^*(\mathbf{y}, \boldsymbol{\eta})\mathbf{z}$$

$$\exists\, \mathbf{C}_M^* > 0 \text{ such that, } \|\mathbf{C}^*(\mathbf{x}, \boldsymbol{\eta})\| \leq \mathbf{C}_M^* \|\mathbf{x}\|$$

This condition is valid as well if the Coriolis and centripetal are represented in the body-fixed frame.

Property 2.3. The damping is dissipative, hence, we have

$$\mathbf{x}^\top \mathbf{D}^*(\boldsymbol{\nu}, \boldsymbol{\eta})\mathbf{x} > 0 \;,\; \forall \mathbf{x}, \boldsymbol{\nu}, \boldsymbol{\eta}$$

Moreover, the damping can be divided into linear and nonlinear terms, i.e. $\mathbf{D}^*(\boldsymbol{\nu}, \boldsymbol{\eta}) = \mathbf{D}_l^*(\boldsymbol{\eta}) + \mathbf{D}_{nl}^*(\boldsymbol{\nu}, \boldsymbol{\eta})$, which satisfies

$$0 < \mathbf{D}_{l\,\min}^* \leq \mathbf{D}_l^*(\boldsymbol{\eta}) \leq \mathbf{D}_{l\,\max}^*$$

$$0 < \mathbf{D}_{nl\,\min}^* \leq \mathbf{D}_{nl}^*(\boldsymbol{\nu}, \boldsymbol{\eta}) \leq \mathbf{D}_{nl\,\max}^*$$

Also under assumption 2.1, we have

$$\delta_m \mathbf{D}_{nl\,\min}^* \|\mathbf{x}\| \leq \mathbf{D}_{nl\,\min}^* \|\mathbf{J}^{-1}(\boldsymbol{\eta}_2)\mathbf{x}\|$$

The quadratic drag is considered to satisfy property 2.2 as well. This condition is valid if the drag matrices are represented in the body-fixed frame.

Property 2.4. The mass matrix $\mathbf{M}^*(\boldsymbol{\eta})$ in inertial frame is positive symmetric, for all angle satisfying assumption 2.1, i.e.

$$0 < \mathbf{M}_{\min}^* < \mathbf{M}^*(\boldsymbol{\eta}) \leq \mathbf{M}_{\max}^*$$

This condition is valid also if the mass is represented in the body-fixed frame **M**.

Property 2.5. The rotation matrix $\mathbf{J}(\boldsymbol{\eta}_2) \in \mathbb{R}^6$ satisfies the following

1. $\mathbf{J}_1(\boldsymbol{\eta}_2)$ is orthogonal, hence, $\|\mathbf{J}_1(\boldsymbol{\eta}_2)\mathbf{x}\| = \|\mathbf{x}\|$ for all $\mathbf{x} \in \mathbb{R}^3$

2. Under assumption 2.1,

$$\|\mathbf{J}_2(\boldsymbol{\eta}_2)\mathbf{x}\| = \sigma_J\|\mathbf{x}\|$$

$$\|\mathbf{J}_2(\boldsymbol{\eta}_2)^{-1}\mathbf{x}\| = \sqrt{3}\|\mathbf{x}\|$$

where $0 < \sigma_J < \infty, \forall \mathbf{x} \in \mathbb{R}^3 - \{0\}$.

Assumption 2.2. The velocity vector defined in the body-fixed frame $\boldsymbol{\nu}$, is bounded by $\boldsymbol{\nu}_{\max}$, i.e.

$$\boldsymbol{\nu}_{\max} = \sup_t \|\boldsymbol{\nu}(t)\|$$

Assumption 2.3. Both bias driven noise $\mathbf{n}$ and measurement noise $\boldsymbol{v}_n$ are both assumed to be zero mean Gaussian white noise and both $\mathbf{n}$ and $\boldsymbol{v}_n$ are not included in the Lyapunov analysis since they are considered negligible.

Assumption 2.4. The true value of the rotation matrix $\mathbf{J}(\boldsymbol{\eta}_2)$ is nearly equal to the value of the rotation matrix as a function of the angle measurement $\mathbf{J}(\mathbf{y}_2)$. This is a good assumption, since noise is assumed small and it is white Gaussian, i.e.

$$\mathbf{J}(\boldsymbol{\eta}_2) \simeq \mathbf{J}(\mathbf{y}_2)$$

2.5 Normed and Function Space

In this section, we briefly review the notation and definitions of normed spaces, $\mathcal{L}_p$ norms and properties of the signals. For a more complete presentation, the reader is referred to [42] or any monograph or text book on functional analysis, [51, 66, 73]. Let E be a linear space over the field K (typically K is $\mathbb{R}$ or the complex field $\mathbb{C}$). The function $\rho(\cdot)$, $\rho : E \to \mathbb{R}^+$ is a norm on E if and only if:

1. $\mathbf{x} \in E$ and $\mathbf{x} \neq \mathbf{0} \Rightarrow \rho(\mathbf{x}) > 0, \rho(\mathbf{0}) = \mathbf{0}$

2. $\rho(\alpha\mathbf{x}) = |\alpha|\rho(\mathbf{x}), \forall \alpha \in K, \forall \mathbf{x} \in E$

3. $\rho(\mathbf{x} + \mathbf{y}) \leq \rho(\mathbf{x}) + \rho(\mathbf{y}), \forall \mathbf{x}, \mathbf{y} \in E$ (triangle inequality)

The linear space E which has the norm operation ρ for all $\mathbf{x} \in E$ is called normed space. We have seen the notion of normed space, next, we consider "function space", specifically, spaces where the vector or elements of space are functions of time. The most important spaces of this kind in control applications are the so-called $\mathcal{L}_p$ spaces. In the following definition we consider a function $\mathbf{u} : \mathbb{R}^+ \to \mathbb{R}^q$, i.e. $\mathbf{u}$ is of the form

$$\mathbf{u} = \begin{bmatrix} u_1(t) \\ u_2(t) \\ \ldots \\ u_q(t) \end{bmatrix}$$

Definition 2.4 (The Space $\mathcal{L}_2$). The Space $\mathcal{L}_2$ consists of all piecewise continuous function $\mathbf{u} : \mathbb{R}^+ \to \mathbb{R}^q$ satisfying

$$\|\mathbf{u}\|_{\mathcal{L}_2} \triangleq \sqrt{\int_0^\infty [|u_1|^2 + |u_2|^2 + \cdots + |u_q|^2]\, dt} < \infty \qquad (2.19)$$

The norm $\|\mathbf{u}\|_{\mathcal{L}_2}$ defined in this equation is the so called $\mathcal{L}_2$ norm of the function $\mathbf{u}$.

Definition 2.5 (The Space $\mathcal{L}_\infty$). The Space $\mathcal{L}_\infty$ consists of all piecewise continuous function $\mathbf{u} : \mathbb{R}^+ \to \mathbb{R}^q$ satisfying

$$\|\mathbf{u}\|_{\mathcal{L}_\infty} \triangleq \sup_{t \in \mathbb{R}^+} \|\mathbf{u}(t)\|_\infty < \infty \tag{2.20}$$

The reader should not confuse the two different norms used in equation (2.20). Indeed, the norm $\|\mathbf{u}\|_{\mathcal{L}_\infty}$ is the $\mathcal{L}_\infty$ norm of the function $\mathbf{u}$, whereas $\|\mathbf{u}(t)\|_\infty$ represents the infinity norm of the vector $\mathbf{u}(t)$ in $\mathbb{R}^q$.

Both $\mathcal{L}_2$ and $\mathcal{L}_\infty$ are special cases of the so called $\mathcal{L}_p$ spaces. Given $p : 1 \le p < \infty$, the $\mathcal{L}_p$ consist of all piecewise continuous functions $\mathbf{u} : \mathbb{R}^+ \to \mathbb{R}^q$ satisfying

$$\|\mathbf{u}\|_{\mathcal{L}_p} \triangleq \sqrt[p]{\int_0^\infty \left[|u_1|^p + |u_2|^p + \cdots + |u_q|^p \right] dt} < \infty \tag{2.21}$$

2.6 Stability Theorem

Here we recall some basic stability theorems for autonomous systems which are taken from [64]. For more details, the readers are referred to standard nonlinear control books such as [64],[31],[42].

Theorem 2.1 (Lyapunov Stability Theorem). *Let $\mathbf{x} = 0$ be an equilibrium point of $\dot{\mathbf{x}} = f(\mathbf{x}), f : \mathcal{D} \to \mathbb{R}^n$ and let $V : \mathcal{D} \to \mathbb{R}$ be a continuously differentiable function such that*

1. *$V(0) = 0$*

2. $V(\mathbf{x}) > 0, \mathbf{x} \in \mathcal{D} - \{0\}$

3. $\dot{V}(\mathbf{x}) \leq 0, \mathbf{x} \in \mathcal{D} - \{0\}$

thus $\mathbf{x} = 0$ is Lyapunov stable.

Theorem 2.2 (Asymptotic Stability Theorem). *Under the conditions of theorem 2.1, if $V(\cdot)$ is such that*

1. $V(0) = 0$

2. $V(\mathbf{x}) > 0, \mathbf{x} \in \mathcal{D} - \{0\}$

3. $\dot{V}(\mathbf{x}) < 0, \mathbf{x} \in \mathcal{D} - \{0\}$

thus $\mathbf{x} = 0$ is Asymptotically stable.

Definition 2.6 (Radially unbounded function). Let $V : \mathcal{D} \to \mathbb{R}$ be a continuously differentiable function. Then $V(\mathbf{x})$ is said to be radially unbounded if

$$V(\mathbf{x}) \to \infty \; as \|\mathbf{x}\| \to \infty \tag{2.22}$$

Theorem 2.3 (Global Asymptotic Stability Theorem). *In addition to the conditions of theorem 2.2, if $V(\mathbf{x})$ is radially unbounded, then $\mathbf{x} = 0$ is globally asymptotically stable.*

Theorem 2.4 (Exponential Stability Theorem). *Suppose that all conditions of theorem 2.2 are satisfied and in addition assume that there exist positive constants K_1, K_2, K_3 and p such that*

$$K_1\|\mathbf{x}\|^p \leq V(\mathbf{x}) \leq K_2\|\mathbf{x}\|^p$$
$$\dot{V}(\mathbf{x}) \leq -K_3\|\mathbf{x}\|^p$$

Then the origin is exponentially stable. Moreover, if the conditions hold globally, the $\mathbf{x} = 0$ *is globally exponentially stable.*

Definition 2.7 (Invariant Set). A set $\mathcal{M}$ is said to be an invariant set with respect to the dynamical system $\dot{\mathbf{x}} = f(\mathbf{x}), f : \mathcal{D} \to \mathbb{R}^n$, if

$$\mathbf{x}(0) \in \mathcal{M} \Rightarrow \mathbf{x}(t) \in \mathcal{M}, \forall t \in \mathbb{R}^+$$

Definition 2.8 (Limit Set). Let $\mathbf{x}(t)$ be a trajectory of the dynamical system $\dot{\mathbf{x}} = f(\mathbf{x}), f : \mathcal{D} \to \mathbb{R}^n$. The set $\mathcal{N}$ is called the limit set (or positive limit set) of $\mathbf{x}(t)$ if for any $p \in \mathcal{N}$ there exist a sequence of times $\{t_n\} \in [0, \infty\}$ such that

$$\mathbf{x}(t_n) \to p \ as \ t_n \to \infty$$

or equivalently

$$\lim_{n \to \infty} \|\mathbf{x}(t_n) - p\| = 0$$

Theorem 2.5 (Invariant Set Stability Theorem). *Let* $\mathbf{x} = 0$ *be an equilibrium point of* $\dot{\mathbf{x}} = f(\mathbf{x}), f : \mathcal{D} \to \mathbb{R}^n$ *and let* $V : \mathcal{D} \to \mathbb{R}$ *be a continuously differentiable function such that*

1. $V(0) = 0$

2. $V(\mathbf{x}) > 0, \mathbf{x} \in \mathcal{D} - \{0\}$

3. $\dot{V}(\mathbf{x}) \leq 0, \mathbf{x} \in \mathcal{D} - \{0\}$

4. $\dot{V}(\mathbf{x})$ *does not vanish identically along any trajectory in* $\mathbb{R}$, *other than the equilibrium point*

thus $\mathbf{x} = 0$ *is asymptotically stable.*

2.7 Dissipativity Theory

In this section, we describe a basic idea of dissipativity, which is summarized from [15]. Dissipativity theory gives a framework for the design and analysis of control systems using an input-output description based on energy-related considerations. Before introducing precise mathematical definitions, we will refer to such input-output properties as dissipative properties Systems with dissipative properties will be termed dissipative systems. When modeling dissipative systems it may be useful to develop the state-space or input-output models so that they reflect the dissipativity of the system and thereby ensure that the dissipativity of the model is invariant with respect to model parameters and to the mathematical representation used in the model.

Models for use in controller design and analysis are usually derived from the basic laws of physics (electrical systems, dynamics, thermodynamics). Then a controller can be designed based on these models. An important problem in controller design is the issue of robustness which relates to how the closed loop system will perform when the physical system differs either in structure or in parameters from the design model. For a system where the basic laws of physics imply dissipative properties, it makes sense to define the model so that it possesses the same dissipative properties regardless of the numerical values of the physical parameters. If a controller is designed so that stability relies on the dissipative properties only, the closed-loop system will be stable whatever the values of the physical parameters. Even a change of the system's order will be tolerated provided it does not destroy the dissipativity. Parallel interconnections and feedback interconnections of dissipative systems inherit the dissipative properties of

the connected subsystems and this simplifies the analysis by the manipulation of block diagrams. It also provides guidelines on how to design control systems.

There is another aspect of dissipativity which is very useful in practical applications. It turns out that dissipativity considerations are helpful as a guide for the choice of a suitable variable for output feedback. This is helpful for selecting where to place sensors for feedback control.

Example 2.1 (System with Mass Spring and Damper). [15] Consider a one-dimensional simple mechanical system with a mass, a spring and a damper. The equation of motion is

$$m\ddot{x}(t) + D\dot{x}(t) + Kx(t) = F(t), \ x(0) = x_0, x(0) = x_0$$

where m is the mass, D is the damper constant, K is the spring stiffness, x is the position of the mass and F is the force acting on the mass. The energy of the system is

$$V(x, \dot{x}) = \frac{1}{2}m\dot{x}^2 + \frac{1}{2}Kx^2$$

The time derivative of the energy when the system moves is

$$\frac{d}{dt}V(x, \dot{x}) = m\ddot{x}\dot{x} + K\dot{x}x$$

Inserting the equation of motion we get

$$\frac{d}{dt}V(x, \dot{x}) = F(t)\dot{x}(t) - D\dot{x}^2(t)$$

Integration of this equation from $t = 0$ to $t = T$ gives

$$V[x(T), x(T)] = V[x(0), x(0)] + \int_0^T F(t)\dot{x}(t)dt - \int_0^T D\dot{x}^2(t)dt$$

25

This means that the energy at time $t = T$ is the initial energy plus the energy supplied to the system by the control force F minus the energy dissipated by the damper. Note that if the input force F is zero and if there is no damping, then the energy $V(\cdot)$ of the system is constant. Here $D \geq 0$ and $V[x(0), x(0)] > 0$ and it follows that the integral of the force F and the velocity $v = \dot{x}$ satisfies

$$\int_0^T F(t)v(t)dt \geq -V[x(0), x(0)] \tag{2.23}$$

The physical interpretation of this inequality is seen from the equivalent inequality

$$-\int_0^T F(t)v(t)dt \leq V[x(0), x(0)] \tag{2.24}$$

which shows that the energy $-\int_0^T F(t)x(t)dt$ that can be extracted from İĞ the system is less than or equal to the initial energy stored in the system. We will show later that (2.23) implies that the system with input F and output v is passive. The Laplace transform of the equation of motion is

$$\left(ms^2 + Ds + K\right) x(s) = F(s)$$

which leads to the transfer function

$$\frac{v}{F} = \frac{s}{ms^2 + Ds + K}$$

It is seen that the transfer function is stable and that for $s = j\omega$ the phase of the transfer function has absolute value less or equal to $90°$, that is,

$$\left| \angle \frac{v}{F}(j\omega) \right| \leq 90° \Rightarrow \mathbf{Re}\left[\frac{v}{F}(j\omega) \right] \geq 0 \tag{2.25}$$

for all $\omega \in [-\infty, +\infty]$. We will see in the following that these properties of the transfer function are consequences of the condition (2.23) and that they are important in controller design.

There are several definitions of dissipativity that will be used later on the development. For our set of definitions, we consider a causal nonlinear system $(\Sigma) : \mathbf{u}(t) \rightarrow \mathbf{y}(t); \mathbf{u}(t) \in \mathcal{L}_{pe}, \mathbf{y}(t) \in \mathcal{L}_{pe}$, represented by the following input-affine state-space representation :

$$\Sigma \begin{cases} \dot{\mathbf{x}} & = f(\mathbf{x}) + g(\mathbf{x})\mathbf{u} \\ \mathbf{y} & = h(\mathbf{x}) + l(\mathbf{x})\mathbf{u} \\ \mathbf{x}(0) & = \mathbf{x}_0 \end{cases} \tag{2.26}$$

Let us call $w(t) = w(\mathbf{u}(t), \mathbf{y}(t))$ the *Supply Rate* and be such that for all admissible $\mathbf{u}(t)$ and $\mathbf{x}(0)$ and for all $t \in \mathbb{R}^+$

$$\int_0^t |w(\mathbf{u}(s), \mathbf{y}(s))| ds < +\infty \tag{2.27}$$

Then the following the definitions are given

Definition 2.9 (Dissipative System). The system (Σ) is said to be dissipative if there exists a so-called storage function $V(\mathbf{x}) \geq 0$ such that the following dissipation inequality holds:

$$V(\mathbf{x}(t)) \leq V(\mathbf{x}(0)) + \int_0^t w(\mathbf{u}(s), \mathbf{y}(s)) ds \tag{2.28}$$

along all possible trajectories of (Σ)starting at $\mathbf{x}(0)$, for all $\mathbf{x}(0)$, $t \geq 0$ (said differently: for all admissible controllers $\mathbf{u}(\cdot)$ that drive the state from $\mathbf{x}(0)$ to $\mathbf{x}(0)$ on

the interval $[0, t]$).

Definition 2.10. The system (Σ) is dissipative with respect to the supply rate $w(\mathbf{u}(t), \mathbf{y}(t))$ if for all admissible $\mathbf{u}(\cdot)$ and all $t_1 \geq t_0$ one has

$$\int_{t_0}^{t_1} w(\mathbf{u}(s), \mathbf{y}(s))ds \geq 0 \tag{2.29}$$

with $\mathbf{x}(t_0) = 0$ and along trajectories of (Σ).

Definition 2.11. The system (Σ) is said dissipative with respect to the supply rate $w(\mathbf{u}(t), \mathbf{y}(t))$ if there exists a locally bounded non-negative function $V : \mathbb{R}^n \to \mathbb{R}$ such that

$$V(\mathbf{x}) \geq \sup_{t \geq 0, \mathbf{u} \in \mathcal{U}} \left\{ V(\mathbf{x}) - \int_0^t w(\mathbf{u}(s), \mathbf{y}(s))ds : \mathbf{x}(0) = \mathbf{x} \right\} \tag{2.30}$$

Definition 2.12 (Available Storage). The available storage $V_a(\cdot)$ of the system (Σ) is given by

$$0 \leq V_a(\mathbf{x}) = \sup_{\mathbf{x} = \mathbf{x}_0, \mathbf{u}, t \geq 0} - \left\{ \int_0^t w(\mathbf{u}(s), \mathbf{y}(s))ds \right\} \tag{2.31}$$

where $V_a(\cdot)$ is the maximum amount of energy which can be extracted from the system with initial state $\mathbf{x} = \mathbf{x}_0$.

2.8   Introduction to MARES

The AUV model selected in this thesis for simulation purposes is a torpedo shaped 1.5m long AUV, called Modular Autonomous Robot for Environment Sampling (MARES) [21, 22, 23], see figure 2.1. MARES can dive up to 100m deep and unlike similar-sized systems has vertical thrusters to allow for purely vertical motion in
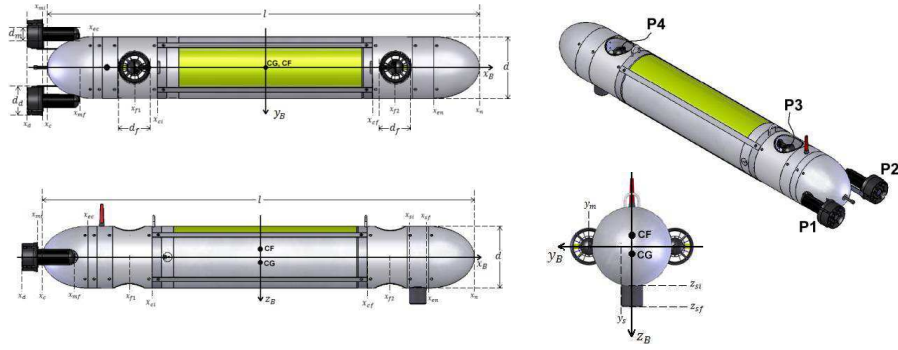
Figure 2.1: MARES vehicle

the water column. Forward velocity can be independently defined, from 0 to about 1.5 m/s. MARES is selected since it has an affine input behaviour that makes the application of previous development straight forward. The following tables list some of MARES properties that are used in simulations. Notice that, MARES has decoupled quadratic drag without linear drag. The hydrodynamic drag matrix of MARES is given by

$$
\mathbf{D}(\boldsymbol{\nu}) \triangleq - \begin{bmatrix}
X_{u|u|}|u| & 0 & 0 & 0 & X_{q|q|}|q| & 0 \\
0 & Y_{v|v|}|v| & 0 & Y_{p|p|}|p| & 0 & Y_{r|r|}|r| \\
0 & 0 & Z_{w|w|}|w| & 0 & Z_{q|q|}|q| & 0 \\
0 & K_{v|v|}|v| & 0 & K_{p|p|}|p| & 0 & 0 \\
M_{u|u|}|u| & 0 & M_{w|w|}|w| & 0 & M_{q|q|}|q| & 0 \\
0 & N_{v|v|}|v| & 0 & 0 & 0 & N_{r|r|}|r|
\end{bmatrix}
\tag{2.32}
$$

From table 2.3,2.4 and 2.5, we can see that MARES inertia matrix and hydrodynamic damping are symmetric.

Properties	Value
Length	1.5 m
Diameter	20 cm
Weight in air	32 kg
Depth rating	100 m
Propulsion	2 horizontal + 2 vertical thrusters
Horizontal velocity	0-1.5 m/s, variable
Energy	Li-Ion batteries, 600 Wh
Autonomy/Range	about 10 hrs / 40 km

Table 2.1: MARES general characteristic

Properties	Value [m]	Description
$[x_{cg}, y_{cg}, z_{cg}]$	$[0, 0, 0]$	Center of gravity
$[x_{cb}, y_{cb}, z_{cb}]$	$[0, 0, 4.40.10^{-3}]$	Center of buoyancy

Table 2.2: MARES location of center of gravity and buoyancy

Properties	Value [$kg.m^2$]
I_{xx}	$1.55.10^{-1}$
I_{yy}	$4.73.10^{0}$
I_{zz}	$4.73.10^{0}$

Table 2.3: MARES moment inertia

Properties	Value	Unit
$X_{\dot{u}}$	$-1.74.10^{0}$	kg
$Y_{\dot{v}}$	$-4.28.10^{1}$	kg
$Z_{\dot{w}}$	$-4.12.10^{1}$	kg
$K_{\dot{p}}$	$-8.61.10^{-3}$	$kg.m^2$
$M_{\dot{q}}$	$-6.07.10^{0}$	$kg.m^2$
$N_{\dot{r}}$	$-6.40.10^{0}$	$kg.m^2$
$X_{\dot{q}}$	$-3.05.10^{-2}$	$kg.m$
$Y_{\dot{p}}$	$3.05.10^{-2}$	$kg.m$
$K_{\dot{v}}$	$3.05.10^{-2}$	$kg.m$
$M_{\dot{u}}$	$-3.05.10^{-2}$	$kg.m$
$Y_{\dot{r}}$	$1.13.10^{-1}$	$kg.m$
$Z_{\dot{q}}$	$-1.23.10^{-1}$	$kg.m$
$M_{\dot{w}}$	$-1.23.10^{-1}$	$kg.m$
$N_{\dot{v}}$	$1.13.10^{-1}$	$kg.m$

Table 2.4: MARES added mass

Properties	Value	Unit
$X_{u\|u\|}$	$-4.05.10^0$	$kg.m^{-1}$
$Y_{v\|v\|}$	$-1.16.10^2$	$kg.m^{-1}$
$Z_{w\|w\|}$	$-1.16.10^1$	$kg.m^{-1}$
$K_{p\|p\|}$	$-7.02.10^{-4}$	$kg.m^2$
$M_{q\|q\|}$	$-1.56.10^1$	$kg.m^2$
$N_{r\|r\|}$	$-1.25.10^1$	$kg.m^2$
$X_{q\|q\|}$	$-4.84.10^{-2}$	$kg.m$
$Y_{p\|p\|}$	$-4.84.10^{-2}$	$kg.m$
$K_{v\|v\|}$	$-2.11.10^{-1}$	kg
$M_{u\|u\|}$	$2.11.10^{-2}$	kg
$Y_{r\|r\|}$	$1.83.10^0$	$kg.m$
$Z_{q\|q\|}$	$-5.95.10^0$	$kg.m$
$M_{w\|w\|}$	$-8.26.10^0$	kg
$N_{v\|v\|}$	$2.13.10^0$	kg

Table 2.5: MARES drag coefficient

2.9 Conclusions

In this chapter, we have covered several basic definitions and preliminaries used in the thesis. Next chapter will cover the literature review for AUV control and observer designs.

Chapter 3

Literature Review

3.1 Introduction

The research activities in the Autonomous Underwater Vehicle (AUV) area are generally covering modelling, observer design, control design as well as instrumentation and sensing. The navigation, guidance and control problem contains several challenging issues mainly imposed by the vehicle working environment. In this chapter, we aim to give a brief review on each of these aspects and present the different approaches. We will review nonlinear observer design, model-based control design and underactuated control design for AUVs. The general architecture of an AUV control system can be seen in the figure 3.1.
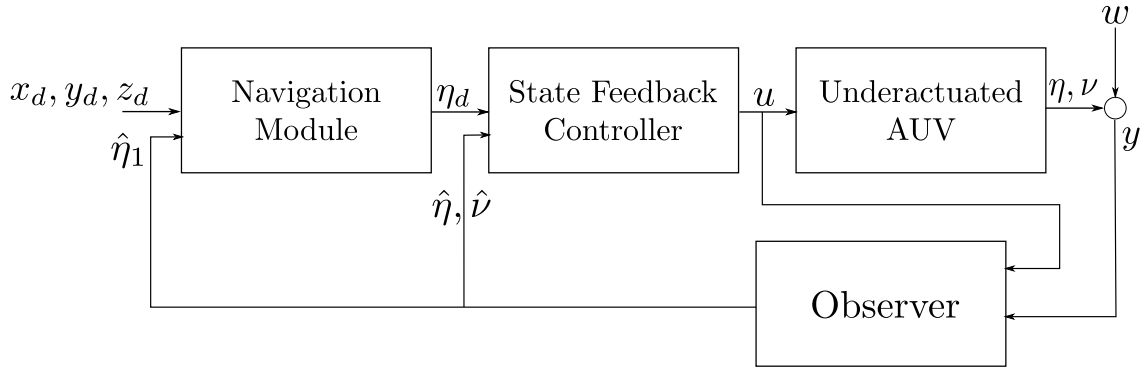
Figure 3.1: Observer, controller and navigation design for under actuated AUV

3.2 Nonlinear Observer Design of AUV

An observer filters available measurements to provide online estimates of the states within a system. Filtering and state estimation are important tasks in AUV control systems. In general, either only inertial position and angle are measured by means of beacon and gyro, or if using Doppler Velocity/Inertial Measurement Unit (IMU), only relative velocities and accelerations are measured. But unfortunately, all of these are required at the same time for designing control law, in addition with stationary (or slowly) varying disturbances due to wind, ocean current and nonlinear wave effects. Therefore, estimates of these signals must be computed from the measured position and heading of the vehicle through a state observer. Furthermore, in case of temporary sensor failure (dead-reckoning), an observer must be able to adequately predict the motion of the ship such that the control operation can continue for a period of time.

To date, the development and implementation of model-based state estimators for underwater vehicle navigation has primarily focused on applying the Kalman Filter (KF), Extended Kalman Filter (EKF), Unscented Kalman Filter (UKF) to a kinematic model. Additional work has investigated using Simultaneous Local-

ization and Mapping (SLAM), trajectory-based observers [38]. Ribas et al. [87], reported the experimental implementation of a dynamic model-based EKF. An extended discussion on the application of state estimators to underwater vehicle navigation is presented in [44]. In [45], decoupled single DOF AUV dynamic observers are proposed employing an experimentally validated vehicle model, whose parameters can be adaptively identified, to estimate the full state of the vehicle. Recently, [39] used dual UKF approach to deal with the simultaneous problem of state estimation and identification of small ROV. Although it is only capable to capture 4 Degrees of Freedom (DOF) decoupled movements of the vehicle, it is able to estimate the inertia and the damping parameters adaptively at the same time with the state estimations.

In [1], an observer-controller scheme is proposed for an Euler-Lagrange system not including the Coriolis and centripetal term, but including a nonlinear damping term. The author assumed that the nonlinear damping term satisfies the monotone damping property, which in general is not satisfied in marine systems. For appropriate choices of the output injection terms, the error dynamics was shown to be globally uniformly asymptotically stable.

In [94], another observer-controller scheme is proposed for a different class of Euler-Lagrange systems. It is assumed that only linear damping is included and a rather special form of the Coriolis and centripetal term is considered there. Notice that in general in marine systems the Coriolis and centripetal term is not of this form.

In underwater applications, the ocean current has severe influence on the vehicle performance. The current influence is difficult to predict even though measurements of both vehicle and water velocities are available. Therefore, a common

approach is to model the disturbance as a constant, or slowly varying bias, see [105], [26]. A drawback of this method is that the hydrodynamic properties of the vehicle are not properly accounted for when modeling the current loads. Other reported methods involve using kinematics and filtering techniques to obtain an estimate of the current velocity. Examples of this can be seen in, e.g., [5], [3] and [10], in which velocity feedback of some kind is required.

In [85], a modeling approach first introduced in [82] and more thoroughly described in [84] are employed. A 3 DOF model in surge, sway and heave is derived to serve as a foundation for current observer design. This is a current-induced vessel model that can be interpreted as a third-order filter with constants obtained based on the vehicle parameters. The goal is to provide an estimate of the current velocity and thereby estimate the influence of the current loads on the vehicle. See figure 3.2
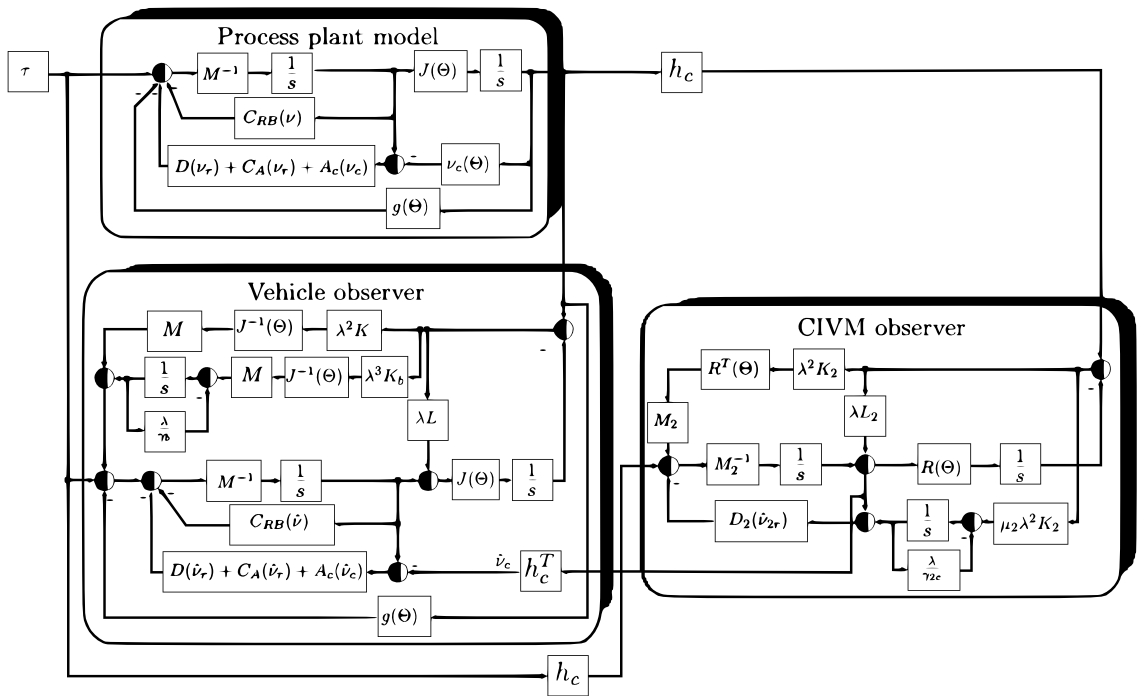
Figure 3.2: Cascaded nonlinear observer design of AUV

35

With this approach, the key hydrodynamic properties are taken into account when estimating the effect of the environmental disturbances, since the estimated current velocity is explicitly used in the calculation of the nonlinear hydrodynamic damping and Coriolis forces. Furthermore, since only the orientation and in particular the position, which can be affected by severe noise, are measured, a higher order model is preferred in order to avoid large jumps and oscillations in the current estimate. Successful experimental results of this observer concept can be found in [86] which report the design of a three DOF current-induced vessel model coworking with a complete nonlinear six DOF vehicle model. An output controller has not yet been tested with the observers in [86].

The problem of nonlinear observer design for AUV is in some aspect, has similarity with the design of nonlinear observer for dynamic positioning system. The first appearance for nonlinear observer design using linear dynamic error has been long time proposed by Fossen, [28]. Later, this work was extended in [35] for weather position control optimization. The problem of output feedback design for dynamic positioning systems using acceleration feedback have been proposed in [58].

Up to now, observer and observer-controller designs are mainly based on Lyapunov and passivity theories. A recent theory, which might be useful for observer design, is contraction theory [59]. The contraction theory basically is the extension of Krasovskii stability criterion for autonomous nonlinear systems. In [37], the contraction theory was applied for the design of Uniformly Globally Exponentially Stable (UGES) nonlinear observers for ships. The observer copies the ship dynamics and takes the earth-fixed measurements as observer feedback. Hence, the observer is analysed using contraction theory and the same result as

36

in Fosen et.al work on the Lyapunov-based nonlinear controller [27], UGES of the observer is obtained.

A region of the state space is called a contraction region with respect to a uniformly positive definite matrix $\mathbf{\Psi}(x, t) = \mathbf{\Theta}^T(x, t)\mathbf{\Theta}(x, t)$ where $\mathbf{\Theta}(x, t)$ stands for a differential coordinate transformation matrix, if equivalently

$$\mathbf{F} = \left(\dot{\mathbf{\Theta}} + \mathbf{\Theta}\frac{\partial}{\partial x} \right) \mathbf{\Theta}^{-1}$$

or

$$\left(\frac{\partial}{\partial x} \right)^T \mathbf{\Psi} + \dot{\mathbf{\Psi}} + \mathbf{\Psi}\frac{\partial}{\partial x}$$

are negative definite. In [37], the authors claim that when using contraction theory, the designer gets a clearer insight of what is being accomplished. Lyapunov based techniques start often with "define a candidate Lyapunov function......" without any further information regarding the interpretability of the chosen function. The authors claim is that by making use of transformation matrices, the designer gets a clearer insight of what has been done in geometrical terms. In particular, the uniform definiteness of the Jacobian imposed by contraction theory simply translates into an angle between the relative displacement δx and the relative virtual velocity $\delta \dot{x}$. This angle norm must be greater than 90 degrees (such an interpretation still holds for linear systems where δx and $\delta \dot{x}$ can be replaced by x and $\dot{x}$).

Furthermore, the contraction analysis also gives a smooth transition from linear-state space control designs to nonlinear ones and thus may be of interest for engineering and educating purposes. In addition, [37] claims that studying the possibly state and time-dependent eigenvalues of the Jacobian also helps to esti-

mate of the rate of decay. The authors claim that, Lyapunov functions lack these properties, mainly because of the underlying energy concept, which is less used in linear control theory.

For wider literature survey on Nonlinear Observer design of AUV, readers are referred to [100],[45].

3.3 Model Based Feedback Control for AUV

There are some reported results on Model Based Feedback Control (MBFC) of AUVs in the literature. In [32], a state feedback controller is proposed for tracking of the NPS ARIES AUV. The NPS ARIES is an underactuated slender-body AUV intended for orientation tracking while maintaining some forward speed. This kind of streamlined AUVs should be distinguished from open box-framed vehicles. These are low-speed vehicles, usually fully actuated and with hydrodynamic and stability properties that may vary significantly. The model is linearized around a constant forward velocity and decoupled into three separate systems: surge, horizontal steering (sway and yaw) and the diving system (heave and pitch). Sliding-mode controllers and observers [17] are proposed to solve the tracking problem. Experimental results, reported in [63], demonstrate successful controller performance.

In [96] and [105], velocity measurements are available for feedback. Successful tracking results of a MBFC derived using the back-stepping theory is presented in [2]. The vehicle, an open-frame hovercraft, is described by a three DOF horizontal model without nonlinear damping. These results have in common that the

velocity is available for feedback and all, except [2], assume that the destabilizing Coriolis forces are dominated by the hydrodynamic damping. Comparing with low-speed applications for ships, e.g., dynamic positioning [60], this is a common approach for control plant modeling. Moreover, the hydrodynamic properties of a box shaped vehicle indicate that the damping is dominant and that the hydrodynamic Coriolis forces are negligible. However, for slender-body vehicles with some forward speed, this assumption is not realistic.

Recent work presented in [85] shows the success application of the model based output feedback design for torpedo shaped AUV. The AUV has relatively small weight compared to the nominal speed which implies that the dynamics are speed dominant and that the nonlinear characteristics of the hydrodynamics become decisive. Moreover it does not carry any velocity or IMU. The available measurements are only beacon based position and attitude of the vehicle from a gyro/inclinometer.

Some higher class vehicles may have speed measurements obtained by using Doppler Velocity Log (DVL) [43] or integrating accelerations measured by the IMU. However, the DVL can only generate accurate velocity measurements provided that the distance to the seafloor is within a certain boundary. Furthermore, IMUs are subject to drift in the derived velocity when integrating faulty acceleration measurements.

3.4   Underactuated Control of AUV

Control design of fully-actuated AUV have been offered extensively in the litera-
ture. In such studies, the design assumes that the vehicle has complete actuation
forces, allowing six DOF movement. In real implementations, similar to many
other mechanical devices, AUV often has less actuation forces than needed to
have a total degrees of freedom movements and control for each observed out-
put. Systems having such characteristics are called *underactuated* systems. In ad-
dition, even in the case of a fully actuated system, unplanned failure may reduce
the number of actuators and change the structure of the system to an underac-
tuated one. Irrespective of the system being originally underactuated or losing
actuation due to a failure, such situation may lead to poor position tracking and
instability.

In the last two decades, many underactuated designs have been proposed in the
literature for general mechanical devices. Most of the work on the underactu-
ated designs are formulated within the Lagrangian mechanics framework, see
[9, 12, 13]. In particular, [54, 53, 55, 52, 56] proposed an underactuated design for
underwater vehicle using the Lagrangian formalism. A state-feedback controller
guaranteeing asymptotic stability of the equilibrium point has been studied by
[80]. In [81], a time-varying control scheme to achieve global exponential stabi-
lization of the equilibrium was proposed.

Recently, [7] extended the work of [56] and [101] in stabilizing control of the un-
deractuated underwater vehicle by considering the problem of stabilization of
classes of relative equilibria associated with the underactuated Kirchhoff's equa-
tions written in Port Controlled Hamiltonian (PCH) formalism. The proposed

controller has been designed using passivity theory. However, the study in [7] neglected hydrodynamic drag and dissipative forces.

There are three different problems in AUV motion control. The first problem is related to point stabilization, which is concerned with steering the vehicle to a single desired position and attitude. The second is the trajectory tracking problem which requires a vehicle to track a time-described path curvature. The last problem is related to path following control which aims at forcing a vehicle to reduce tracking error ideally to zero and makes it follow a desired spatial path without any specific time-based performance specifications. Based on a previous work [20], [50] considered a kinematic model with three degrees of freedom for AUV to design a nonlinear control for path tracking.

The work in [2] and its further development in [3] address the issue of position tracking for general underactuated autonomous vehicle for both two and three dimensions. The proposed control algorithms are based on integrator backstepping (see for instance design[49],[89]). Although the controller was successfully implemented in a particular type of AUV, the work assumes that the vehicle has its center of gravity coinciding with the origin of the body frame and the added mass related to translational motion and added mass related to rotational motion are decoupled. In addition, the authors assume that the damping force acting for translational motion is an affine function to the angular body velocity . This assumption restricts the class of AUV to the one characterized by the decoupled quadratic drag . Although this assumption can be considered valid for most slender type AUV at low speed, the coupled term cannot be neglected at higher speed. In addition, the desired trajectory has to have a smooth third derivative, which restricts the trajectory selections. The designed control also suffers from

the cancellation of non-linearities coming from the Coriolis and drag forces and computation of the derivative of restoring force and drag forces where the possibility of discontinuity are present.

Recently, [68] assumes that both buoyancy and gravitational forces are equal to zero or cancel each other in the nonactuated body frame. Such assumption is a consequence of having the center of gravity lying below the center of buoyancy. Such condition is necessary for a stable submersible body. Further more, [68] assumes that the damping terms of the nonactuated part is sufficiently larger than their inertia when both are presented in the inertial frame. In addition, the controller design was carried without considering the nonactuated roll angle dynamics based on the assumption that the restoring effects allow to self-stabilize effectively.

In this section we briefly present the work of [2, 3]. Later on, we will tackle several issues of their design in our underactuated AUV designs. We will modify the notations in [2, 3] development to follow our previous notations so the reader can easily grasp the meaning. Consider the following kinematic relations

$$\dot{\boldsymbol{\eta}}_1 = \mathbf{J}_1(\boldsymbol{\eta}_2)\boldsymbol{\nu}_1 \tag{3.1}$$

$$\dot{\mathbf{J}}_1(\boldsymbol{\eta}_2) = \mathbf{J}_1(\boldsymbol{\eta}_2)\mathbf{S}(\boldsymbol{\nu}_2) \tag{3.2}$$

Here, underactuated vehicles are considered having dynamic equations of motion of the following form

$$\mathbf{M}_1\dot{\boldsymbol{\nu}}_1 = -\mathbf{S}(\boldsymbol{\nu}_2)\mathbf{M}_1\boldsymbol{\nu}_1 + f_1(\boldsymbol{\nu}_1, \boldsymbol{\eta}_1, \boldsymbol{\eta}_2) + g_1 u_1 \tag{3.3}$$

$$\mathbf{M}_2\dot{\boldsymbol{\nu}}_2 = -\mathbf{S}(\boldsymbol{\nu}_1)\mathbf{M}_1\boldsymbol{\nu}_1 - \mathbf{S}(\boldsymbol{\nu}_2)\mathbf{M}_2\boldsymbol{\nu}_2 + f_2(\boldsymbol{\nu}_1, \boldsymbol{\nu}_2, \boldsymbol{\eta}_1, \boldsymbol{\eta}_2) + \mathbf{G}_2\mathbf{u}_2 \tag{3.4}$$

Where $\mathbf{M}_1, \mathbf{M}_2 \in \mathbb{R}^{3\times3}$ are top left and lower right block of total inertia matrix $\mathbf{M}$, $u_1 \in \mathbb{R}, \mathbf{u}_2 \in \mathbb{R}^3$ denote the control inputs, which act upon the system through a constant nonzero vector $g_1 \in \mathbb{R}^3$ and a constant nonsingular matrix $\mathbf{G}_2 \in \mathbb{R}^{3\times3}$, respectively; the terms $-\mathbf{S}(\boldsymbol{\nu}_2)\mathbf{M}_1\boldsymbol{\nu}_1$ in (3.3) and the $-\mathbf{S}(\boldsymbol{\nu}_1)\mathbf{M}_1\boldsymbol{\nu}_1 - \mathbf{S}(\boldsymbol{\nu}_2)\mathbf{M}_2\boldsymbol{\nu}_2$ matrix in (3.4) are the Coriolis terms and the functions $f_1, f_2 \in \mathcal{C}^1$,represent all the remaining forces and torques acting on the body. After defining the dynamic equations, Control-Lyapunov functions are introduced iteratively borrowing from the techniques of backstepping [49].

1. Coordinate Transformation : Consider the global diffeomorphic coordinate transformation

$$\mathbf{e} \triangleq \mathbf{J}_1^\top \left(\boldsymbol{\eta}_1 - \boldsymbol{\eta}_{1,d} \right) \tag{3.5}$$

which expresses the tracking error $\boldsymbol{\eta}_1 - \boldsymbol{\eta}_{1,d}$ in the body-fixed frame. The dynamic equation of the body-fixed tracking error is given by

$$\dot{\mathbf{e}} = -\mathbf{S}(\boldsymbol{\nu}_2)\mathbf{e} + \boldsymbol{\nu}_1 - \mathbf{J}_1^\top \dot{\boldsymbol{\eta}}_{1,d} \tag{3.6}$$

2. Convergence of $\mathbf{e}$: Define the control-Lyapunov function

$$V_1 = \frac{1}{2}\mathbf{e}^\top\mathbf{e} \tag{3.7}$$

and computing its time derivative to obtain

$$\dot{V}_1 = \mathbf{e}^\top \left[\boldsymbol{\nu}_1 - \mathbf{J}_1^\top \dot{\boldsymbol{\eta}}_{1,d} \right] \tag{3.8}$$

$\boldsymbol{\nu}_1$ is regarded as a virtual control that one would use to make $\dot{V}_1$ negative. This could be achieved, by setting $\boldsymbol{\nu}_1$ equal to $\mathbf{J}_1^\top \dot{\boldsymbol{\eta}}_{1,d} - k_e \mathbf{M}_1^{-1}\mathbf{e}$, for some

positive constant k_e. To accomplish this, we introduce the error variable

$$\mathbf{z}_1 = \boldsymbol{\nu}_1 - \mathbf{J}_1^\top \dot{\boldsymbol{\eta}}_{1,d} + k_e \mathbf{M}_1^{-1} \mathbf{e} \tag{3.9}$$

that we would like to drive to zero and re-write (3.8) as

$$\dot{V}_1 = -\mathbf{e}^\top k_e \mathbf{M}_1^{-1} \mathbf{e} + \mathbf{e}^\top \mathbf{z}_1 \tag{3.10}$$

3. Backstepping for $\mathbf{z}_1$: After straightforward algebraic manipulations, the dynamic equation of the error $\mathbf{z}_1$ can be written as

$$\mathbf{M}_1 \dot{\mathbf{z}}_1 = \mathbf{S}(\mathbf{M}_1 \mathbf{z}_1) + \boldsymbol{\Gamma}(\cdot) + g_1 u_1 + h(\cdot) \tag{3.11}$$

where

$$\boldsymbol{\Gamma} \triangleq \mathbf{S}(\mathbf{M}_1 \mathbf{J}_1^\top \dot{\boldsymbol{\eta}}_{1,d}) - \mathbf{M}_1 \mathbf{S}(\mathbf{J}_1^\top \dot{\boldsymbol{\eta}}_{1,d})$$

$$h = f_1 - \mathbf{M}_1 \mathbf{J}_1^\top \ddot{\boldsymbol{\eta}}_{1,d} + k_e \mathbf{z}_1 - k_e^2 \mathbf{M}_1^{-1} \mathbf{e}$$

It turns out that it will not always be possible to drive $\mathbf{z}_1$ to zero. We need to explore the coupling of the translation dynamics with the rotational inputs. To this effect, we will drive $\mathbf{z}_1$ to a constant design vector $\boldsymbol{\delta} \in \mathbb{R}^3$. To achieve this, we define $\boldsymbol{\varphi} \triangleq \mathbf{z}_1 - \boldsymbol{\delta}$ as new error variable that will be driven to zero and consider the augmented control-Lyapunov function

$$V_2 = V_1 + \frac{1}{2} \boldsymbol{\varphi}^\top \mathbf{M}_1^2 \boldsymbol{\varphi} \tag{3.12}$$

44

The time derivative of V_2 can be written as

$$\dot{V}_2 = -k_e \mathbf{e}^\top \mathbf{M}_1^{-1}\mathbf{e} + \mathbf{e}^\top\boldsymbol{\delta} + \boldsymbol{\varphi}^\top\left(\mathbf{M}_1\mathbf{B}(\cdot)\boldsymbol{\zeta} + \mathbf{M}_1 h(\cdot) + \mathbf{e}\right) \tag{3.13}$$

where

$$\mathbf{B} \triangleq \begin{bmatrix} g_1 & \mathbf{S}(\mathbf{M}_1\boldsymbol{\delta}) + \boldsymbol{\Gamma} \end{bmatrix} \tag{3.14}$$

$$\boldsymbol{\zeta} \triangleq \mathrm{col}(u_1, \boldsymbol{\nu}_2) \in \mathbb{R}^4 \tag{3.15}$$

It can be shown [3] that $\mathbf{B}$ can always be made full-rank by choosing suitable $\boldsymbol{\delta}$. One can now regard $\boldsymbol{\zeta}$ as a virtual control (actually its first component is already a "real" control) that one would like to use to make $\dot{V}_2$ negative. This could be achieved by setting $\boldsymbol{\zeta}$ equal to

$$\boldsymbol{\alpha} \triangleq \mathbf{B}^\top\left(\mathbf{B}\mathbf{B}^\top\right)^{-1}\left[-h - \mathbf{M}_1^{-1}\mathbf{e} - \mathbf{M}_1^{-1}\mathbf{K}_\varphi\boldsymbol{\varphi}\right] \tag{3.16}$$

where $\mathbf{K}_\varphi \in \mathbb{R}^{3\times3}$ is a symmetric positive definite matrix. To accomplish this we set u_1 to be equal to the first entry of $\boldsymbol{\alpha}$,

$$u_1 = \begin{bmatrix} 1 & 0_{1\times3} \end{bmatrix} \boldsymbol{\alpha} \tag{3.17}$$

and introduce the error variable

$$\mathbf{z}_2 \triangleq \boldsymbol{\nu}_2 - \begin{bmatrix} 0_{3\times1} & \mathbf{I}_3 \end{bmatrix} \boldsymbol{\alpha} \tag{3.18}$$

that one would like to set to zero. Now, (3.13) can be rewritten with u_1 given

45

by (3.17) as

$$\dot{V}_2 = -k_e \mathbf{e}^\top \mathbf{M}_1^{-1} \mathbf{e} + \mathbf{e}^\top \boldsymbol{\delta} - \boldsymbol{\varphi}^\top \mathbf{K}_\varphi \boldsymbol{\varphi} + -\boldsymbol{\varphi}^\top \mathbf{M}_1 \left[\mathbf{S}(\mathbf{M}_1 \boldsymbol{\delta}) + \boldsymbol{\Gamma} \right] \mathbf{z}_2 \qquad (3.19)$$

4. Backstepping for $\mathbf{z}_2$: Now consider a thrid control Lyapunov function given by

$$V_3 \triangleq V_2 + \frac{1}{2} \mathbf{z}_2^\top \mathbf{M}_2 \mathbf{z}_2 \qquad (3.20)$$

Computing its time derivative, one obtains

$$\dot{V}_3 = -k_e \mathbf{e}^\top \mathbf{M}_1^{-1} \mathbf{e} + \mathbf{e}^\top \boldsymbol{\delta} - \boldsymbol{\varphi}^\top \mathbf{K}_\varphi \boldsymbol{\varphi} + \mathbf{z}_2^\top (\mathbf{G}_2 \mathbf{u}_2 + \boldsymbol{\beta}) \qquad (3.21)$$

where

$$\boldsymbol{\beta} = -\mathbf{S}(\boldsymbol{\nu}_1)\mathbf{M}_1\boldsymbol{\nu}_1 - \mathbf{S}(\boldsymbol{\nu}_2)\mathbf{M}_2\boldsymbol{\nu}_2 + f_2 - \begin{bmatrix} 1 & 0_{1\times 3} \end{bmatrix} \dot{\boldsymbol{\alpha}} + \left(\boldsymbol{\Gamma}^\top - \mathbf{S}(\mathbf{M}_1 \boldsymbol{\delta}) \right) \mathbf{M}_1 \boldsymbol{\varphi}$$

If $\mathbf{u}_2$ is chosen as

$$\mathbf{u}_2 = -\mathbf{G}_2^{-1} \boldsymbol{\beta} - \mathbf{K}_{z_2} \mathbf{z}_2 \qquad (3.22)$$

where $\mathbf{K}_{z_2} \in \mathbb{R}^{3\times 3}$ is a symmetric positive definite matrix, the time derivative of V_3 becomes

$$\dot{V}_3 = -k_e \mathbf{e}^\top \mathbf{M}_1^{-1} \mathbf{e} + \mathbf{e}^\top \boldsymbol{\delta} - \boldsymbol{\varphi}^\top \mathbf{K}_\varphi \boldsymbol{\varphi} - \mathbf{z}_2^\top \mathbf{K}_{z_2} \mathbf{z}_2 \qquad (3.23)$$

Note that although $\dot{V}_3$ is not necessarily always negative, this will be sufficient to prove boundedness and convergence to a neighbourhood of the origin.

3.5   Conclusions

In this chapter we have reviewed some main results in nonlinear observer of under water vehicle, model based control design and the underactuated control of AUV. We will complete the literature review by adding at the beginning of every chapter an additional introduction that also contains some literature regarding the proposed design. We think this arrangement is more effective to keep the reading smooth.

Chapter 4

Controller Design

4.1 Introduction

In this chapter, first we will transform the Autonomous Underwater Vehicle (AUV) dynamic into Port Controlled Hamiltonian (PCH) form. Next, we will develop a general passivity-based control design for PCH. Based on this controller, an $\mathcal{L}_2$ disturbance attenuation controller is presented. Furthermore, the adaptive scheme of the developed $\mathcal{L}_2$ disturbance attenuation controller is elaborated. The three proposed control design are then simulated using the Modular Autonomous Robot for Environment Sampling (MARES) AUV model to evaluate their performance. We also present the analysis of stability in the presence of both parameter uncertainty and exogenous disturbance. In addition, we estimate the rate of convergence of the state dynamics to equilibrium. In the next chapter, we will address the case of the underactuated AUV within the PCH framework. The contribution of this chapter are

1. Representation of AUV dynamic in PCH formalism.

2. Extension of Shen's et.al work [91] in the design of an $\mathcal{L}_2$ disturbances attenuation controller in the PCH form.

3. Design of a passivity-based controller for AUV in PCH form.

4. Analysis of the AUV's PCH system stability

4.2 Port Controlled Hamiltonian of Autonomous Underwater Vehicle

The objective of this section is to represent AUV equations of motion in the PCH realization. To do this, we transform the second order Lagrangian system into Hamiltonian using Legendre transformation. The motivation stems from the fact that, constructing the dynamic equations in PCH offers many advantages, such as

1. The Hamiltonian function in many systems (not only mechanical ones) can act as a Lyapunov function or energy storage function crucial in dissipativity formalism.

2. Representing the nonlinear dynamics of a system in the PCH form provides a convenient structure that can be exploited when dealing with $\mathcal{L}_2$ disturbance rejection. This is a major benefit compared to the usual practice in solving disturbance rejection problems where it uses Hamilton Jacobi Issac (HJI) inequality which is recognized as a bottle neck in nonlinear optimization problems. Despite the fact that many studies already proposed several

approaches to overcome the difficulty of solving HJI in several special cases, finding a general solution is still an open problems. As will be seen in section 4.4. Using straight forward manipulation of PCH structure will avoid computing the HJI [102, 65].

We begin our formulation with the definition of PCH form and then show the transformation of the AUV dynamics given in the previous chapter, into PCH form. In general, the PCH form with dissipation can be described by

$$\dot{\mathbf{x}} = [\mathcal{J}(\mathbf{x}) - \mathcal{R}(\mathbf{x})]\,\nabla\mathcal{H}(\mathbf{x}) + \mathbf{G}(\mathbf{x})\mathbf{u}$$

$$\mathbf{y} = \mathbf{G}(\mathbf{x})^{\top}\nabla\mathcal{H}(\mathbf{x}) \tag{4.1}$$

where the state is $\mathbf{x}(t) \in \mathcal{D} \subseteq \mathbb{R}^n$, and $\mathcal{D}$ is an open set. The input is $\mathbf{u}(t) \in \mathcal{U} \subseteq \mathbb{R}^m$ and the output is $\mathbf{y}(t) \in \mathcal{Y} \subseteq \mathbb{R}^l$. The Hamiltonian function is given by $\mathcal{H} : \mathcal{D} \to \mathbb{R}$. The function $\mathcal{J}(\mathbf{x}) = -\mathcal{J}^{\top}(\mathbf{x})$ an antisymmetric interconnection matrix, and the damping matrix $\mathcal{R}(\mathbf{x}) : \mathcal{D} \to \mathbb{S}^n$, are both semi positive definite in $\mathcal{D}$, i.e. $\mathcal{R}(\mathbf{x}) \geq 0, \forall \mathbf{x} \in \mathcal{D}$. It is assumed also that the function $[\mathcal{J}(\mathbf{x}) - \mathcal{R}(\mathbf{x})]\,\nabla\mathcal{H}(\mathbf{x})$ is Lipschitz continuous in $\mathcal{D}$. $\mathbf{G} : \mathcal{D} \to \mathbb{R}^{m \times n}$ is the input affine matrix.

Recall from the previous chapter, eq. (2.6), that ,

$$\dot{\boldsymbol{\nu}} = \mathbf{M}^{-1}\left[\boldsymbol{\tau} - g(\boldsymbol{\eta}) - (\mathbf{C}(\boldsymbol{\nu}) + \mathbf{D}(\boldsymbol{\nu}))\,\boldsymbol{\nu} + \mathbf{J}^{-1}(\boldsymbol{\eta})\mathbf{b}\right]$$

$$\dot{\boldsymbol{\nu}} = \mathbf{M}^{-1}\left[\boldsymbol{\tau} - g(\boldsymbol{\eta}) - \bar{\mathbf{D}}(\boldsymbol{\nu})\boldsymbol{\nu} + \mathbf{J}^{-1}(\boldsymbol{\eta})\mathbf{b}\right] \tag{4.2}$$

$$\dot{\boldsymbol{\eta}} = \mathbf{J}(\boldsymbol{\eta}) \tag{4.3}$$

Let $\mathcal{H}$ be the Hamiltonian and $\mathbf{p}$ the momentum of the AUV, such that $\mathcal{H} = \frac{1}{2}\boldsymbol{\nu}^\top \mathbf{M}\boldsymbol{\nu}$, $\mathbf{p} \equiv \mathbf{M}\boldsymbol{\nu}$ and $\mathbf{q} \equiv \boldsymbol{\eta}$. The dynamics of the system can be rewritten as a function of $\mathcal{H}$ and $\mathbf{p}$ as follows

$$\frac{\partial \mathcal{H}}{\partial \mathbf{q}} = 0_{1\times 6}$$

$$\frac{\partial \mathcal{H}}{\partial \mathbf{p}} = \boldsymbol{\nu}^\top$$

$$\nabla \mathcal{H}(\mathbf{x}) = \left[\frac{\partial \mathcal{H}}{\partial \mathbf{q}} \frac{\partial \mathcal{H}}{\partial \mathbf{p}} \right]^\top$$

Where $\mathbf{x} = \left[\boldsymbol{\eta}^\top \mathbf{p}^\top \right]^\top$ is the new state vector. The AUV equations of motion can be transformed in the following PCH form

$$\begin{bmatrix} \dot{\boldsymbol{\eta}} \\ \dot{\mathbf{p}} \end{bmatrix} = \begin{bmatrix} 0 & \mathbf{J} \\ -\mathbf{J}^\top & -\bar{\mathbf{D}} \end{bmatrix} \nabla \mathcal{H}(\mathbf{x}) + \begin{bmatrix} 0 \\ \mathbf{I} \end{bmatrix} \left[\boldsymbol{\tau} - g(\boldsymbol{\eta}) + \mathbf{J}^{-1}(\boldsymbol{\eta})\mathbf{b} \right]$$

$$\mathcal{J}(\mathbf{x}) \equiv \begin{bmatrix} 0 & \mathbf{J} \\ -\mathbf{J}^\top & 0 \end{bmatrix}$$

$$\mathcal{R}(\mathbf{x}) \equiv \begin{bmatrix} 0 & 0 \\ 0 & \bar{\mathbf{D}} \end{bmatrix}$$

$$\mathbf{G} = \begin{bmatrix} 0 \\ \mathbf{I} \end{bmatrix} \tag{4.4}$$

with $\mathbf{u} = \boldsymbol{\tau}$ and slowly varying disturbance $\mathbf{b}$, which represents the lumped term from other ocean current and other external non-control forces. In the next section, we will develop the stabilizing controller of the AUV's PCH system (4.4). The essence of our contribution in the control design is the idea that the design

of an $\mathcal{L}_2$ disturbance rejection controller can be constructed as an additional term into the stabilizing controller that shapes the Hamiltonian.

4.3   Stabilizing Controller Through Reshaping of The Hamiltonian

The design of the proposed stabilizing controller exploits the advantages of having the system described in PCH structure. In addition, the approach can be seen as a passivation of the open loop PCH system. Indeed, the interconnection and the damping matrix functions of the open loop system is shaped to preserve the PCH structure of the closed loop system. Moreover, passivity-based control design for PCH systems is extremely appealing for the control action has a clear *physical* energy interpretation which can considerably simplify the controller's implementation.

To proceed with the formulation of the stabilizing controller [31], consider the PCH system given by (4.1) and let $\phi : \mathcal{D} \to \mathcal{U}$ and define $\mathbf{u}(t) = \phi(\mathbf{x}(t)), t \geq 0$, such that the closed loop system has the form

$$\dot{\mathbf{x}} = [\mathcal{J}(\mathbf{x}) - \mathcal{R}(\mathbf{x})] \nabla \mathcal{H}(\mathbf{x}) + \mathbf{G}(\mathbf{x})\phi(\mathbf{x}(t)$$

Theorem 4.1 states that under proper selection of $\phi(\mathbf{x})$, the closed loop system can be rewritten in the following PCH form

$$\dot{\mathbf{x}} = [\mathcal{J}_s(\mathbf{x}) - \mathcal{R}_s(\mathbf{x})] \nabla \mathcal{H}_s(\mathbf{x}) \tag{4.5}$$

where $\mathcal{H}_s : \mathcal{D} \to \mathcal{U}$ is a *shaped Hamiltonian function* for the closed loop system (4.5), $\mathcal{J}_s : \mathcal{D} \to \mathbb{R}^{n \times n}$ is a shaped interconnection matrix function for the closed loop system with $\mathcal{J}_s(\mathbf{x}) = -\mathcal{J}_s^\top(\mathbf{x})$, and $\mathcal{R}_s(\mathbf{x}) : \mathcal{D} \to \mathbb{S}^n$ is a shaped dissipation matrix function for the closed loop system and satisfies $\mathcal{R}_s(\mathbf{x}) \geq 0, x \in \mathcal{D}$.

Theorem 4.1. *Consider the nonlinear PCH given by (4.1). Assume there exists a function $\phi : \mathcal{D} \to \mathcal{U}, \mathcal{H}_s, \mathcal{H}_c : \mathcal{D} \to \mathbb{R}, \mathcal{J}_s, \mathcal{J}_a : \mathcal{D} \to \mathbb{R}^{n \times n}, \mathcal{R}_s, \mathcal{R}_a : \mathcal{D} \to \mathbb{R}^{n \times n}$, such that $\mathcal{H}_s(\mathbf{x}) = \mathcal{H}(\mathbf{x}) + \mathcal{H}_c(\mathbf{x})$ is continuously differentiable, $\mathcal{J}_s = \mathcal{J}_a + \mathcal{J} = -\mathcal{J}_s^\top, \mathcal{R}_s(\mathbf{x}) = \mathcal{R}(\mathbf{x}) + \mathcal{R}_a(\mathbf{x}), \mathcal{R}_s = \mathcal{R}_s^\top \geq 0, \mathbf{x} \in \mathcal{D}$ and let the equilibrium solution $\mathbf{x}(t) \equiv \mathbf{x}_e$ of the closed loop system eq (4.5) and*

$$\frac{\partial \mathcal{H}_c}{\partial \mathbf{x}_e} = -\frac{\partial \mathcal{H}}{\partial \mathbf{x}_e} \tag{4.6}$$

$$\frac{\partial^2 \mathcal{H}_c}{\partial^2 \mathbf{x}_e} > -\frac{\partial^2 \mathcal{H}}{\partial^2 \mathbf{x}_e} \tag{4.7}$$

$$[\mathcal{J}_s(\mathbf{x}) - \mathcal{R}_s(\mathbf{x})] \nabla \mathcal{H}_c(\mathbf{x}) = -[\mathcal{J}_a(\mathbf{x}) - \mathcal{R}_a(\mathbf{x})] \nabla \mathcal{H}(\mathbf{x})$$

$$+ \mathbf{G}(\mathbf{x})\phi(\mathbf{x}) \tag{4.8}$$

Then the equilibrium point $\mathbf{x}_e$ of closed loop system (4.5) is Lyapunov stable. If in addition, $\mathcal{D}_c \subseteq \mathcal{D}$ is compact positively invariant set with respect to (4.5) and the largest invariant set contained in $\mathcal{N} \triangleq \{\mathbf{x} \in \mathcal{D}_c : (\nabla \mathcal{H}_s)^\top \mathcal{R}_s(\mathbf{x})\nabla \mathcal{H}_s = 0\}$ is $\mathcal{M} = \mathbf{x}_e$, then $\mathbf{x}_e$ is locally asymptotically stable and $\mathcal{D}_c$ is a subset of the domain of attraction of eq (4.5).

Proof. Condition (4.8) implies that with feedback controller $\mathbf{u}(t) = \phi(\mathbf{x}(t))$ the closed loop system has a Hamiltonian structure given by (4.5). Furthermore, it follows from (4.6) and (4.7) that the energy function $\mathcal{H}_s$ has a local minimum at $\mathbf{x} = \mathbf{x}_e$. Hence, $\mathbf{x} = \mathbf{x}_e$ is an equilibrium point of the closed loop system. Next, consider the Lyapunov function candidate for the closed loop system (4.5) given by $V(\mathbf{x}) = \mathcal{H}_s(\mathbf{x}) - \mathcal{H}_s(\mathbf{x}_e)$. Now the corresponding Lyapunov derivative of $V(\mathbf{x})$

along the closed loop state trajectories $\mathbf{x}(t), t \geq 0$ is given by

$$\dot{V}(\mathbf{x}) = \dot{\mathcal{H}}_s = -\nabla \mathcal{H}_s^\top \mathcal{R}_s \nabla \mathcal{H}_s \leq 0, t \geq 0 \tag{4.9}$$

Thus, it follows from Lyapunov stability theorem, that the solution $\mathbf{x} = \mathbf{x}_e$, is Lyapunov stable. Asymptotic stability of the closed loop system follows immediately from *LaSalle's invariant sets principle* [42]. □

Remark 4.1. Using simple manipulation, one can see that the matching condition in (4.8), is equivalent to (4.5).

4.4 $\mathcal{L}_2$ Disturbance Attenuation

In the literature, several studies addressed $\mathcal{L}_2$ disturbance attenuation of PCH systems, (see for eaxmple [29, 90, 91, 103, 57]). The industrial application of the mentioned technique has been in power systems, [90, 91, 98, 57] and nuclear reactors [18, 19]. The technique presented in this chapter is an extension of [91]. The approach target a relaxation of $\mathbf{G}(\mathbf{x})$ selection by allowing the disturbance to have different input gain matrix $\mathbf{G}_2$. Such relaxation has been considered in previous work [57] where the derivation was for adaptive control case. In the present case, model (4.1) is modified to include the effect of an additive disturbance as follows

$$\dot{\mathbf{x}} = [\mathcal{J}(\mathbf{x}) - \mathcal{R}(\mathbf{x})] \nabla \mathcal{H}(\mathbf{x}) + \mathbf{G}_1(\mathbf{x})\mathbf{u} + \mathbf{G}_2(\mathbf{x})\mathbf{w} \tag{4.10}$$

where $\mathbf{w} \in \mathbb{R}^m$ is a bounded unknown disturbance such that the state trajectory $\mathbf{x}(t)$ remains in $\mathcal{D}$ for any initial state $\mathbf{x}(0) \in \mathcal{D}$. The $\mathcal{L}_2$ disturbance attenuation assumes a

- given desired equilibrium point $\mathbf{x}_e \in \mathcal{D}$,

- given penalty signal $\mathbf{z} = q(\mathbf{x})$, where $q(\mathbf{x}_e) = 0$ and

- given disturbance attenuation level γ.

The objective is to find a state feedback control law $\mathbf{u} = \phi(\mathbf{x})$ and a positive definite storage function $V(\mathbf{x})$ with respect to the equilibrium state $\mathbf{x}_e$, such that for the closed loop configuration of (4.10) under a state feedback control law, the γ-dissipation inequality given by

$$\dot{V}(\mathbf{x}) + \mathcal{Q}(\mathbf{x}) \leq \frac{1}{2} \left(\gamma^2 \|\mathbf{w}\|^2 - \|\mathbf{z}\|^2 \right) \tag{4.11}$$

holds along all trajectories within $\mathcal{D}$, where $\mathcal{Q}(\mathbf{x}), \mathcal{Q}(\mathbf{x}_e) \equiv 0$ is a non-negative definite function. As pointed out in [11], the γ-dissipation inequality (4.11) guaranties the following performances

P 1. $\mathcal{L}_2$ gain from the disturbance $\mathbf{w}$ to the penalty signals $\mathbf{z}$ is less than the given level, γ;

P 2. When $\mathbf{w} = 0$, $\mathbf{x}_e$ is a Lyapunov stable equilibrium of unperturbed systems in $\mathcal{D}$. Furthermore, $\mathbf{x}_e$ asymptotically stable provided that

$$\mathcal{Q}(\mathbf{x}) + \frac{1}{2} \|q(\mathbf{x})\|^2 = 0 \Rightarrow \mathbf{x} = \mathbf{x}_e; \tag{4.12}$$

P 3. If $\mathbf{w}$ is square integrable then $\mathbf{x}$ is uniformly bounded.

55

For the perturbed system (4.10) and according to Theorem 4.1, there exists a feedback law $\mathbf{u} = \phi_1(\mathbf{x})$ which preserves the Hamiltonian structure of the closed loop system. Using Theorem 4.1, the best approach is to incorporate an additional term into $\mathbf{u} = \phi_1(\mathbf{x})$ to provide the controller with the means to attenuate the unknown disturbance. Therefore, let the penalty signal be described as follows

$$\mathbf{z} = h(\mathbf{x})\mathbf{G}_1^\top(\mathbf{x})\nabla\mathcal{H}(\mathbf{x}) \tag{4.13}$$

where, $h(\mathbf{x})$ is a weighting matrix such that $h(\mathbf{x}_e) \equiv 0$. In such case the $\mathcal{L}_2$ disturbance attenuation can be achieved by injecting new damping term into (4.10), i.e. under a proper selection of a feedback law, the Hamiltonian $\mathcal{H}_s$ can serve as the storage function for the closed loop system.

Theorem 4.2. *Consider the system (4.10). For any given $\gamma > 0$, the $\mathcal{L}_2$ disturbance attenuation objective can be achieved using the following feedback control law*

$$\mathbf{u} = \phi_1(\mathbf{x}) + \phi_2(\mathbf{x}) \tag{4.14}$$

$$\phi_2(\mathbf{x}) = -\frac{1}{2}\left[\frac{1}{\gamma^2}\mathbf{I} + h^\top(\mathbf{x})h(\mathbf{x})\right]\mathbf{G}_1^\top(\mathbf{x})\nabla\mathcal{H}_s(\mathbf{x}) \tag{4.15}$$

where $\phi_1(\mathbf{x})$ satisfies Theorem 4.1

Before starting the proof, we state the following property

Property 4.1 (Vector inner product inequality). For given a a and $b \in \mathbb{R}^n$, the following inequalities apply

$$\mathbf{a}^\top\mathbf{b} = -\frac{1}{2}\left((\mathbf{a} - \mathbf{b})^\top(\mathbf{a} - \mathbf{b}) - (\mathbf{a}^\top\mathbf{a} + \mathbf{b}^\top\mathbf{b})\right)$$

$$\mathbf{a}^\top\mathbf{b} \leq \frac{1}{2}\left(\mathbf{a}^\top\mathbf{a} + \mathbf{b}^\top\mathbf{b}\right)$$

Proof. Note that under the feedback control (4.14), the closed loop system with the modified Hamiltonian function $\mathcal{H}_s$ can be represented by

$$\dot{\mathbf{x}} = [\mathcal{J}_s(\mathbf{x}) - \mathcal{R}_s(\mathbf{x})]\, \nabla\mathcal{H}_s + \mathbf{G}_1(\mathbf{x})\phi_2(\mathbf{x}) + \mathbf{G}_2(\mathbf{x})\mathbf{w} \tag{4.16}$$

$$\mathbf{z} = h(\mathbf{x})\mathbf{G}_1(\mathbf{x})\nabla\mathcal{H}(\mathbf{x}) \tag{4.17}$$

and

$$\dot{\mathcal{H}}_s = -(\nabla\mathcal{H}_s(\mathbf{x}))^\top \mathcal{R}_s \nabla\mathcal{H}_s(\mathbf{x}) + (\nabla\mathcal{H}_s(\mathbf{x}))^\top \mathbf{G}_1(\mathbf{x})\phi_2(\mathbf{x})$$
$$+ (\nabla\mathcal{H}_s(\mathbf{x}))^\top \mathbf{G}_2(\mathbf{x})\mathbf{w} \tag{4.18}$$

Next, we select $\phi_2(\mathbf{x})$ as follows

$$\phi_2(\mathbf{x}) \equiv \mathbf{K}_1(\mathbf{x})\mathbf{G}_1^\top(\mathbf{x})\nabla\mathcal{H}_s(\mathbf{x}) \tag{4.19}$$

$$\mathbf{K}_1(\mathbf{x}) = -\frac{1}{2}\left[\frac{1}{\gamma^2}\mathbf{I} + h^\top(\mathbf{x})h(\mathbf{x})\right] \tag{4.20}$$

Using property 4.1 for last the term of (4.18), we obtain

$$\mathbf{a} \equiv \frac{1}{\gamma}\mathbf{G}_2^\top(\mathbf{x})\nabla\mathcal{H}_s(\mathbf{x})$$

$$\mathbf{b} \equiv \gamma\mathbf{w}$$

$$\mathbf{a}^\top\mathbf{a} = \frac{1}{\gamma^2}(\nabla\mathcal{H}_s(\mathbf{x}))^\top \mathbf{G}_2(\mathbf{x})\mathbf{G}_2^\top(\mathbf{x})\nabla\mathcal{H}_s(\mathbf{x})$$

$$\mathbf{b}^\top\mathbf{b} = \gamma^2\mathbf{w}^\top\mathbf{w}$$

Finally, $\dot{\mathcal{H}}_s$ is obtained as follows

$$\dot{\mathcal{H}}_s \leq -(\nabla\mathcal{H}_s(\mathbf{x}))^\top (\mathcal{R}_s^*) \nabla\mathcal{H}_s(\mathbf{x}) + \gamma^2 \mathbf{w}^\top \mathbf{w}$$

$$\mathcal{R}_s^* \equiv \mathcal{R}_s^{**} + \frac{1}{2}\mathbf{G}_1(\mathbf{x})h^\top(\mathbf{x})h(\mathbf{x})\mathbf{G}_1^\top \qquad (4.21)$$

$$\mathcal{R}_s^{**} \equiv \mathcal{R}_s + \frac{1}{2\gamma^2}\left(\mathbf{G}_1(\mathbf{x})\mathbf{G}_1^\top(\mathbf{x}) - \mathbf{G}_2(\mathbf{x})\mathbf{G}_2^\top(\mathbf{x})\right)$$

Note that $(\nabla\mathcal{H}_s^\top \left(\mathbf{G}_1 h^\top h \mathbf{G}_1^\top\right)(\nabla\mathcal{H}_s) = \mathbf{z}^\top \mathbf{z}$ and hence

$$\dot{\mathcal{H}}_s \leq -(\nabla\mathcal{H}_s(\mathbf{x}))^\top \mathcal{R}_s^{**} \nabla\mathcal{H}_s(\mathbf{x}) + \frac{1}{2}\left[\gamma^2\|\mathbf{w}\|^2 - \|\mathbf{z}\|^2\right]$$

$$\dot{\mathcal{H}}_s + (\nabla\mathcal{H}_s(\mathbf{x}))^\top \mathcal{R}_s^{**} \nabla\mathcal{H}_s(\mathbf{x}) \leq \frac{1}{2}\left[\gamma^2\|\mathbf{w}\|^2 - \|\mathbf{z}\|^2\right]$$

If $\mathcal{R}_s$ can be selected big enough such that $\mathcal{R}_s^{**} \geq 0$, $\dot{\mathcal{H}}_s$ then satisfies the γ-dissipation inequality (4.11),

$$\dot{\mathcal{H}}_s + \mathcal{Q}(\mathbf{x}) \leq \frac{1}{2}\left(\gamma^2\|\mathbf{w}\|^2 - \|\mathbf{z}\|^2\right) \qquad (4.22)$$

$\square$

Comparing equation (4.22) with (4.11), one can see that the shaped Hamiltonian function $\mathcal{H}_s$ acts as a storage function for closed loop system.

Remark 4.2. The approach of shaping Hamiltonian is composed of two stages. In the first stage we calculate the feedback $\phi_1(\mathbf{x})$ which shapes the energy and adds damping such that the unforced system when $\mathbf{w} = 0$ is stable around the equilibrium point $\mathbf{x}_e$. In the second stage, we use Theorem 4.2 in order to render the closed loop system γ-dissipative by injecting additional damping as follows

$$\mathcal{R}_s \to \mathcal{R}_s^* \qquad (4.23)$$

58

which defines the additional feedback $\phi_2(\mathbf{x})$. In addition, $\phi_2(\mathbf{x})$ has *lie derivative* of Lyapunov function against G, $(L_G V)$, i.e. it is of the form $k(\mathbf{x})L_G \mathcal{H}_s$. The relation between the disturbance attenuation level γ and the gain $k(\mathbf{x})$ is given in Theorem 4.2.

Remark 4.3. The closed loop system with controller (4.14) ensures both the performance **P 1,P 3** and the stability of the equilibrium point. In order to achieve asymptotic stability, the weighting matrix $h(\mathbf{x})$,the structure of the matrix $\mathcal{R}_s$ and the shaped Hamiltonian $\mathcal{H}_s$ should be selected such that (4.12) is satisfied, i.e.

$$(\nabla \mathbf{H}_s(\mathbf{x}))^\top \mathcal{R}_s^* (\nabla \mathbf{H}_s(\mathbf{x})) = 0$$
$$\Rightarrow \mathbf{x} = \mathbf{x}_e,$$

given that $\mathcal{H}_s$ has a strictly isolated minimum at $\mathbf{x}_e$. This technical assumption is locally satisfied if $\mathcal{R}_s^*$ in (4.21) has a full rank which in turn, depends on the degree of freedom available for damping injection and disturbance attenuation performance. This is essentially determined through the rank of $\mathbf{G}_1(\mathbf{x})$,$\mathbf{G}_2(\mathbf{x})$ and $h(\mathbf{x})$.

4.5   Adaptive $\mathcal{L}_2$ Disturbance Attenuation

This section present the adaptive control version of $\mathcal{L}_2$ disturbance attenuation developed in the previous section. We assume that the PCH system can have some parameter uncertainties. Our work is an extension of [57]. We relax $\mathbf{G}(\mathbf{x})$ restriction to allow the input and the disturbance matrix to have some uncertainties, i.e. $\mathbf{G}_i(\mathbf{x}, \epsilon)$. We will start with the model given in eq. (4.1) and add

disturbance and parameter uncertainties,

$$\dot{\mathbf{x}} = \left[\mathcal{J}(\mathbf{x}, \epsilon) - \mathcal{R}(\mathbf{x}, \epsilon)\right] \nabla \mathcal{H}(\mathbf{x}, \epsilon) + \mathbf{G}_1(\mathbf{x}, \epsilon)\mathbf{u} + \mathbf{G}_2(\mathbf{x}, \epsilon)\mathbf{w} \qquad (4.24)$$

$\mathbf{u}$ consists of two part similar to the last section, $\phi_1(\mathbf{x})$ for stabilizing and $\phi_2(\mathbf{x})$ for disturbance attenuation. Since the parameter uncertainty ϵ is present, to stabilize the system in (4.24), ϕ_1 has to be function of $\mathbf{x}$ and ϵ. This is impossible due to the fact that the unknown perturbation ϵ introduces a term $\Delta \phi_1(\mathbf{x}, \epsilon)$ that should be considered in the closed loop analysis. Using the matching condition developed in sec 4.3,the controlled system will be

$$\dot{\mathbf{x}} = \left[\mathcal{J}_s(\mathbf{x}, \epsilon) - \mathcal{R}_s(\mathbf{x}, \epsilon)\right] \nabla \mathcal{H}_s(\mathbf{x}, \epsilon) - \mathbf{G}_1(\mathbf{x}, \epsilon)\Delta \phi_1(\mathbf{x}, \epsilon)$$
$$+ \mathbf{G}_1(\mathbf{x}, \epsilon)\phi_2(\mathbf{x}) + \mathbf{G}_2(\mathbf{x}, \epsilon)\mathbf{w} \qquad (4.25)$$

Furthermore, for simplicity reasons we also assume that $\nabla \mathcal{H}_s(\mathbf{x}, \epsilon)$ is separable, i.e.

$$\nabla \mathcal{H}_s(\mathbf{x}, \epsilon) \equiv \nabla \mathcal{H}_s(\mathbf{x}) + \Delta \mathcal{H}_s(\mathbf{x}, \epsilon)$$

The unknown parameter θ is a linear function of the perturbations ϵ. Both disturbance attenuation control input ϕ_2 and the unknown parameter estimate $\hat{\theta}$ are assumed to satisfy the following equalities

$$\phi_2(\mathbf{x}) = \mathbf{K}_1(\mathbf{x})\nabla \mathcal{H}_s(\mathbf{x}) + \mathbf{L}_1(\mathbf{x})\hat{\theta} \qquad (4.26)$$
$$\dot{\hat{\theta}} = \mathbf{K}_2(\mathbf{x})\nabla \mathcal{H}_s(\mathbf{x}) \qquad (4.27)$$

Thus, we may note that $\phi_2(\mathbf{x})$ has an additional term related to unknown parameter estimate $\hat{\theta}$. This term is considered as the third stage of our controller design.

In the remaining of this chapter, we will omit $\mathbf{x}$ and ϵ from our notation and place small ϵ below any matrix or vector to indicate that it is a function of $\mathbf{x}$ and ϵ. Other matrices without small ϵ are function of $\mathbf{x}$. The $\mathbf{Q}$ matrix and the identity matrix $\mathbf{I}$ are both constant and independent of $\mathbf{x}$ and ϵ.

Theorem 4.3. *Consider the system* (4.25) *with the penalty signal* (4.13). *Assume that there exists a function* $\boldsymbol{\Phi}(\mathbf{x})$ *such that,*

$$[\mathcal{J}_{s,\epsilon} - \mathcal{R}_{s,\epsilon}]\,\Delta\mathcal{H}_{s,\epsilon} - \mathbf{G}_{1,\epsilon}\Delta\phi_{1,\epsilon} = \mathbf{G}_{1,\epsilon}\boldsymbol{\Phi}^{\top}\theta \qquad (4.28)$$

for all $\mathbf{x}$. *Then For any given* $\gamma > 0$ *and unknown bounded* ϵ, *the adaptive* $\mathcal{L}_2$ *disturbance attenuation can be achieved by the following control law*

$$\phi_2 = -\frac{1}{2}\left[\frac{1}{\gamma^2}\mathbf{I} + hh^{\top}\right]\mathbf{G}_1^{\top}\nabla\mathcal{H}_s - \boldsymbol{\Phi}^{\top}\hat{\theta}$$

$$\dot{\hat{\theta}} = \left(\mathbf{G}_1\boldsymbol{\Phi}^{\top}\mathbf{Q}\right)^{\top}\nabla\mathcal{H}_s$$

Proof. Using the assumption in (4.28), we can write (4.25) as

$$\dot{\mathbf{x}} = [\mathcal{J}_{s,\epsilon} - \mathcal{R}_{s,\epsilon}]\,\nabla\mathcal{H}_s + \mathbf{G}_{1,\epsilon}\boldsymbol{\Phi}^{\top}\theta + \mathbf{G}_{1,\epsilon}(\mathbf{K}_1\nabla\mathcal{H}_s + \mathbf{L}_1\hat{\theta}) + \mathbf{G}_{2,\epsilon}\mathbf{w}$$

$$\dot{\mathbf{x}} = [\mathcal{J}_{s,\epsilon} - \mathcal{R}_{s,\epsilon}]\,\nabla\mathcal{H}_s + \mathbf{G}_{1,\epsilon}\left(\boldsymbol{\Phi}^{\top}\theta + \mathbf{L}_1\hat{\theta}\right) + \mathbf{G}_{1,\epsilon}\mathbf{K}_1\nabla\mathcal{H}_s + \mathbf{G}_{2,\epsilon}\mathbf{w}$$

where,

$$\mathbf{K}_1 = -\frac{1}{2}\mathbf{k}_1\mathbf{G}_1^\top \tag{4.29}$$

$$\mathbf{k}_1 = \frac{1}{\gamma^2}\mathbf{I} + hh^\top \tag{4.30}$$

If we select $\mathbf{L}_1 = -\mathbf{\Phi}^\top$ then we obtain

$$\dot{\mathbf{x}} = [\mathcal{J}_{s,\epsilon} - \mathcal{R}_{s,\epsilon}]\nabla\mathcal{H}_s + \mathbf{G}_{1,\epsilon}\left(\mathbf{\Phi}^\top\tilde{\theta}\right) + \mathbf{G}_1\mathbf{K}_1\nabla\mathcal{H}_s + \mathbf{G}_{2,\epsilon}\mathbf{w}$$

At this stage, we define another *shaped Hamiltonian function* where we add a term of weighted quadratic unknown parameter estimation error as follows

$$\mathcal{H}_r = \mathcal{H}_s + \frac{1}{2}\tilde{\theta}^\top\mathbf{Q}^{-1}\tilde{\theta} \tag{4.31}$$

The partial derivative of $\mathcal{H}_r$ with respect to $\mathbf{x}$ and $\hat{\theta}$ is given by

$$\nabla\mathcal{H}_{r,x} \equiv \nabla\mathcal{H}_s \tag{4.32}$$

$$\nabla\mathcal{H}_{r,\hat{\theta}} = -\mathbf{Q}^{-1}\tilde{\theta} \tag{4.33}$$

Furthermore, we augment the system state $\mathbf{x}$ with the unknown parameter θ to have the augmented state $\mathcal{X}$ which obeys the following dynamic equation

$$\dot{\mathcal{X}} = \begin{bmatrix} \mathcal{J}_{s,\epsilon} - \mathcal{R}_{s,\epsilon} + \mathbf{G}_1\mathbf{K}_1 & -\mathbf{G}_1\mathbf{\Phi}^\top\mathbf{Q} \\ \mathbf{K}_2 & 0 \end{bmatrix}\nabla\mathcal{H}_r + \begin{bmatrix} \mathbf{G}_{2,\epsilon} \\ 0 \end{bmatrix}\mathbf{w} + \begin{bmatrix} \Delta\mathbf{G}_{1,\epsilon} \\ 0 \end{bmatrix}\mathbf{\Phi}^\top\tilde{\theta} \tag{4.34}$$

Where $\mathbf{G}_{1,\epsilon} = \mathbf{G}_1 + \Delta\mathbf{G}_{1,\epsilon}$. Examining the last term in the right hand side of eq. (4.34), we can see that $\mathbf{\Phi}^\top\tilde{\theta}$ is acting as a *fictitious additional disturbance* to the

system. For that reason, we redefine three terms as follows

$$\mathbf{G}_{3,\epsilon} \equiv \Delta\mathbf{G}_{1,\epsilon}$$

$$\mathbf{w}_2 \equiv \mathbf{\Phi}\tilde{\theta}$$

$$\mathbf{w}_1 \equiv \mathbf{w}$$

To preserve the anti-symmetric properties of the first matrix in (4.34), we select

$$\mathbf{K}_2 = \left(\mathbf{G}_1\mathbf{\Phi}^\top\mathbf{Q}\right)^\top$$

Let $\mathcal{G} = -\mathbf{G}_1\mathbf{\Phi}^\top\mathbf{Q}$, we rewrite (4.34) in more compact form as

$$\dot{\mathcal{X}} = \left(\begin{bmatrix} \mathcal{J}_{s,\epsilon} & \mathcal{G} \\ -\mathcal{G}^\top & 0 \end{bmatrix} - \begin{bmatrix} \mathcal{R}_{s,\epsilon} - \mathbf{G}_{1,\epsilon}\mathbf{K}_1 & 0 \\ 0 & 0 \end{bmatrix}\right)\nabla\mathcal{H}_r + \begin{bmatrix} \mathbf{G}_{2,\epsilon} \\ 0 \end{bmatrix}\mathbf{w}_1 + \begin{bmatrix} \mathbf{G}_{3,\epsilon} \\ 0 \end{bmatrix}\mathbf{w}_2$$

$$(4.35)$$

The time derivative of the shaped Hamiltonian $\dot{\mathcal{H}}_r$ is then evaluated along the trajectory. Deploying the anti-symmetric properties of the matrix in (4.35), the time derivative of the shaped Hamiltonian $\dot{\mathcal{H}}_r$ can be expressed as

$$\dot{\mathcal{H}}_r = -(\nabla\mathcal{H}_s)^\top\left(\mathcal{R}_s - \mathbf{G}_{1,\epsilon}\mathbf{K}_1\right)\nabla\mathcal{H}_s + (\nabla\mathcal{H}_s)^\top\mathbf{G}_{2,\epsilon}\mathbf{w}_1 + (\nabla\mathcal{H}_s)^\top\mathbf{G}_{3,\epsilon}\mathbf{w}_2 \quad (4.36)$$

Recall that from (4.29), $\mathbf{K}_1$ can be rewritten as follows

$$\mathbf{K}_1 \equiv -\frac{1}{2}\mathbf{k}_1\mathbf{G}_1^\top$$

$$\mathbf{K}_1 \equiv -\frac{1}{2}\mathbf{k}_1\mathbf{G}_{1,\epsilon}^\top - \mathbf{k}_1\Delta\mathbf{G}_{1,\epsilon}^\top$$

$$\mathbf{k}_1(\mathbf{x}) \equiv \left[\frac{1}{\gamma^2}\mathbf{I} + hh^\top\right]$$

Using property 4.1, it follows that

$$\dot{\mathcal{H}}_r \leq -(\nabla\mathcal{H}_s)^\top (\mathcal{R}_s^*) \nabla\mathcal{H}_s + \gamma^2\mathbf{w}_1^\top\mathbf{w}_1 + \gamma^2\mathbf{w}_2^\top\mathbf{w}_2$$

$$\mathcal{R}_s^* = \mathcal{R}_s^{**} + \frac{1}{2}\mathbf{G}_{1,\epsilon}hh^\top\mathbf{G}_{1,\epsilon}^\top$$

$$\mathcal{R}_s^{**} \equiv \mathcal{R}_{s,\epsilon} + \frac{1}{2\gamma^2}\left(\mathbf{G}_{1,\epsilon}\mathbf{G}_{1,\epsilon}^\top - \mathbf{G}_{2,\epsilon}\mathbf{G}_{2,\epsilon}^\top - \mathbf{G}_{3,\epsilon}\mathbf{G}_{3,\epsilon}^\top\right) + \boldsymbol{\mu}_\epsilon$$

$$\boldsymbol{\mu}_\epsilon \equiv -\frac{1}{2}\left(\mathbf{G}_{1,\epsilon}\mathbf{k}_1\Delta\mathbf{G}_{1,\epsilon}^\top\right)$$

Since $(\nabla\mathcal{H}_s)^\top \left(\mathbf{G}_{1,\epsilon}h^\top h\mathbf{G}_{1,\epsilon}^\top\right)(\nabla\mathcal{H}_s) = \mathbf{z}^\top\mathbf{z}$, we get

$$\dot{\mathcal{H}}_r + (\nabla\mathcal{H}_s)^\top\mathcal{R}_s^{**}\nabla\mathcal{H}_s \leq \frac{1}{2}\left[\gamma^2(\|\mathbf{w}_1\|^2 + \|\mathbf{w}_2\|^2) - \|\mathbf{z}\|^2\right]$$

□

Remark 4.4. As stated in [8], $\mathcal{J}$, $\mathcal{R}$, $\mathcal{H}$ and often $\mathbf{G}$ are functions of θ. Therefore, $\hat{\theta}$ is not required to converge to any particular equilibrium, but merely remains bounded. However, in many cases it is possible to establish also the global stability of the equilibrium $\{\mathbf{x}, \hat{\theta}\} = \{\mathbf{x}_d, \theta\}$ as can be shown in the next remark.

Remark 4.5. In case $\mathbf{w}_1 = 0$, the estimation errors of the unknown parameter $\hat{\theta}$ converge to zero. This is due to the fact that if the controlled system without exogenous disturbances and parameter uncertainties is asymptotically stable and

$\mathbf{x}_d$ is strictly isolated minimum of $\mathcal{H}_s$ with $\nabla \mathcal{H}_s|_{\mathbf{x}=\mathbf{x}_d} = 0$, then from the augmented equation (4.36) and *La Salle invariant set* theorem, we conclude that the largest invariant set is contained in

$$\mathcal{N} \triangleq \{\mathcal{X} \in \mathcal{D}_c : (\nabla \mathcal{H}_s)^\top \left(\mathcal{R}_s^- \mathbf{G}_{1,\epsilon} \mathbf{K}_1 \right) \nabla \mathcal{H}_s + (\nabla \mathcal{H}_s)^\top \mathbf{G}_{3,\epsilon} \mathbf{w}_2 = 0\} \tag{4.37}$$

which is equal to $\{\mathcal{X} \in \mathcal{D}_c : \mathbf{x} = \mathbf{x}_d\}$. In addition to that, if $\mathbf{G}_{1,\epsilon} \mathbf{\Phi}^\top$ is non singular, and using the fact that for every $\mathcal{X} \in \mathcal{N}$, $\dot{\mathbf{x}} = \mathbf{G}_{1,\epsilon} \mathbf{\Phi}^\top \tilde{\theta} = 0$, if and only if $\tilde{\theta} = 0$, then it follows that the largest invariant set contained in $\mathcal{N}$ is given by $\mathcal{M} = \{\mathbf{x}_d, \theta^*\}$.

Remark 4.6. From the matching condition (4.28), the adaptive scheme presented in this section is restricted to systems having the dimension of the unknown parameters θ equal to the number of the input variables.

The following example illustrates how the estimation error of the unknown parameter will converge to zero

Example 4.1. Consider the following second order system which already stabilized using ϕ_1, where $\Delta \phi_1 = 0$

$$\begin{bmatrix} x_1 \\ x_2 \end{bmatrix} = \begin{bmatrix} 0 & 1 \\ -1 & -1 \end{bmatrix} \begin{bmatrix} x_1 - (\epsilon_1 + \epsilon_2) \\ x_2 + \epsilon_1 \end{bmatrix} + \begin{bmatrix} 1 & 0 \\ 0 & 1 \end{bmatrix} \phi_2 \tag{4.38}$$

The corresponding Hamiltonian is given below

$$\mathcal{H}_s = \frac{1}{2} \left(x_1^2 + x_2^2 \right) - (\epsilon_1 + \epsilon_2) x_1 + \epsilon_1 x_2 \tag{4.39}$$

From the matching condition we have

$$\begin{bmatrix} 0 & 1 \\ -1 & -1 \end{bmatrix} \begin{bmatrix} -(\epsilon_1 + \epsilon_2) \\ \epsilon_1 \end{bmatrix} = \begin{bmatrix} 1 & 0 \\ 0 & 1 \end{bmatrix} \mathbf{\Phi}^\top \theta \qquad (4.40)$$

if we select $\theta = \begin{bmatrix} \epsilon_1 & \epsilon_2 \end{bmatrix}^\top$, then $\mathbf{\Phi}^\top$ is equals to the identity matrix and consequently the condition in remark 4.5 is satisfied. Since our purpose is just to show the convergence of the unknown parameter estimation errors, we select $\mathbf{K}_1 = 0$ for the simulation without the presence of exogenous disturbances. The simualtion results indicate that the nominal model has the origin as its asymptotic equilibrium point. By means of the state feedback $\phi_2 = -\mathbf{\Phi}^\top \hat{\theta}$, the unknown parameter vector converges to its true value and makes the system behaves like the nominal model. The effect of parameter uncertainties is cancelled by the feedback ϕ_2. The simulation results use $\epsilon_1 = 0.2, \epsilon_2 = 0.1, \mathbf{Q} = \mathbf{I}$ and $\mathbf{x}(0) = \begin{bmatrix} 1 & 1 \end{bmatrix}^\top$. Figure 4.1 hints that the estimations of the unknown parameter vector converges to its true value and the asymptotic stability behaviour of the nominal model is preserved as well.

(a) $\hat{\theta}$

(b) $\mathbf{x}$
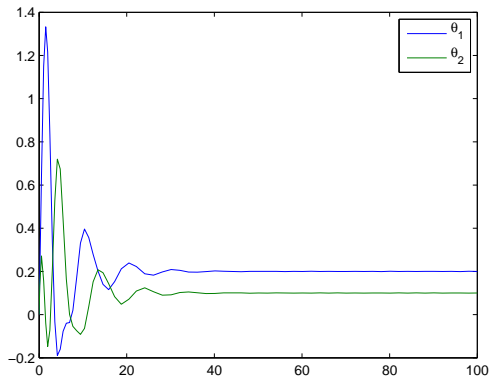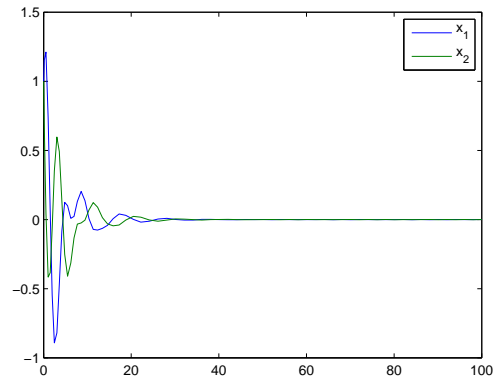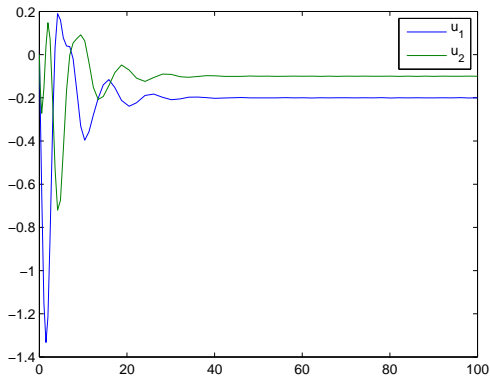
(c) ϕ_2

Figure 4.1: Simulation result of example 4.1

4.6 PCH Based Control Design for AUV

In this section, we apply the two steps of PCH-based control design to the AUV model. To obtain a general solution for a wider class of AUV, we ignore the issue related to force and torque allocation from the actuator. For instance, we do not take into account the problem of thruster nonlinear behaviour and whether the vehicle is fully-actuated or underactuated. Therefore, we assume that there is a sufficient actuator effort available to perform the control actions as needed. The underactuated AUV control design will be developed in the next chapter.

4.6.1 Stabilizing Controller: First Stage

For trajectory tracking purpose, we will apply theorem 4.1 for AUV dynamics. For the time being, we will ignore the exogenous disturbance and we will consider it in the next subsection. For trajectory tracking design, we define the equilibrium point $\mathbf{x}_d \equiv \left[\boldsymbol{\eta}_d^\top, 0 \right]$. Next, adapting the approach presented in [70], we select the *shaped Hamiltonian function* to be the combination of the kinetic energy and weighted quadratic trajectory tracking error as follows,

$$
\mathcal{H}_s = \frac{1}{2} \boldsymbol{\nu}^\top \mathbf{M} \boldsymbol{\nu} + \frac{1}{2} \tilde{\boldsymbol{\eta}}^\top \hat{\mathbf{Q}} \tilde{\boldsymbol{\eta}}
$$
$$
\mathcal{H}_s = \frac{1}{2} \mathbf{p}^\top \mathbf{M}^{-1} \mathbf{p} + \frac{1}{2} \tilde{\boldsymbol{\eta}}^\top \hat{\mathbf{Q}} \tilde{\boldsymbol{\eta}} \tag{4.41}
$$

, where $\tilde{\boldsymbol{\eta}} = \boldsymbol{\eta} - \boldsymbol{\eta}_d$. Next we select

$$\mathcal{J}_a = 0$$

$$\mathcal{R}_a = \begin{bmatrix} 0 & 0 \\ 0 & \mathbf{D}_a \end{bmatrix} \tag{4.42}$$

where $\mathbf{D}_a$ is an additional damping term. From (4.41), we have

$$\frac{\partial \mathcal{H}_s}{\partial \mathbf{p}} = \boldsymbol{\nu}^\top , \frac{\partial \mathcal{H}_c}{\partial \mathbf{p}} = 0$$
$$\frac{\partial \mathcal{H}_s}{\partial \boldsymbol{\eta}} = \tilde{\boldsymbol{\eta}}^\top \hat{\mathbf{Q}} , \frac{\partial \mathcal{H}_c}{\partial \boldsymbol{\eta}} = \tilde{\boldsymbol{\eta}}^\top \hat{\mathbf{Q}} \tag{4.43}$$

Using Theorem 4.1, the matching condition (considering the gravity and buoyancy term $g(\boldsymbol{\eta})$ as well) becomes

$$\mathbf{G}\phi(\mathbf{x}) = \mathbf{G}g(\boldsymbol{\eta}) + [\mathcal{J}_s(\mathbf{x}) - \mathcal{R}_s(\mathbf{x})] \nabla\mathcal{H}_c(\mathbf{x}) + [\mathcal{J}_a(\mathbf{x}) - \mathcal{R}_a(\mathbf{x})] \nabla\mathcal{H}(\mathbf{x})$$

$$\begin{bmatrix} 0 \\ \mathbf{I} \end{bmatrix} \phi(\mathbf{x}) = \begin{bmatrix} 0 \\ \mathbf{I} \end{bmatrix} g(\boldsymbol{\eta}) + \begin{bmatrix} 0 \\ -\mathbf{D}_a\boldsymbol{\nu} - \mathbf{J}^\top\hat{\mathbf{Q}}\boldsymbol{\eta} \end{bmatrix}$$

$$\phi(\mathbf{x}) = g(\boldsymbol{\eta}) - \mathbf{J}^\top\hat{\mathbf{Q}}\tilde{\boldsymbol{\eta}} - \mathbf{D}_a\boldsymbol{\nu}$$

$$\phi(\mathbf{x}) = g(\boldsymbol{\eta}) - \mathbf{K}\nabla\mathcal{H}_s \tag{4.44}$$

$$\mathbf{K} \equiv \begin{bmatrix} \mathbf{J}^\top & \mathbf{D}_a \end{bmatrix} \tag{4.45}$$

Up to here the Lyapunov stability condition is proven by invoking the theorem 4.1. Furthermore, To prove the asymptotic stability, the following conditions are required:

C 1. $\bar{\mathbf{D}} + \mathbf{D}_a = \mathbf{D}_s > 0$, i.e strictly positive definite. From antisymmetric proper-

ties of Coriolis (properties 2.2) and dissipativity properties of AUV drag (properties 2.3), $\mathbf{D}_a$ can be selected as semi-positive definite matrix and hence, different from [68], $\mathbf{D}_a$ doesn't have to cancel the nonlinearity in the Coriolis and AUV's drag. Thus, such design gives more robust closed loop response, since the cancellation of Coriolis and drag in real application may require high amplitude of actuator forces and drive the closed loop unstable in case of high uncertainties or dynamic mismatch.

C 2. $\hat{\mathbf{Q}}$ is selected such that $\mathbf{J}^\top \hat{\mathbf{Q}}$ is non-singular.

From (4.43), invariant set of system (4.1) is contained in the set

$$\mathcal{N} \triangleq \{\mathbf{x} \in \mathcal{D}_c : (\nabla \mathcal{H}_s)^\top \mathcal{R}_s(\mathbf{x}) \nabla \mathcal{H}_s = 0\}$$

which can be reduced in our case to $\{\mathbf{x} \in \mathcal{D}_c : \tilde{\boldsymbol{\nu}} = 0\}$. Since for every $\mathbf{x} \in \mathcal{N}$ and under condition C2, $\dot{\mathbf{p}} = \mathbf{J}^\top \hat{\mathbf{Q}} \tilde{\boldsymbol{\eta}} = 0$ if and only if $\tilde{\boldsymbol{\eta}} = 0$, it follows that the largest invariant set contained in $\mathcal{N}$ is given by the singleton $\mathcal{M} = \{\mathbf{0}\}$. Furthermore since the shaped Hamiltonian is radially unbounded, then the equilibrium solution $\mathbf{x}(t) \equiv \mathbf{0}$ of the closed loop system equation (4.5) is Uniformly Globally Asymptotically Stable (UGAS).

4.6.2 Determining The Rate of Convergence

Our analysis in the previous subsection tells nothing about the rate of convergence. We are only able to deduce the asymptotic stability properties of the origin using *LaSalle* theorem, which are less strong compared to the exponential stability ones. There are two ways to estimate the convergence rate. The first way is to

determine the convergence rate using a manipulation in the shaped Hamiltonian function (4.41) and the second is to choose a Lyapunov function other than the shaped Hamiltonian.

Convergence Rate using shaped Hamiltonian

Recall that the shaped Hamiltonian and its time derivative are given respectively by

$$\mathcal{H}_s = \frac{1}{2}\boldsymbol{\nu}^\top \mathbf{M}\boldsymbol{\nu} + \frac{1}{2}\tilde{\boldsymbol{\eta}}^\top \hat{\mathbf{Q}}\tilde{\boldsymbol{\eta}}$$

$$\dot{\mathcal{H}}_s = -\boldsymbol{\nu}^\top \mathbf{D}_s \boldsymbol{\nu}$$

$\mathcal{H}_s$ and $\dot{\mathcal{H}}_s$ are both bounded as follows

$$\lambda_{\min}(\mathbf{M})\|\boldsymbol{\nu}\|^2 + \lambda_{\min}(\hat{\mathbf{Q}})\|\tilde{\boldsymbol{\eta}}\|^2 \le 2\mathcal{H}_s \le \lambda_{\max}(\mathbf{M})\|\boldsymbol{\nu}\|^2 + \lambda_{\max}(\hat{\mathbf{Q}})\|\tilde{\boldsymbol{\eta}}\|^2$$

$$\dot{\mathcal{H}}_s \le -\lambda_{\min}(\mathbf{D}_s)\|\boldsymbol{\nu}\|^2$$

since $\|\boldsymbol{\nu}\|^2 \ge \dfrac{2\mathcal{H}_s - \lambda_{\max}(\hat{\mathbf{Q}})\|\tilde{\boldsymbol{\eta}}\|^2}{2\lambda_{\max}(\mathbf{M})}$, we have

$$\dot{\mathcal{H}}_s \le -\frac{\lambda_{\min}(\mathbf{D}_s)}{\lambda_{\max}(\mathbf{M})}\mathcal{H}_s + \xi$$

where

$$\xi = \frac{\lambda_{\max}(\hat{\mathbf{Q}})\lambda_{\min}(\mathbf{D}_s)}{2\lambda_{\max}(\mathbf{M})}\|\tilde{\boldsymbol{\eta}}\|^2$$

71

Writing $\sigma = \dfrac{\lambda_{\min}(\mathbf{D}_s)}{\lambda_{\max}(\mathbf{M})}$, the upper bound of the shaped Hamiltonian may be given by

$$\mathcal{H}_s(t) \le \mathcal{H}_s(0) \exp \left(-\sigma t + \int_0^t \frac{\xi}{\mathcal{H}_s} d\tau \right) \tag{4.46}$$

From the definition of shaped Hamiltonian, $\int_0^t \frac{\xi}{\mathcal{H}_s} d\tau$ is a function of $\tilde{\mathbf{Q}}$. The state evolution along the time can be roughly bounded by

$$\|\mathbf{x}(t)\| \le \sqrt{\frac{\mathcal{H}_s(0)}{\min \left(\lambda_{\min}(\mathbf{M}), \lambda_{\min}(\hat{\mathbf{Q}}) \right)}} \exp \left(-\frac{\sigma}{2} t + \int_0^t \frac{\xi}{2\mathcal{H}_s} d\tau \right) \tag{4.47}$$

Convergence rate of system using other Lyapunov functions

Consider the following Lyapunov function $\mathcal{V}$ defined as

$$\mathcal{V} = \mathcal{H}_s + \mathcal{V}_c \tag{4.48}$$

Where $\mathcal{V}_c$ is an additional coupling term that we add to ensure the exponential stability properties. Since $\mathcal{H}_s$ contains no coupled term between $\tilde{\boldsymbol{\eta}}$ and $\boldsymbol{\nu}$ and $\dot{\mathcal{H}}_s$ is only quadratic function of $\boldsymbol{\nu}$, the coupled term $\mathcal{V}_c$ might help us to get $\dot{\mathcal{V}}$ also a quadratic function in both $\tilde{\boldsymbol{\eta}}$ and $\boldsymbol{\nu}$. With this in mind, we select also

$$\mathcal{V}_c = \frac{1}{2} \left[\tilde{\boldsymbol{\eta}}^\top \mathbf{S} \boldsymbol{\nu} + \boldsymbol{\nu}^\top \mathbf{S}^\top \tilde{\boldsymbol{\eta}} \right] \tag{4.49}$$

Where $\mathbf{S}$ is unknown matrix that can be a constant matrix or function of $\boldsymbol{\eta}_2$, i.e. $\mathbf{S}(\boldsymbol{\eta}_2)$. In this case The Lyapunov function can be written in quadratic form as

below

$$\mathcal{V} = \frac{1}{2} \begin{bmatrix} \tilde{\boldsymbol{\eta}}^\top & \boldsymbol{\nu}^\top \end{bmatrix} \begin{bmatrix} \hat{\mathbf{Q}} & \mathbf{S} \\ \mathbf{S}^\top & \mathbf{M} \end{bmatrix} \begin{bmatrix} \tilde{\boldsymbol{\eta}} \\ \boldsymbol{\nu} \end{bmatrix} \tag{4.50}$$

$$\mathcal{V} = \begin{bmatrix} \tilde{\boldsymbol{\eta}}^\top & \boldsymbol{\nu}^\top \end{bmatrix} \bar{\mathbf{P}} \begin{bmatrix} \tilde{\boldsymbol{\eta}} \\ \boldsymbol{\nu} \end{bmatrix} \tag{4.51}$$

Given the above equation, we evaluate the time derivative of the Lyapunov function along the trajectory as below

$$\dot{\mathcal{V}} = \nabla_x \mathcal{H}_s^\top \dot{\mathbf{x}} + \nabla_x \mathcal{V}_c^\top \dot{\mathbf{x}} \tag{4.52}$$

The first term of the above equation is the shaped Hamiltonian time derivative and

$$\nabla_x \mathcal{V}_c^\top = \frac{\partial \mathcal{V}_c}{\partial \mathbf{x}}$$
$$\frac{\partial \mathcal{V}_c}{\partial \mathbf{x}} = \begin{bmatrix} \dfrac{\partial \mathcal{V}_c}{\partial \boldsymbol{\eta}} & \dfrac{\partial \mathcal{V}_c}{\partial \mathbf{p}} \end{bmatrix}$$
$$\frac{\partial \mathcal{V}_c}{\partial \boldsymbol{\eta}} = \boldsymbol{\nu}^\top \left(\mathbf{S}^\top + \frac{\partial \mathbf{S}^\top}{\partial \boldsymbol{\eta}_2} \tilde{\boldsymbol{\eta}}_2 \right) = \boldsymbol{\nu}^\top \bar{\mathbf{S}}^\top$$
$$\frac{\partial \mathcal{V}_c}{\partial \mathbf{p}} = \tilde{\boldsymbol{\eta}}^\top \mathbf{S} \mathbf{M}^{-1}$$

Combining the time derivative of the Hamiltonian given in (4.43) and the time

derivative of $\mathcal{V}_c$, we obtain the time derivative of Lyapunov function as

$$\dot{\mathcal{V}} = - \begin{bmatrix} \tilde{\boldsymbol{\eta}}^\top & \boldsymbol{\nu}^\top \end{bmatrix} \begin{bmatrix} \mathbf{SM}^{-1}\mathbf{J}^\top\hat{\mathbf{Q}} & \frac{1}{2}\mathbf{SM}^{-1}\mathbf{D}_s \\ \frac{1}{2}(\mathbf{SM}^{-1}\mathbf{D}_s)^\top & \mathbf{D}_s - \bar{\mathbf{S}}^\top\mathbf{J} \end{bmatrix} \begin{bmatrix} \tilde{\boldsymbol{\eta}} \\ \boldsymbol{\nu} \end{bmatrix} \tag{4.53}$$

$$\dot{\mathcal{V}} = - \begin{bmatrix} \tilde{\boldsymbol{\eta}}^\top & \boldsymbol{\nu}^\top \end{bmatrix} \bar{\mathbf{Q}} \begin{bmatrix} \tilde{\boldsymbol{\eta}} \\ \boldsymbol{\nu} \end{bmatrix} \tag{4.54}$$

The presence of $\mathbf{S}$, follows from the fact that the closed-loop of the AUV dynamics is Uniformly Locally Exponentially Stable (ULES), with the following explanations. Consider that the Jacobian of the AUV dynamics at the desired equilibrium point $\mathbf{x}_d = \{\boldsymbol{\eta}_d, 0\}$ is given by

$$\mathbf{f} = [\mathcal{J}_s - \mathcal{R}_s]\nabla_x\mathcal{H}_s$$

$$\mathbf{A} = \left.\frac{\partial\mathbf{f}}{\partial\mathbf{x}}\right|_{x=x_d}$$

$$\mathbf{A} = \begin{bmatrix} 0 & \mathbf{J}(\boldsymbol{\eta}_{d,2})\mathbf{M}^{-1} \\ -\mathbf{J}(\boldsymbol{\eta}_{d,2})^\top\hat{\mathbf{Q}} & -\mathbf{D}_s\mathbf{M}^{-1} \end{bmatrix}$$

The eigenvalues of $\mathbf{A}$ are the solution of the following second order matrix determinant equations

$$\det\left[s^2\mathbf{I} + s\mathbf{D}_s\mathbf{M}^{-1} + \mathbf{J}(\boldsymbol{\eta}_{d,2})^\top\hat{\mathbf{Q}}\mathbf{J}(\boldsymbol{\eta}_{d,2})\mathbf{M}^{-1}\right] = 0 \tag{4.55}$$

It can be easily proven that the eigenvalues of $\mathbf{A}$ are always in the left hand side of the imaginary axis, provided that the pitch angle of the AUV is not equal to $\pi/2$. The eigenvalues will be distributed inside a region $(-\lambda_{max}(\mathbf{D}_s\mathbf{M}^{-1}), 0)$ and separated into two groups, the faster eigenvalues are mostly related to velocity

74

and the slower are related to position. In the special case of diagonal $\mathbf{D}_s$, $\mathbf{M}$ and $\hat{\mathbf{Q}}$ and the pitch angle is zero (horizontal plane mission), we have six independent second order equations of eigenvalues as given below

$$\lambda_i = -\frac{d_{s,i}m_i}{2} \pm \frac{1}{2}\sqrt{(d_{s,i}m_i)^2 - 4q_im_i} \tag{4.56}$$

Where $d_{s,i}$, m_i and q_i are the ith diagonal element of $\mathbf{D}_s$, $\mathbf{M}^{-1}$ and $\hat{\mathbf{Q}}$. λ_i will equal to zero if q_i is zero, otherwise it always less than zero.

Following theorem 4.6 in [42], the origin of the nonlinear AUV dynamics is an exponentially stable equilibrium point, or more precisely ULES and by *Converse Lyapunov Theorem*, there exist $\mathbf{S}$ such that $\bar{\mathbf{P}}$ and $\bar{\mathbf{Q}}$ are positive definite. The minimum rate of convergence of the Lyapunov function $\mathcal{V}$ is then given by

$$\mathcal{V}(t) = \mathcal{V}(0)e^{-\sigma t} \tag{4.57}$$

where $\sigma = \dfrac{2\lambda_{min}(\bar{\mathbf{Q}})}{\lambda_{max}(\bar{\mathbf{P}})}$. The state evolution along the time is bounded by

$$\|\mathbf{x}(t)\| \leq \sqrt{\frac{\mathcal{V}(0)}{\lambda_{\min}(\bar{\mathbf{P}})}} \exp -\frac{\sigma}{2}t \tag{4.58}$$

Note that, although the closed loop system is UGAS as seen in the previous section, it is also ULES with different rate of convergence. σ will vary depending on the Euler angle of the AUV. In addition, while the existence of $\mathbf{S}$ is guaranteed, finding the right choice of $\mathbf{S}$ is also challenging. One initial guess that one can make, is to select $\mathbf{S} = \rho\,\mathbf{J}^{-\top}$, since in the matrix $\bar{\mathbf{Q}}$ the only non-constant matrix involved is $\mathbf{J}$. The parameter ρ is selected as a gain to tune the behaviour of $\bar{\mathbf{P}}$ and $\bar{\mathbf{Q}}$, based on selected controller parameter $\hat{\mathbf{Q}}$ and $\mathbf{D}_s$. Putting ρ too big might lead

to semi or non-definite behaviour, i.e. presence of zero or negative eigenvalue in $\bar{\mathbf{P}}$ and $\bar{\mathbf{Q}}$. While selecting ρ too small might defy the purpose of introducing $\mathcal{V}_c$ and may lead to a conservative convergence rate.

4.6.3 Stability Analysis of Stabilizing Controller in The Presence of Parameter Uncertainties and Exogenous Disturbance

In this subsection we study the stability of the controller in the presence of parameter uncertainty and exogenous disturbances. Suppose that the AUV's inertia matrix can be written as $\mathbf{M}_\epsilon = \mathbf{M} + \Delta \mathbf{M}_\epsilon$, where $\mathbf{M}_0$ is the nominal value of inertia matrix and $\Delta \mathbf{M}_\epsilon$ is it's perturbation from nominal value due to added mass for instance. The Hamiltonian of the system along with the stabilizing controller can be expressed as follows

$$\mathcal{H}_{s,\epsilon} = \frac{1}{2}\mathbf{p}^\top \mathbf{M}_\epsilon^{-1}\mathbf{p} + \frac{1}{2}\tilde{\boldsymbol{\eta}}^\top \hat{\mathbf{Q}}\tilde{\boldsymbol{\eta}} \tag{4.59}$$

Since the Hamiltonian of the perturbed system is related to $\mathbf{M}_\epsilon^{-1}$, we need to state the following lemma to write $\mathbf{M}_\epsilon^{-1} = \mathbf{M}^{-1} + \Delta\mathcal{M}$.

Lemma 4.1 (Inverse of Sum of Matrices). *Given $\mathbf{A}$ and $\mathbf{B}$, where $\mathbf{A}$ and $\mathbf{A} + \mathbf{B}$ are invertible, them*

$$(\mathbf{A} + \mathbf{B})^{-1} = \mathbf{A}^{-1} + \mathbf{X}$$

where

$$\mathbf{X} = -(\mathbf{I} + \mathbf{A}^{-1}\mathbf{B})^{-1}\mathbf{A}^{-1}\mathbf{B}\mathbf{A}^{-1}$$

Proof. To prove this, $(\mathbf{A} + \mathbf{B})^{-1}$ can be evaluated knowing only $\mathbf{A}^{-1}$ and $\mathbf{B}$. Suppose that we can express $(\mathbf{A} + \mathbf{B})^{-1} = \mathbf{A}^{-1} + \mathbf{X}$, then $\mathbf{X}$ can be computed as follows

$$(\mathbf{A} + \mathbf{B})^{-1} = \mathbf{A}^{-1} + \mathbf{X}$$
$$(\mathbf{A}^{-1} + \mathbf{X})(\mathbf{A} + \mathbf{B}) = \mathbf{I}$$
$$\mathbf{A}^{-1}\mathbf{A} + \mathbf{X}\mathbf{A} + \mathbf{A}^{-1}\mathbf{B} + \mathbf{X}\mathbf{B} = \mathbf{I}$$
$$\mathbf{X}(\mathbf{A} + \mathbf{B}) = -\mathbf{A}^{-1}\mathbf{B}$$
$$\mathbf{X} = -\mathbf{A}^{-1}\mathbf{B}(\mathbf{A} + \mathbf{B})^{-1}$$
$$\mathbf{X} = -\mathbf{A}^{-1}\mathbf{B}(\mathbf{A}^{-1} + \mathbf{X})$$
$$(\mathbf{I} + \mathbf{A}^{-1}\mathbf{B})\mathbf{X} = -\mathbf{A}^{-1}\mathbf{B}\mathbf{A}^{-1}$$
$$\mathbf{X} = -(\mathbf{I} + \mathbf{A}^{-1}\mathbf{B})^{-1}\mathbf{A}^{-1}\mathbf{B}\mathbf{A}^{-1}$$

$\square$

This lemma is simplified version of the one presented by Ken Miller, 1981, see [67]. Using Lemma 4.1, we have

$$\Delta\mathcal{M} = -(\mathbf{I} + \mathbf{M}^{-1}\Delta\mathbf{M})^{-1}\mathbf{M}^{-1}\,(\Delta\mathbf{M})\,\mathbf{M}^{-1} \qquad (4.60)$$

The partial derivative of the Hamiltonian associated with the perturbed system can be computed as

$$\nabla\mathcal{H}_{s,\epsilon} = \nabla\mathcal{H}_s = \begin{bmatrix} \hat{\mathbf{Q}}\tilde{\eta} \\ (\mathbf{M}^{-1} + \Delta\mathcal{M})\,\mathbf{p} \end{bmatrix} \qquad (4.61)$$

If we assume that the body fixed velocity ν vector is measured, we can write

$\boldsymbol{\nu} = \left(\mathbf{M}^{-1} + \Delta\mathcal{M}\right)\mathbf{p}$. In addition, knowing that for AUV, $\mathcal{J}_{s,\epsilon} = \mathcal{J}_s = \mathcal{J}$ and $\mathbf{D}_a = \mathbf{D}_s - \hat{\mathbf{D}}$, then from the matching condition we have

$$\dot{\mathbf{x}} = [\mathcal{J} - \mathcal{R}_\epsilon]\,\nabla\mathcal{H}_\epsilon + \mathbf{G}_1\phi_{1,\epsilon} + \mathbf{G}_2\mathbf{w}$$

$$\dot{\mathbf{x}} = \begin{bmatrix} 0 & \mathbf{J} \\ -\mathbf{J}^\top & -(\mathbf{D}_s + (\bar{\mathbf{D}}_\epsilon - \hat{\mathbf{D}})) \end{bmatrix} \nabla\mathcal{H}_{s,\epsilon} + \mathbf{G}_2\mathbf{w}$$

Next, we compute the time derivative of the *Shaped Hamiltonian* along a trajectory as given below,

$$\dot{\mathcal{H}}_s = -\nabla\mathcal{H}_{s,\epsilon}^\top \begin{bmatrix} 0 & \mathbf{J} \\ -\mathbf{J}^\top & (\mathbf{D}_s + (\bar{\mathbf{D}}_\epsilon - \hat{\mathbf{D}})) \end{bmatrix} \nabla\mathcal{H}_{s,\epsilon} + \nabla\mathcal{H}_{s,\epsilon}^\top \mathbf{G}_2\mathbf{w} \qquad (4.62)$$

$$= -\nabla\mathcal{H}_{s,\epsilon}^\top \mathcal{R}_{s,\epsilon} \nabla\mathcal{H}_{s,\epsilon} + \nabla\mathcal{H}_{s,\epsilon}^\top \mathbf{G}_2\mathbf{w} \qquad (4.63)$$

$$(4.64)$$

Where $\mathcal{R}_{s,\epsilon}$ is the desired damping matrix in the presence of the uncertainties. Using properties 4.1, we have

$$\dot{\mathcal{H}}_s \leq -\nabla\mathcal{H}_{s,\epsilon}^\top \left[\mathcal{R}_{s,\epsilon} - \frac{1}{2}\left(\mathbf{G}_2\mathbf{G}_2^\top\right)\right]\nabla\mathcal{H}_{s,\epsilon} + \frac{1}{2}\|\mathbf{w}\|^2$$

$$\leq -\nabla\mathcal{H}_{s,\epsilon}^\top \mathcal{R}_{s,\epsilon}^* \nabla\mathcal{H}_{s,\epsilon} + \frac{1}{2}\|\mathbf{w}\|^2 \qquad (4.65)$$

From equation (4.65), we see that the closed loop system is still stable provided

that the following inequality is satisfied.

$$-\nabla\mathcal{H}_{s,\epsilon}^{\top}\mathcal{R}_{s,\epsilon}^{*}\nabla\mathcal{H}_{s,\epsilon} + \frac{1}{2}\|\mathbf{w}\|^2 \leq 0 \tag{4.66}$$

For AUV dynamics in the PCH structure as given in eq. (4.4), eq. (4.66) is equivalent to

$$\boldsymbol{\nu}^{\top}\left(\mathbf{D}_a + \bar{\mathbf{D}}_\epsilon - \frac{1}{2}\mathbf{J}^{-1}\mathbf{J}^{-\top}\right)\boldsymbol{\nu} \geq \frac{1}{2}\|\mathbf{w}\|^2 \tag{4.67}$$

When there is no exogenous disturbance, the closed loop of perturbed system is Lyapunov stable and furthermore, asymptotically stable using *LaSalle* theorem, provided that $\mathbf{D}_a + \bar{\mathbf{D}}_\epsilon \geq 0$. The uncertainties $\mathbf{M}$ contributed in $\nabla\mathcal{H}_{s,\epsilon}$ do not affect the system stability. The remaining effects are only in $\bar{\mathbf{D}}_\epsilon$ which is function of the Coriolis and centripetal matrix $\mathbf{C}$. Fortunately since Coriolis and centripetal matrix $\mathbf{C}$ is always skew symmetric (property 2.2) and natural damping is also always positive definite (property 2.3), the stability conditions for the perturbed systems are preserved.

4.6.4 $\mathcal{L}_2$ Disturbance Attenuation Controller: Second Stage

Theorem 4.2 is directly applicable to our AUV PCH model. In AUV dynamics, $\mathbf{G}_2$ is given by $\mathbf{J}^{-1}$ and $\mathcal{R}_s^*$ given by

$$\mathcal{R}_s^* = \mathcal{R}_s + \frac{1}{2\gamma^2}\left(\mathbf{G}_1(\mathbf{x})\mathbf{G}_1^{\top}(\mathbf{x}) - \mathbf{G}_2(\mathbf{x})\mathbf{G}_2^{\top}(\mathbf{x})\right) + \frac{1}{2}\mathbf{G}_1(\mathbf{x})h^{\top}(\mathbf{x})h(\mathbf{x})\mathbf{G}_1^{\top}$$

$$\mathcal{R}_s^* = \mathcal{R}_s + \frac{1}{2\gamma^2}\left(\begin{bmatrix} 0 & 0 \\ 0 & \mathbf{I} \end{bmatrix} - \begin{bmatrix} 0 & 0 \\ 0 & \mathbf{J}^{-1}\mathbf{J}^{-\top} \end{bmatrix}\right) + \frac{1}{2}\mathbf{G}_1(\mathbf{x})h^{\top}(\mathbf{x})h(\mathbf{x})\mathbf{G}_1^{\top} \tag{4.68}$$

In normal operational conditions, when the vehicle is moving in the horizontal plane, the pitch $\theta = 0$,hence, the value of $\mathbf{J}$ is orthogonal and $\mathbf{J}^{-1}\mathbf{J}^{-\top} = \mathbf{I}$, hence we have

$$\frac{1}{2\gamma^2}\left(\mathbf{G}_1(\mathbf{x})\mathbf{G}_1^\top(\mathbf{x}) - \mathbf{G}_2(\mathbf{x})\mathbf{G}_2^\top(\mathbf{x})\right) = 0.$$

The above equation means that the dissipativity of the closed loop system with exogenous disturbance, exhibits the same dissipativity of the closed loop system without exogenous disturbance. For penalty signal, we can select $h(\mathbf{x})$ to be

$$h(\mathbf{x}) = \boldsymbol{\nu}^\top \hat{\mathbf{Q}} \tag{4.69}$$

since $h(\mathbf{x}_d) = 0$. For a given desired disturbance attenuation level γ and using direct substitution into (4.14) we get

$$\phi_2(\mathbf{x}) = \frac{1}{2}\left(\frac{1}{\gamma^2}\mathbf{I} + \hat{\mathbf{Q}}\boldsymbol{\nu}\boldsymbol{\nu}^\top\hat{\mathbf{Q}}\right)\boldsymbol{\nu} \tag{4.70}$$

From equation (4.68) we can conclude that $\mathcal{R}_s^*$ will not be full rank. In such case, we use *La Salle* invariance principle in a similar approach as described in the previous subsections and under the same condition mentioned therein. The invariant set of system (4.10) is contained in $\mathcal{N} \triangleq \{\mathbf{x} \in \mathcal{D}_c : (\nabla\mathcal{H}_s)^\top\mathcal{R}_s^*(\mathbf{x})\nabla\mathcal{H}_s = 0\}$ which is equal to $\{\mathbf{x} \in \mathcal{D}_c : \boldsymbol{\nu} = 0\}$. Since for every $\mathbf{x} \in \mathcal{N}$, $\dot{\boldsymbol{\nu}} = \mathbf{J}^\top\hat{\mathbf{Q}}\tilde{\boldsymbol{\eta}} = 0$, if and only if $\tilde{\boldsymbol{\eta}} = 0$, it follows that the largest invariant set contained in $\mathcal{N}$ is given by $\mathcal{M} = \{\mathbf{x}_d\}$.

4.6.5   Adaptive $\mathcal{L}_2$ Attenuation Controller: Third Stage

In this subsection, theorem 4.3 is applied to the AUV problem. We select $\mathbf{D}_a$ such that it has to cancels the natural damping of the AUV to give more decoupling effect on the closed loop. We consider only uncertainties in system equation only that occur in drag matrix $\mathbf{D}$. This may happen due to imprecise parameters in $\mathbf{D}$, or higher order terms that are neglected during the modelling, see [24].

Suppose AUV drag matrix can be written as $\mathbf{D}_\epsilon = \mathbf{D} + \Delta\mathbf{D}_\epsilon$, where $\mathbf{D}_0$ is the nominal value of the drag matrix and $\Delta\mathbf{D}_\epsilon$ is its perturbation from nominal value. Since for slender type of AUV with Y-Z and X-Z body symmetry, the diagonal terms of the drag matrix are dominant, we assume that the perturbations occur on the diagonal terms only, i.e. $\Delta\mathbf{D}_\epsilon = \mathrm{diag}\{\begin{bmatrix} \epsilon_1 & \epsilon_2 & \epsilon_3 & \epsilon_4 & \epsilon_5 & \epsilon_6 \end{bmatrix}\}$.

Next, we develop the matching conditions of the adaptive controller as stated in theorem 4.3. Note that, since we consider only uncertainty in the drag matrix, the shaped Hamiltonian $\mathcal{H}_s$ is the same in the nominal case and the perturbed case and hence we can write

$$[\mathcal{J}_{s,\epsilon} - \mathcal{R}_{s,\epsilon}] \Delta\mathcal{H}_{s,\epsilon} - \mathbf{G}_{1,\epsilon}\Delta\phi_{1,\epsilon} = \mathbf{G}_{1,\epsilon}\mathbf{\Phi}^\top\theta$$

$$0 - \mathbf{G}_{1,\epsilon}\Delta\phi_{1,\epsilon} = \mathbf{G}_{1,\epsilon}\mathbf{\Phi}^\top\theta$$

$$\Delta\mathbf{K}_\epsilon\nabla\mathcal{H}_s = \mathbf{\Phi}^\top\theta$$

$$\Delta\mathbf{D}_\epsilon\boldsymbol{\nu} == \mathbf{\Phi}^\top\theta \tag{4.71}$$

If we select $\theta = \begin{bmatrix} \epsilon_1 & \epsilon_2 & \epsilon_3 & \epsilon_4 & \epsilon_5 & \epsilon_6 \end{bmatrix}^\top$, with $\Delta\mathbf{K}_\epsilon$ linear in θ,then we can write

the last equation to obtain $\mathbf{\Phi}^\top$ as follows

$$\frac{\partial\left(\Delta\mathbf{D}_\epsilon\boldsymbol{\nu}\right)}{\partial\theta} = \mathbf{\Phi}^\top \tag{4.72}$$

Evaluating the equation (4.72) for AUV model, $\mathbf{\Phi}^\top$ will be

$$- \begin{bmatrix} |u| & 0 & 0 & 0 & 0 & 0 \\ 0 & |v| & 0 & 0 & 0 & 0 \\ 0 & 0 & |w| & 0 & 0 & 0 \\ 0 & 0 & 0 & |p| & 0 & 0 \\ 0 & 0 & 0 & 0 & |q| & 0 \\ 0 & 0 & 0 & 0 & 0 & |r| \end{bmatrix} = -\text{diag}\{|\boldsymbol{\nu}|\} = \mathbf{\Phi}^\top \tag{4.73}$$

Substituting this in the controller equation ϕ_2 as in theorem 4.3, the solution of *Adaptive $\mathcal{L}_2$ disturbance attenuation* for fully actuated AUV with uncertainties in the drag matrix is solved.

Remark 4.7. From remark 4.5 in section 4.5, we require $\mathbf{G}_{1,\epsilon}\mathbf{\Phi}^\top$ to be non singular to achieve asymptotic stability of the desired augmented equilibrium point $\{\mathbf{x}_d, \theta^*\}$. However, the matching condition for the AUV model shows that $\mathbf{\Phi}^\top$ can be singular if $\mathbf{x} = \mathbf{x}_d$. This makes the stability of adaptive closed loop system downgraded into Lyapunov stable conditions only and the estimation of the unknown parameters might converge to the wrong values. Fortunately, the stability of the desired position and velocity $\mathbf{x_d} = \{\boldsymbol{\eta}_d, 0\}$ is preserved.

4.7 Simulation Results

In this section, we apply the controller design procedure presented in the previous section to MARES for trajectory tracking. We divide this section into three subsections. First we design a stabilizing controller based on PCH structure of AUV, applied to MARES. Next, the $\mathcal{L}_2$ disturbance attenuation is designed. Last, an adaptive scheme of $\mathcal{L}_2$ disturbance attenuation is designed for MARES vehicle with uncertainties in the drag matrix diagonal elements. Based on the controller law design presented in subsection 4.6.1, to meet asymptotic stability requirement, $\mathbf{D}_a$ has to be selected such that during the operation, $\left(\bar{\mathbf{D}} + \mathbf{D}_a\right) > 0$.
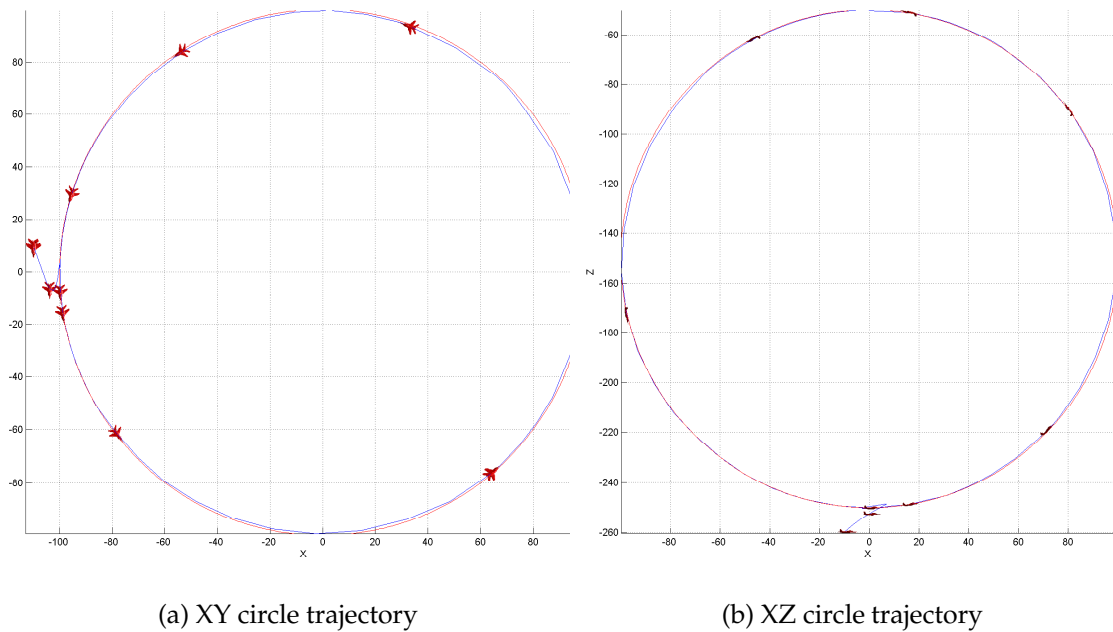

(a) XY circle trajectory

(b) XZ circle trajectory

Figure 4.2: Trajectory simulation result

From figures 4.2a, 4.2b,4.3a and 4.3b, we see that the designed controller are able to drive the AUV tracking the correct trajectory, even it is able to pass the critical condition where the pitch angle equal to $\pi/2$.
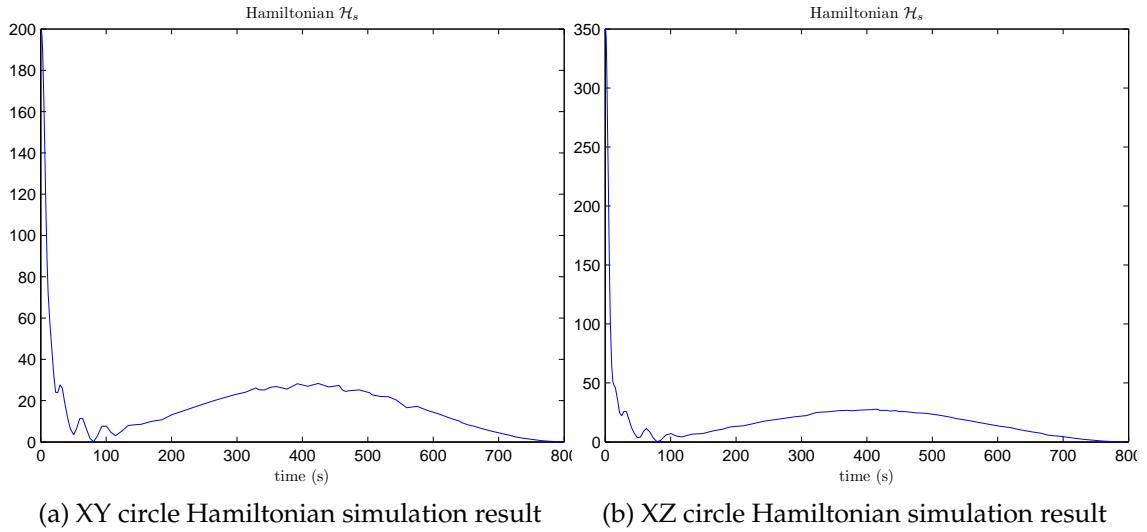
(a) XY circle Hamiltonian simulation result   (b) XZ circle Hamiltonian simulation result

Figure 4.3: Hamiltonian

To show the effectiveness of the proposed design against parameter uncertainties, here we show the simulation with 50%, 80% and 500% error on diagonal element of added mass matrix $\mathbf{M}_A$ and 5% error on drag matrix $\mathbf{D}$. The simulations are shown in figure 4.4 below. It can be seen that the selecting of $\mathbf{D}_a$ makes the AUV trajectory robust enough to encounter added mass and drag uncertainties.

4.7.1 $\mathcal{L}_2$ Disturbance Attenuation: Second Stage

Next we continue to apply the $\mathcal{L}_2$ disturbance attenuation design, where we add the exogenous disturbance. Using the same controller as before, the simulation results are given in figure 4.5 with shuttle space mark. As can be seen, the trajectory is highly disturbed, although the AUV generally still follow the desired trajectory. By means of the $\mathcal{L}_2$ disturbance attenuation controller, the disturbance effect on the trajectory can be attenuated. The simulation result of $\mathcal{L}_2$ disturbance attenuation controller is given in figure 4.5 with 'mig' mark. One of the draw-
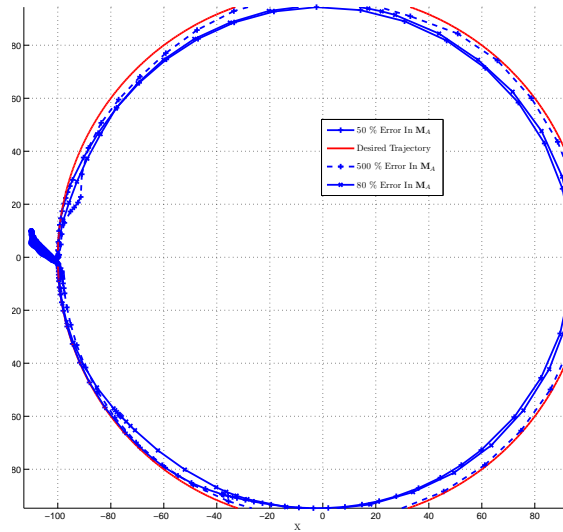
Figure 4.4: XY circle simulation results with different uncertainties in $\mathbf{M}$

backs of applying the $\mathcal{L}_2$ disturbance attenuation controller is that it makes the AUV not follow the desired trajectory exactly. This happens due to the presence of additional damping from the $\mathcal{L}_2$ disturbance attenuation. This is the common trade off, between disturbance rejection and controller performance.

4.7.2 Adaptive $\mathcal{L}_2$ Attenuation Controller: Third Stage

In this subsection we will show the simulation of the designed adaptive $\mathcal{L}_2$ attenuation controller. First, we will show the simulation result of the AUV system having 5 % uncertainties in the drag matrix $\mathbf{D}$ without any exogenous disturbance and no uncertainty in the inertia matrix M. This simulation aims to show the behaviour of the unknown parameters estimation. For this simulation, we set $\phi_2 = 0$. Second simulation will carry all types of uncertainties and exogenous disturbances as well, where we choose $\gamma = 0.1$. From both simulation results
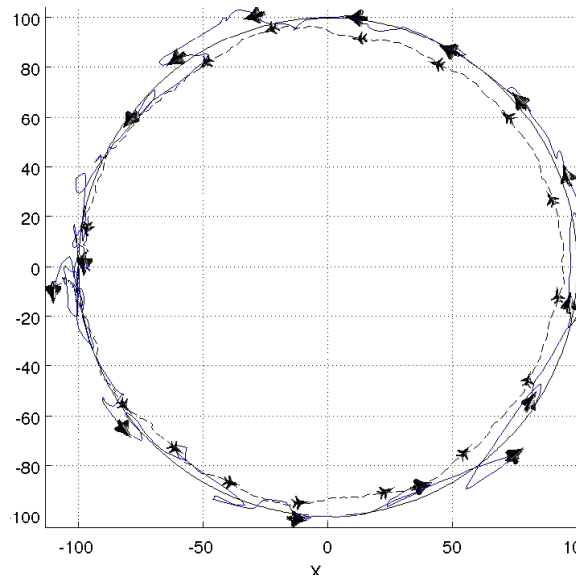
Figure 4.5: XY circle trajectory simulation results, $\mathcal{L}_2$ disturbance attenuation with $\gamma = 0.1$

given in figure 4.6, we can see that the stability of the AUV is still preserved, even when there is exogenous disturbances, except that the AUV becomes miss-headed. Also from figure 4.7 and 4.8, we can see -as in our previous derivations- that the unknown parameters tend to be bounded, although they are not converging to the correct values, see remark 4.4.

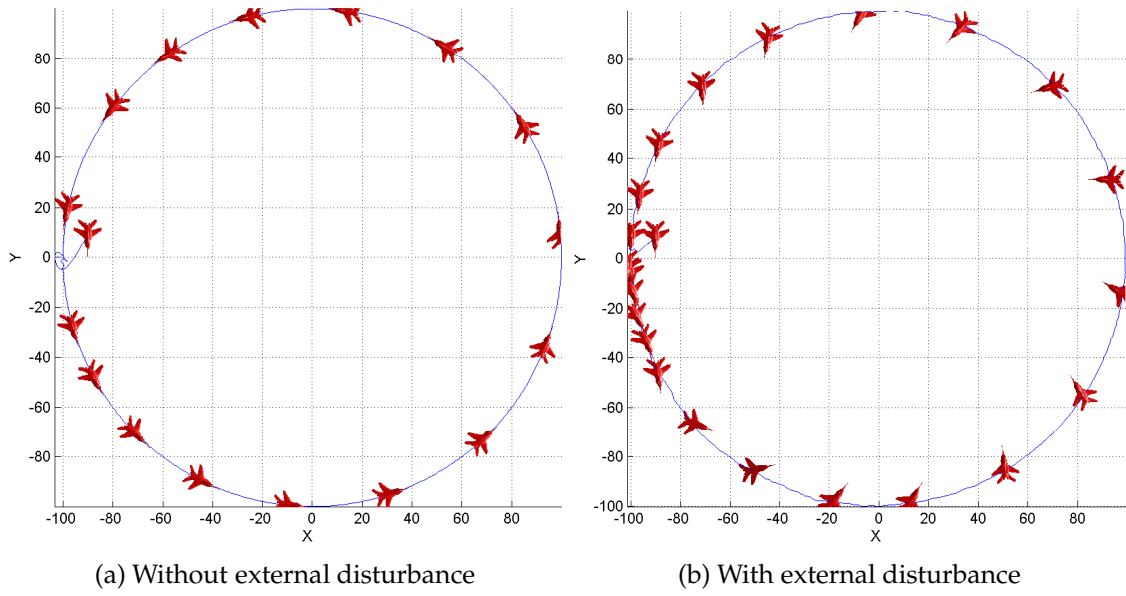(a) Without external disturbance   (b) With external disturbance

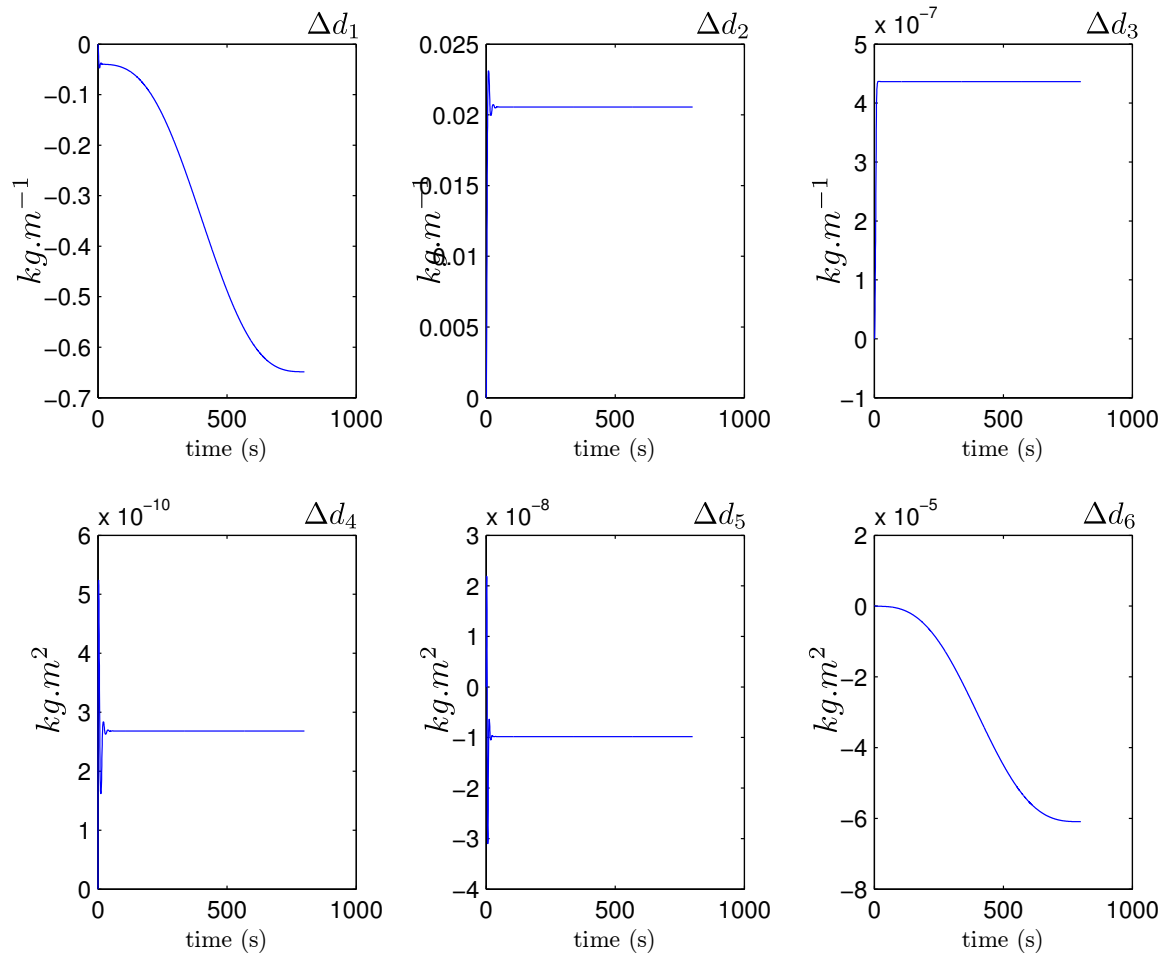Figure 4.6: Adaptive scheme simulation trajectory

Figure 4.7: Unknown parameter estimates - without exogenous disturbance
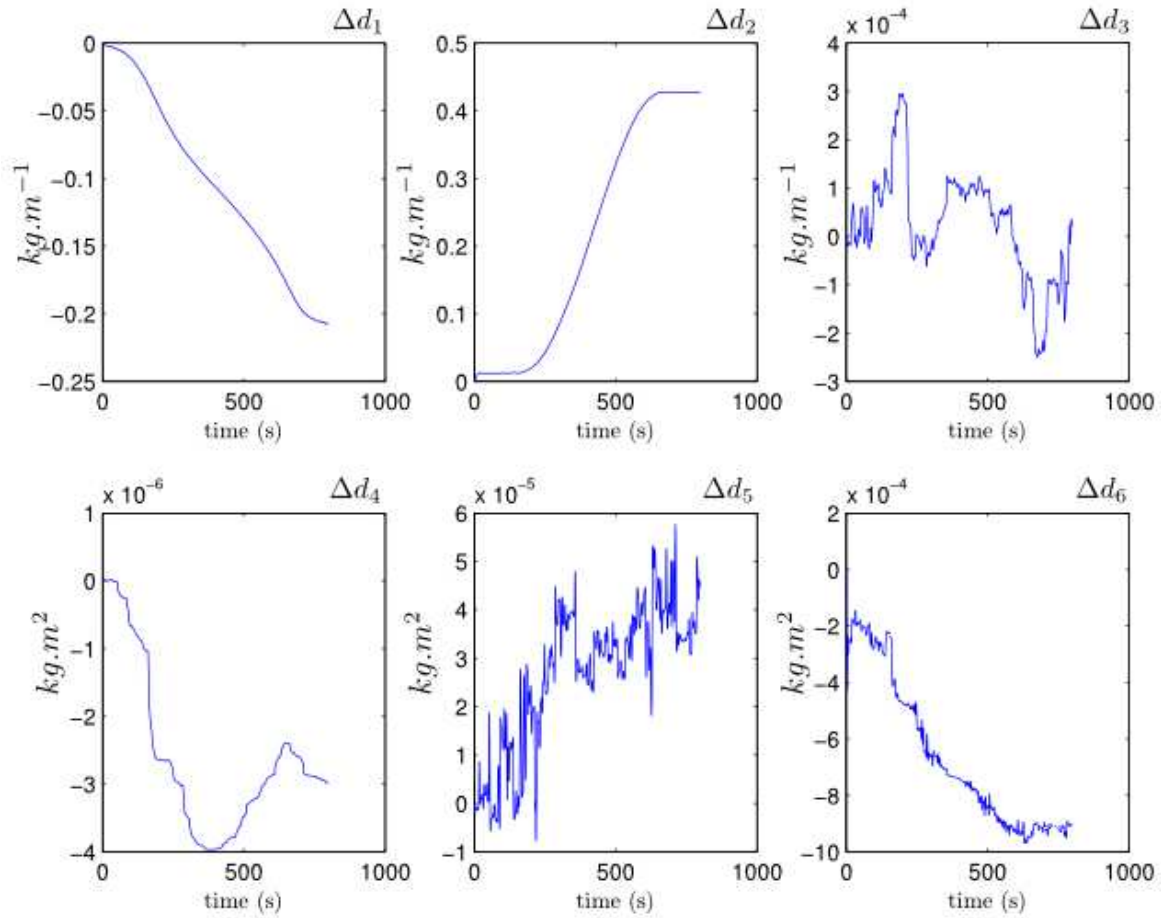
Figure 4.8: Unknown parameter estimates - with exogenous disturbance

4.8 Conclusions

In this chapter, we have established the passivity-based controller design for AUV. We stated a PCH formulation of AUV dynamics. Then we proposed a design of a nonlinear passivity-based controller for AUV PCH framework. Furthermore, we presented an extension of [91] in $\mathcal{L}_2$ disturbance attenuation for general PCH system, where we relaxed $\mathbf{G(x)}$ restriction to allow the disturbance to have different input gain matrix $\mathbf{G}_2$. In addition to that, we also presented an extension to [57], in the adaptive $\mathcal{L}_2$ disturbance attenuation. We relaxed $\mathbf{G(x)}$ restriction, where the input and disturbance matrix are allowed to have some uncertainties.

Rate of convergence analysis of the closed loop AUV system has been presented as well. Furthermore, the stability analysis of the designed closed loop AUV system in the presence of parameter uncertainties and exogenous disturbance is elaborated.

Finally, we presented an application of the passivity-based control of AUV system in the PCH framework, its $\mathcal{L}_2$ extension and adaptive $\mathcal{L}_2$ attenuation. Simulation results showed the robustness of the controller with respect to both parameter uncertainties and exogenous disturbances. All results presented were developed for fully-actuated AUV. In the next chapter, we will extend the controller design to cover the underactuated AUV.

Chapter 5

Underactuated Controller Design

5.1 Introduction

In the previous chapter, we have shown the passivity-based controller design for Autonomous Underwater Vehicle (AUV) in Port Controlled Hamiltonian (PCH) framework. While the design seems straight forward and simple, it assumes that the vehicle has a complete actuating force to move in six degrees of freedom. In real implementation, similar to other mechanical devices, many AUVs have less actuating forces than the total degrees of freedom. Such systems are called *underactuated*. The presence of this restriction may lead to poor position tracking and even to instability.

In this chapter,we address the problem of trajectory tracking for a class of AUV having actuating forces over four degrees of freedom namely surge, heave, pitch and sway motions. Unlike the previous designs which appeared in the literature, we do not assume any restrictions on the nonactuated damping or assume that

it has to be larger than the inertia. In addition, none of the nonactuated motions is neglected. We analyze the dynamics of the AUV in full six degrees of freedom within PCH framework as proposed and motivated in the previous chapter. Our approach to address the underactuated conditions is based on the underactuated PCH design presented in [30] and [75].

In summary, this chapter contributes to the literature by

1. proposing a detailed design method that constructs a nonlinear trajectory tracking controller for both two and three-dimensional underactuated AUV. Although the design is implemented in an AUV model that has four degrees of actuating forces, i.e heave, surge, pitch and sway, the analysis and design are general and can also be implemented for those vehicles having actuating forces only in three degrees of freedom, i.e surge, pitch and sway.

2. covering a broader AUV types compared to [2, 3], where in the proposed design, we allow the AUV to have non zero z-axes of center of buoyancy. In addition to that, we also allow the AUV to have a coupled quadratic damping,

3. proposing a robust trajectory tracking with respect to the ocean currents. Indeed, the proposed design allows the closed loop AUV system to have a passive mapping of the ocean disturbance, as well as $\mathcal{L}_2$ Input to State Stable (ISS) properties,

4. proposing a simple controller design that does not suffer from Coriolis and nonlinear drag force cancellation which is different from the work in [2, 3, 68]. Consequently, without the cancellations, the controller is considerably more robust to parameter uncertainties.

5. relaxing the constraints of a smooth, time differentiable desired trajectory restriction. Indeed, the desired trajectory does not need to be smooth and is allowed to have piecewise continuous profile. This condition cannot be handled in previous designs, such as in[2, 3] where the desired trajectory has to be in $\mathcal{C}^3$.

5.2 Desired Attitude Determination

In the previous chapter, the desired attitude of the AUV can be determined at the beginning, because AUV has enough actuating forces to move into the desired position and attitude. However, for the underactuated AUV, the attitude cannot be independently determined over the desired inertia position, due to the lack of two actuating forces. The desired attitude has to be designed such that the AUV heading is pointing to the desired position. The common approach to achieve this design is to use inverse tangent rule, commonly known as Line of Sight (LOS), [92, 25], as shown in figure 5.1
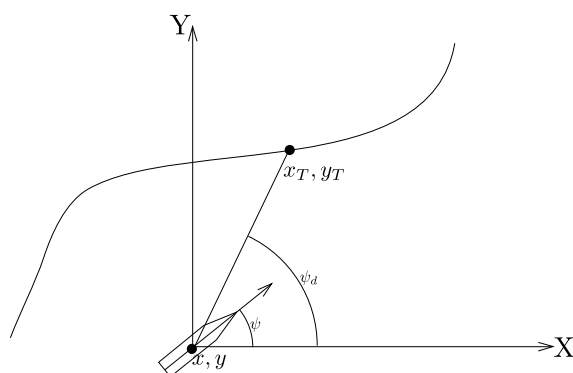

Figure 5.1: Line of Sight in two dimensions

The desired heading angle (yaw) and desired pitch angle are given by the follow-

93

ing equations respectively

$$\psi_d = \tan^{-1}\left(\frac{\Delta y}{\Delta x}\right) \tag{5.1}$$

$$\theta_d = \tan^{-1}\left(\frac{-\Delta z}{\sqrt{\Delta x^2 + \Delta y^2}}\right) \tag{5.2}$$

Due to the lack of the actuating torque for rolling motion, the desired roll angle ϕ_d is kept equal to the vehicle roll angle ϕ. Worth to mention that care should be taken when computing the $\tan^{-1}$, since it is only valid in the range $\left(-\frac{\pi}{2}, \frac{\pi}{2}\right)$. Using a specialized function that uses Δx and Δy as input to handle $\tan^{-1}$, we can extend the range to $(0, 2\pi)$. However, since $\tan^{-1}$ has several discontinuities in a range wider than $(0, 2\pi)$, LOS system with switching algorithm and memories has to be implemented (see for example [14]).

We propose the following attitude determination module as shown in figure 5.2 below
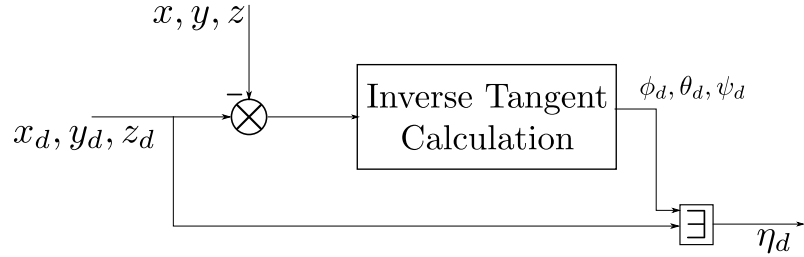

Figure 5.2: AUV desired attitude diagram

5.3 PCH Based Underactuated AUV Design

Underactuated conditions of AUV are addressed in this section using the extended version of the matching condition stated in theorem 4.1(eq. (4.8)). We

begin by defining two sets formed by a transformation matrix $\mathbf{T}$ that separates the body-fixed velocity into the actuated and nonactuated states respectively. The transformation matrix is an orthogonal matrix and does not change the magnitude of the velocity vector, it only reorder its elements, where the actuated velocities reindexed first while the nonactuated are put last.

Note that, the separation of body-fixed velocities into actuated and nonactuated modes is more appealing when compared to the separation of vehicle inertial positions as considered in [68]. The reason behind the selection stems from the fact that the Degrees of Freedom (DOF)'s are better seen in the vehicle body-fixed frame and not in the inertial frame. For example, most AUV's have only three DOF actuators covering surge, pitch and yaw. The lack of actuation in heave and sway does not mean that the vehicle cannot move in y and z axises of the inertial frame. For the current study, we selected Modular Autonomous Robot for Environment Sampling (MARES) AUV. MARES has only four thrusters. These thrusters can produce a force on surge and heave and creates a torque in sway and pitch angles respectively. Actuated body velocity are then given by u, w, q, r

and the nonactuated velocities are v and p. Consequently we have

$$\mathbf{T}\boldsymbol{\nu} = \hat{\boldsymbol{\nu}}$$

$$\mathbf{T} = \begin{bmatrix} 1 & 0 & 0 & 0 & 0 & 0 \\ 0 & 0 & 1 & 0 & 0 & 0 \\ 0 & 0 & 0 & 0 & 1 & 0 \\ 0 & 0 & 0 & 0 & 0 & 1 \\ 0 & 1 & 0 & 0 & 0 & 0 \\ 0 & 0 & 0 & 1 & 0 & 0 \end{bmatrix} \tag{5.3}$$

$$\hat{\boldsymbol{\nu}} = \begin{bmatrix} u & w & q & r & v & p \end{bmatrix}^{\top} \tag{5.4}$$

At the beginning following the original dynamics representation of MARES in [21, 22, 23], we assume that $g(\boldsymbol{\eta})$ has zeros on nonactuated motion, due to the assumption that the roll angle is negligible. Then, in section 5.3.2 we will discuss the case where $g(\boldsymbol{\eta})$ has non zero component on nonactuated modes. $g(\boldsymbol{\eta})$ is generally given by [24]

$$g(\boldsymbol{\eta}) = \begin{bmatrix} (W - B)s\theta \\ -(W - B)c\theta s\phi \\ -(W - B)c\theta c\phi \\ -(y_G W - y_B B)c\theta c\phi + (z_G W - z_B B)c\theta s\phi \\ (z_G W - z_B B)s\theta + (x_G W - x_B B)c\theta c\phi \\ -(x_G W - x_B B)c\theta s\phi - (y_G W - y_B B)s\theta \end{bmatrix} \tag{5.5}$$

Recall that the AUV dynamics under affine control characteristic can be expressed

as follows

$$\mathbf{M}\dot{\boldsymbol{\nu}} + \bar{\mathbf{D}}(\boldsymbol{\nu})\boldsymbol{\nu} + g(\boldsymbol{\eta}) = \mathbf{G}\mathbf{u} + \mathbf{J}^{-1}\mathbf{b} \tag{5.6}$$

Where $\mathbf{G}_1 \in \mathbb{R}^{6\times 4}$ is full column rank input gain matrix and $\mathbf{u} \in \mathbb{R}^4$ is the input for underactuated AUV. Using the separation based on the transformation matrix $\mathbf{T}$ of the dynamic equation, (5.6) can be rewritten as

$$\mathbf{M}\mathbf{T}^{\top}\dot{\boldsymbol{\nu}} + \bar{\mathbf{D}}(\hat{\boldsymbol{\nu}})\mathbf{T}^{\top}\hat{\boldsymbol{\nu}} + g(\boldsymbol{\eta}) = \mathbf{G}\mathbf{u} + \mathbf{J}^{-1}\mathbf{b} \tag{5.7}$$

Next, we define the transformed inertia $\hat{\mathbf{M}} = \mathbf{TMT}^{\top}$ and hence, we have the dynamics of AUV, arranged in actuated and non actuated manner as below

$$\dot{\boldsymbol{\nu}} = \hat{\mathbf{M}}^{-1}\left[\mathbf{TGu} + \mathbf{TJ}^{\top}\mathbf{b} - \mathbf{T\bar{D}}(\boldsymbol{\nu})\mathbf{T}^{\top}\hat{\boldsymbol{\nu}} + \mathbf{T}g(\boldsymbol{\eta})\right]$$

$$\dot{\boldsymbol{\nu}} = \hat{\mathbf{M}}^{-1}\left[\hat{\mathbf{G}}_1\mathbf{u} + \hat{\mathbf{G}}_2\mathbf{b} - \hat{\bar{\mathbf{D}}}(\hat{\boldsymbol{\nu}})\hat{\boldsymbol{\nu}} + \hat{g}(\boldsymbol{\eta})\right] \tag{5.8}$$

where $\hat{\mathbf{G}}_1 = \mathbf{TG}, \hat{\mathbf{G}}_2 = \mathbf{TJ}^{-1}, \hat{\bar{\mathbf{D}}}(\hat{\boldsymbol{\nu}}) = \mathbf{T\bar{D}}(\hat{\boldsymbol{\nu}})\mathbf{T}^{\top}, \hat{g}(\boldsymbol{\eta}) = \mathbf{T}g(\boldsymbol{\eta})$. The first four rows of $\hat{\mathbf{G}}_1$ are non-zero rows for the actuated body velocities, while the last two rows are zeros for the nonactuated. For coordinate transformation, we have

$$\dot{\boldsymbol{\eta}} = \mathbf{J}(\boldsymbol{\eta}_2)\boldsymbol{\nu}$$

$$\dot{\boldsymbol{\eta}} = \mathbf{J}(\boldsymbol{\eta}_2)\mathbf{T}^{\top}\hat{\boldsymbol{\nu}}$$

$$\dot{\boldsymbol{\eta}} = \hat{\mathbf{J}}(\boldsymbol{\eta}_2)\hat{\boldsymbol{\nu}} \tag{5.9}$$

Having the dynamics arranged in this manner, we rewrite the Hamiltonian as follows

$$\mathcal{H} = \frac{1}{2}\hat{\boldsymbol{\nu}}^{\top}\hat{\mathbf{M}}\hat{\boldsymbol{\nu}} \tag{5.10}$$

Due to the orthogonality of $\mathbf{T}$, the Hamiltonian in the transformed coordinates is equal to the original Hamiltonian. For a given arranged body-fixed momentum $\hat{\mathbf{p}} = \hat{\mathbf{M}}\hat{\boldsymbol{\nu}}$, the AUV dynamics in PCH form is given by

$$
\begin{bmatrix} \dot{\boldsymbol{\eta}} \\ \dot{\hat{\mathbf{p}}} \end{bmatrix} = \begin{bmatrix} 0 & \hat{\mathbf{J}} \\ -\hat{\mathbf{J}}^\top & -\hat{\mathbf{D}}(\hat{\boldsymbol{\nu}}) \end{bmatrix} \begin{bmatrix} \nabla_{\boldsymbol{\eta}}\mathcal{H} \\ \nabla_{\hat{\mathbf{p}}}\mathcal{H} \end{bmatrix} + \begin{bmatrix} 0 \\ \hat{\mathbf{G}}_1 \end{bmatrix} \mathbf{u} + \begin{bmatrix} 0 \\ \hat{\mathbf{G}}_2 \end{bmatrix} \mathbf{b} - \begin{bmatrix} 0 \\ \mathbf{I} \end{bmatrix} \hat{\mathbf{g}}(\boldsymbol{\eta}) \qquad (5.11)
$$

Furthermore, for the trajectory tracking problem, we define the new shaped Hamiltonian in transformed body-fixed velocities as

$$
\mathcal{H}_s = \frac{1}{2}\hat{\boldsymbol{\nu}}^\top \hat{\mathbf{M}}\hat{\boldsymbol{\nu}} + \frac{1}{2}\tilde{\boldsymbol{\eta}}^\top \hat{\mathbf{Q}}\tilde{\boldsymbol{\eta}} \qquad (5.12)
$$

$$
\hat{\mathbf{Q}} = \begin{bmatrix} q_{pos}\mathbf{I}_{3\times3} & 0 \\ 0 & q_{ang}\mathbf{I}_{3\times3} \end{bmatrix} \qquad (5.13)
$$

where $q_{pos}, q_{ang} > 0$ are two positive scalars representing the weights selected for the errors in inertial position and angle respectively.

According to the matching condition in theorem 4.1,

$$
\begin{bmatrix} 0 & \hat{\mathbf{J}} \\ -\hat{\mathbf{J}}^\top & -\hat{\mathbf{D}}(\hat{\boldsymbol{\nu}}) \end{bmatrix} \begin{bmatrix} \nabla_{\boldsymbol{\eta}}\mathcal{H} \\ \nabla_{\hat{\mathbf{p}}}\mathcal{H} \end{bmatrix} + \begin{bmatrix} 0 \\ \hat{\mathbf{G}}_1 \end{bmatrix} \mathbf{u} + \begin{bmatrix} 0 \\ \hat{\mathbf{G}}_2 \end{bmatrix} \mathbf{b} - \begin{bmatrix} 0 \\ \mathbf{I} \end{bmatrix} \hat{g}(\boldsymbol{\eta}) = \begin{bmatrix} 0 & \hat{\mathbf{J}} \\ -\hat{\mathbf{J}}^\top & -\hat{\mathbf{D}}_s(\hat{\boldsymbol{\nu}}) \end{bmatrix} \begin{bmatrix} \nabla_{\boldsymbol{\eta}}\mathcal{H}_s \\ \nabla_{\hat{\mathbf{p}}}\mathcal{H}_s \end{bmatrix}
$$
(5.14)

From now on, for simplicity, we will omit $\boldsymbol{\eta}$ and $\boldsymbol{\nu}$ from $\hat{g}$ and $\hat{\mathbf{D}}$. The biases, which represent the ocean current disturbances and other external forces will also be ignored for the time being. Analysis of the AUV stability in the presence of biases will be developed in the next section, see remark 5.1. Evaluating equation (5.14), we obtain

$$
\hat{\mathbf{G}}_1\mathbf{u} = \hat{g} - \left[\hat{\mathbf{D}}_s - \hat{\mathbf{D}}\right]\hat{\boldsymbol{\nu}} - \hat{\mathbf{J}}^\top \hat{\mathbf{Q}}\tilde{\boldsymbol{\eta}} \qquad (5.15)
$$

If $\hat{\mathbf{G}}_1$ is invertible, i.e., if the system is fully-actuated, then we may uniquely solve for the control input $\mathbf{u}$, given any $\mathcal{H}_s$. However, in the underactuated case, $\hat{\mathbf{G}}_1$ is not invertible, but it is only full column rank and $\mathbf{u}$ can only influence the terms in the range space of $\hat{\mathbf{G}}_1$. This leads to the following set of constraint equations, which must be satisfied for any choice of $\mathbf{u}$

$$\hat{\mathbf{G}}_1^{\perp} \left(\hat{g} - \left[\hat{\mathbf{D}}_s - \hat{\hat{\mathbf{D}}} \right] \hat{\nu} - \hat{\mathbf{J}}^{\top} \hat{\mathbf{Q}} \tilde{\eta} \right) = 0 \qquad (5.16)$$

where $\hat{\mathbf{G}}_1^{\perp}$ is a full rank left annihilator of $\hat{\mathbf{G}}_1$, i.e. $\hat{\mathbf{G}}_1^{\perp} \hat{\mathbf{G}}_1 = 0$. In the transformed AUV dynamics, $\hat{\mathbf{G}}_1 = \begin{bmatrix} \hat{\mathbf{G}}_{1,a} \\ 0_{2 \times 4} \end{bmatrix}$.

The left annihilator of $\hat{\mathbf{G}}_1$ could be selected as $\hat{\mathbf{G}}_1^{\perp} = \begin{bmatrix} 0_{2 \times 4} \mathbf{I}_{2 \times 2} \end{bmatrix}$. From (5.16), the last two entries in the vector $\hat{g} - \left[\hat{\mathbf{D}}_s - \hat{\hat{\mathbf{D}}} \right] \hat{\nu} - \hat{\mathbf{J}}^{\top} \hat{\mathbf{Q}} \tilde{\eta}$ have to be equal to zeros. $\hat{g}$ will satisfy this condition, since it is assumed to have two zeros as the last two entries and can be removed from the equation for its contribution is zero. The remaining terms can be decomposed with respect to their dependency with the body-fixed velocities and the inertial position errors as follows,

$$\hat{\mathbf{G}}_1^{\perp} \left[\hat{\mathbf{D}}_s - \hat{\hat{\mathbf{D}}} \right] \hat{\nu} = \begin{bmatrix} 0 \\ 0 \end{bmatrix} \qquad (5.17)$$

$$\hat{\mathbf{G}}_1^{\perp} \left[\hat{\mathbf{J}}^{\top} \hat{\mathbf{Q}} \tilde{\eta} \right] = \begin{bmatrix} 0 \\ 0 \end{bmatrix} \qquad (5.18)$$

One can think that $\hat{\mathbf{J}}^{\top} \hat{\mathbf{Q}} \tilde{\eta}$ is the weighted position error represented in body-fixed frame which is arranged by transformation matrix $\mathbf{T}$ into the actuated and

nonactuated body-fixed frame position error $\begin{bmatrix} \tilde{\mathbf{q}}_a^\top & \tilde{\mathbf{q}}_u^\top \end{bmatrix}^\top$. Equation (5.18) hints that the body-fixed frame position errors in the nonactuated coordinates are always zero. Consequently, at a certain direction, some position errors cannot be reduced using the available control effort which is a consequence of having underactuated restrictions. However, this restriction can be tackled using a proper design of navigation module like LOS. In the next section, we will show that the use of the navigation module will help the controller to achieve the stability conditions for trajectory tracking problem.

On the other hand, equation (5.17) restricts the selection of additional drag $\hat{\mathbf{D}}_a$ to be added in $\hat{\hat{\mathbf{D}}}$ on its lower block. The orthogonal transformation on $\mathbf{D}_s$ decomposes it into four blocks, namely, AA, NN, AN, NA, where N stand for nonactuated, A for actuated, given as follows,

$$\hat{\mathbf{D}}_s = \begin{bmatrix} \hat{\mathbf{D}}_{s,AA} & \hat{\mathbf{D}}_{s,AN} \\ \hat{\mathbf{D}}_{s,NA} & \hat{\mathbf{D}}_{s,NN} \end{bmatrix}$$

$$\hat{\hat{\mathbf{D}}} = \begin{bmatrix} \hat{\hat{\mathbf{D}}}_{AA} & \hat{\hat{\mathbf{D}}}_{AN} \\ \hat{\hat{\mathbf{D}}}_{NA} & \hat{\hat{\mathbf{D}}}_{NN} \end{bmatrix}$$

$$\hat{\mathbf{D}}_{s,NA} = \hat{\mathbf{D}}_{s,AU}^\top = -\hat{\hat{\mathbf{D}}}_{NA}$$

$$\hat{\mathbf{D}}_{a,NA} = \hat{\mathbf{D}}_{a,AU}^\top = \mathbf{0}_{2\times 4}$$

$$\hat{\mathbf{D}}_{s,NN} = -\hat{\hat{\mathbf{D}}}_{NN}$$

$$\hat{\mathbf{D}}_{a,NN} = \mathbf{0}_{2\times 2} \tag{5.19}$$

Equation (5.19) shows that since underactuated condition is present, we cannot

put extra damping term on the nonactuated body-fixed velocity and this means that $\hat{\mathbf{D}}_a$ are zeros in its bottom part. This is a result from the actuators limitations, which implies that we cannot manipulate the drag behaviour of the nonactuated body-fixed velocities. However, since the natural damping properties of the AUV are dissipative as mentioned in properties 2.3, at some degree we can rely on the natural damping of AUV to keep the nonactuated body-fixed velocities bounded. The stability analysis will be detailed in the following subsection.

5.3.1   Stability Analysis

Theorem 5.1. *Using PCH formalism combined with LOS navigation, the underactuated AUV is asymptotically stable.*

The proof theorem will be done in two steps,

1. in the first step we show that when the restoring force has two zeros in the nonactuated modes, the Uniformly Globally Asymptotically Stable (UGAS) condition of the equilibrium point can be achieved. This statement is presented in proposition 5.1.

2. in the second step, we show that when the restoring force is not assumed zero in the nonactuated modes, the UGAS condition of the equilibrium point is preserved as well. This statement is presented in proposition 5.2.

We will begin with the first case analysis in this subsection. The second will be presented in the following subsection.

We have shown some restrictions that are present in the underactuated conditions of PCH AUV controller design. The stability of the closed loop system is

101

evaluated by studying the value and sign of the time derivatives of the shaped Hamiltonian $\mathcal{H}_s$ along the trajectory. Using the dynamics given on the right hand side of (5.14), we obtain

$$\dot{\mathcal{H}}_s = -\hat{\boldsymbol{\nu}}^\top \hat{\mathbf{D}}_s \hat{\boldsymbol{\nu}} + \hat{\boldsymbol{\nu}}^\top \hat{\mathbf{G}}^\perp \hat{\mathbf{J}}^\top \hat{\mathbf{Q}} \tilde{\boldsymbol{\eta}}$$

$$\dot{\mathcal{H}}_s \le -\hat{\boldsymbol{\nu}}^\top \hat{\mathbf{D}}_s \hat{\boldsymbol{\nu}} + \hat{\boldsymbol{\nu}}_u^\top \tilde{\mathbf{q}}_u$$

$$\dot{\mathcal{H}}_s \le -\hat{\boldsymbol{\nu}}_a^\top \hat{\mathbf{D}}_{s,a} \hat{\boldsymbol{\nu}}_a - \hat{\boldsymbol{\nu}}_u^\top \hat{\mathbf{D}}_{s,u} \hat{\boldsymbol{\nu}}_u + \hat{\boldsymbol{\nu}}_u^\top \tilde{\mathbf{q}}_u \tag{5.20}$$

The term $\hat{\boldsymbol{\nu}}_u^\top \tilde{\mathbf{q}}_u$ in (5.20) prevents the closed loop system to converge to the desired inertial position and zero velocities, due to the integration effect of the position reflected on $\tilde{\mathbf{q}}_u$. Generally

$$\left\| \hat{\boldsymbol{\nu}}_u^\top \hat{\mathbf{D}}_{s,u} \hat{\boldsymbol{\nu}}_u \right\| \le \left\| \hat{\boldsymbol{\nu}}_u^\top \tilde{\mathbf{q}}_u \right\| \text{ as } t \to \infty$$

Evaluating $\tilde{\mathbf{q}}_u$ when the attitude are equal to the desired attitude ($\psi = \psi_d, \theta = \theta_d, \phi_d = \phi$), and the weighting matrix $\hat{\mathbf{Q}}$ given in (5.13), we have the following

$$\tilde{\mathbf{q}}_u = \begin{bmatrix} q_{pos} \left(a_1 \tilde{x} + a_2 \tilde{y} + a_3 \tilde{z} \right) \\ q_{ang} \tilde{\phi} \end{bmatrix}$$

$$a_1 = -\sin(\psi)\cos(\phi) + \cos(\psi)\sin(\theta)\sin(\phi)$$

$$a_2 = \cos(\psi)\cos(\phi) + \sin(\phi)\sin(\theta)\sin(\psi)$$

$$a_3 = \cos(\theta)\sin(\phi)$$

where a_i are the i-th element of the second column of $\mathbf{J}_1$ and $\tilde{\phi} = 0$. Substituting

102

the values of $\tilde{y}$ and $\tilde{z}$ in term of $\tilde{x}$ using the equation (5.1), we have the following,

$$\tilde{\mathbf{q}}_u = \begin{bmatrix} q_{pos}\tilde{x}\left(a_1 + a_2\tan(\psi) - a_3\sqrt{1 + \tan(\psi)^2}\tan(\theta)\right) \\ q_{ang}\tilde{\phi} \end{bmatrix}$$

A straight forward trigonometric substitution confirms that the first element of $\tilde{\mathbf{q}}_u$ will always be equal to zero. By equation (5.20), the actuated part of body-fixed velocities will be forced to zero by the controller, which is also true for $\tilde{\mathbf{q}}_a$. Furthermore, by means of desired attitude computation as presented in (5.1), we are able to force the error in position in sway direction to go to zero, provided that the pitch and yaw angles of the vehicle reach the desired values with faster dynamics. This will give $\hat{\boldsymbol{\nu}}_u^\top\tilde{\mathbf{q}}_u = 0$ and the time derivative of the shaped Hamiltonian will be negative definite. Therefore the position error on sway axis will asymptotically return to zero. This result can be summarized in proposition 5.1.

Proposition 5.1 (Stability of Underactuated AUV, where nonactuated entries of $\hat{g}$ are zeros)**.** *For a given underactuated AUV where nonactuated entries of $\hat{g}$ are assumed zeros, using desired attitude computation given by* (5.1)*, asymptotic stability condition of equilibrium point $\{x_d, y_d, z_d, \phi, \theta_d, \psi_d, \mathbf{0}\}$ given in theorem 4.1 is satisfied.*

5.3.2 Rolling Motion Over Trajectory

In the last subsection, we have seen the stability analysis of underactuated AUV trajectory tracking problem when the restoring forces are zeros in the nonactuated modes. However, this condition is an over-simplification of real restoring force [24] when roll angle is close to zero. When we take into account the real restoring force, the $\hat{g}$ can not be extracted from the underactuated constraint in

eq. (5.16).

Proposition 5.2 (General stability condition for Underactuated AUV). *Using desired attitude computation given by* (5.1), *there exists an uniform ultimate bound defined by manifold $\mathcal{F}$ described by*

$$\mathcal{F} \triangleq \{\mathbf{x} \in \mathbb{R}^n : \hat{\boldsymbol{\nu}}^\top \hat{\mathbf{D}}_s \hat{\boldsymbol{\nu}} \leq (W - B) \, |v| + \lambda |q|\} \tag{5.21}$$

where the $\dot{\tilde{\mathcal{H}}}_s$ is not strictly negative and all trajectories outside $\mathcal{F}$ are directed towards it. Furthermore, the equilibrium point $\{x_d, y_d, z_d, \phi, \theta_d, \psi_d \, \mathbf{0}\}$ is asymptotically stable.

Proof. Assume that the following equation satisfies proposition 5.1

$$\hat{\mathbf{G}}^\perp \left[\bar{g} - \mathbf{D}_a \hat{\boldsymbol{\nu}} - \hat{\mathbf{J}}^\top \mathbf{Q} \tilde{\boldsymbol{\eta}} \right] = 0 \tag{5.22}$$

where the restoring forces $\hat{g}$ are decomposed into actuated restoring forces $\bar{g}$ which are cancelled by feedback and nonactuated restoring forces $\tilde{g}$ which still remain. The remaining restoring forces on nonactuated motion $\tilde{g}$ are given below (assuming that the center of gravity lies on the origin,center of buoyancy horizontal axis x_b, y_b also equal to zero, [24]).

$$\tilde{g}(\boldsymbol{\eta}) = \begin{bmatrix} \mathbf{0}_{4 \times 1} \\ -(W - B) \cos(\theta) \sin(\phi) \\ -z_b B \cos(\theta) \sin(\phi) \end{bmatrix} \tag{5.23}$$

The rolling motion on the AUV due to the restoring forces behaves like the damped inverted pendulum dynamics. Inspired by the analogy to the damped inverted pendulum dynamics to analyse the stability of roll motion, we propose a modi-

104

fied Lyapunov function as follows

$$\bar{\mathcal{H}}_s = \mathcal{H}_s + \lambda \left[1 - \cos(\theta) \cos(\phi) \right] = \mathcal{H}_s + \bar{\mathcal{H}}_c \tag{5.24}$$

where $\mathcal{H}_s$ given by (5.12). Evaluating the time derivative of $\bar{\mathcal{H}}_s$ along the trajectory we have

$$\dot{\bar{\mathcal{H}}}_s = -\hat{\boldsymbol{\nu}}^\top \hat{\mathbf{D}}_s \hat{\boldsymbol{\nu}} + \hat{\boldsymbol{\nu}}^\top \tilde{g}(\boldsymbol{\eta}) + \frac{\partial \bar{\mathcal{H}}_c}{\partial \boldsymbol{\eta}} \dot{\boldsymbol{\eta}}$$

$$\hat{\boldsymbol{\nu}}^\top \tilde{g}(\boldsymbol{\eta}) = - \left[v \left(W - B \right) + p z_b B \right] \cos(\theta) \sin(\phi)$$

$$\frac{\partial \bar{\mathcal{H}}_c}{\partial \boldsymbol{\eta}} \dot{\boldsymbol{\eta}} = \lambda \left[\cos(\theta) \sin(\phi) \dot{\phi} + \sin(\theta) \cos(\phi) \dot{\theta} \right]$$

$$\dot{\phi} = p + \sin(\phi) \tan(\theta) q + \cos(\phi) \tan(\theta) r$$

$$\dot{\theta} = \cos(\phi) q - \sin(\phi) r$$

$$\frac{\partial \bar{\mathcal{H}}_c}{\partial \boldsymbol{\eta}} \dot{\boldsymbol{\eta}} = \lambda \left[p \cos(\theta) \sin(\phi) + q \sin(\theta) \right]$$

if we select $\lambda = z_b B$

$$\dot{\bar{\mathcal{H}}}_s = -\hat{\boldsymbol{\nu}}^\top \hat{\mathbf{D}}_s \hat{\boldsymbol{\nu}} - v \left(W - B \right) \cos(\theta) \sin(\phi) + \lambda q \sin(\theta) \tag{5.25}$$

$$\dot{\bar{\mathcal{H}}}_s \leq -\hat{\boldsymbol{\nu}}^\top \hat{\mathbf{D}}_s \hat{\boldsymbol{\nu}} + \left(W - B \right) |v| + \lambda |q| \tag{5.26}$$

We can see from eq. (5.25) that, when the vehicle is moving in the horizontal plane with $\phi = 0, \theta = 0$, the stability of the motion is guaranteed.

For general conditions, there exists a manifold $\mathcal{F}$

$$\mathcal{F} \triangleq \{ \mathbf{x} \in \mathbb{R}^n : \hat{\boldsymbol{\nu}}^\top \hat{\mathbf{D}}_s \hat{\boldsymbol{\nu}} \leq \left(W - B \right) |v| + \lambda |q| \} \tag{5.27}$$

where the $\dot{\hat{\mathcal{H}}}_s$ is not strictly negative. Note that $\mathbf{x}_d = \{x_d, y_d, z_d, \phi, \theta_d, \psi_d, \mathbf{0}\} \in \mathcal{F}$.

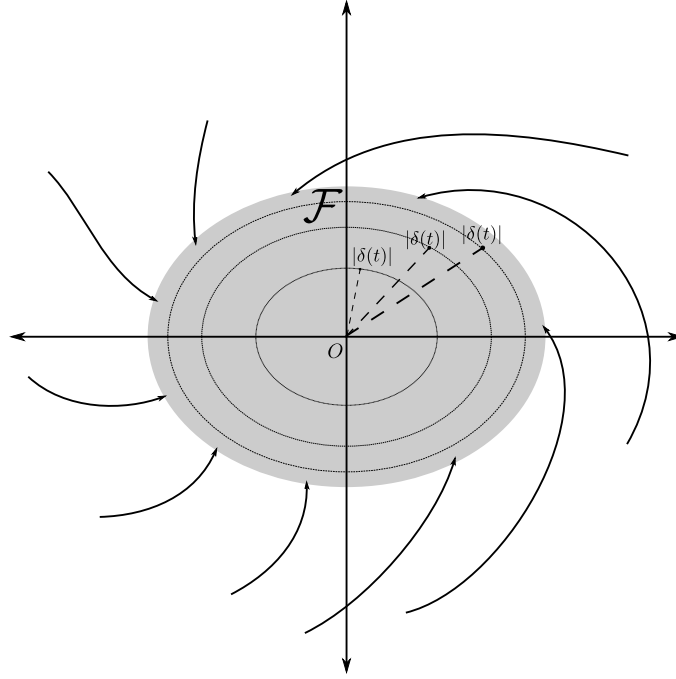Figure 5.3: Illustration of AUV trajectory and closed set $\mathcal{F}$

Outside $\mathcal{F}$, the trajectory will be pushed into $\mathcal{F}$, because of the negative definiteness of $\dot{\hat{\mathcal{H}}}_s$ due to the dominance of $\hat{\boldsymbol{\nu}}^\top \hat{\mathbf{D}}_s \hat{\boldsymbol{\nu}}$ and hence the Lyapunov stability condition is satisfied. Furthermore, inside $\mathcal{F}$, the term

$$\delta(\boldsymbol{\nu}_n, \boldsymbol{\eta}_n) = -v\,(W - B)\cos(\theta)\sin(\phi) + \lambda q \sin(\theta)$$

$$\boldsymbol{\nu}_n \triangleq [v\ q]^\top$$

$$\boldsymbol{\eta}_n \triangleq [\phi\ \theta]^\top$$

is dominant and cannot be neglected. Indeed, inside $\mathcal{F}$, $\dot{\hat{\mathcal{H}}}_s$ can be positive. However, there exist a class $\mathcal{KL}$ function β, where $|\delta| \leq \beta(\boldsymbol{\nu}_n, t)$ due to the damping in v and q. Since the largest invariant set in $\mathcal{F}$ is the origin, invoking *LaSalle* Invariant principle leads to the asymptotic stability of the origin. (See figure 5.3 for the

106

illustration).   □

Except for hovering condition, most of the time the vehicle will be outside $\mathcal{F}$ and hence, the stability condition will be similar to the previous case, where $\tilde{g}$ are assumed to be zero.

This condition is similar to the one found in [81], where the exponential stabilization of AUV can be achieved without using roll control torque, if the hydrodynamics restoring forces in roll motion are large enough. The same condition also appeared in [3], where the Lyapunov time derivative of the closed loop AUV system using the back-stepping design has a similar term due to null space of the input matrix $\mathbf{G}$.

Remark 5.1 (Disspativity of the closed loop). In the case that the effect of ocean disturbances are considered as in equation (2.15), one can transform equation (2.15) into actuated - nonactuated part as in the previous section. Then using the similar convergence analysis mentioned in section 4.6.2, it is shown that using the Lyapunov $\mathcal{V}$ and evaluating the time derivative along the trajectory, we obtain

$$\dot{\mathcal{V}} \le - \begin{bmatrix} \tilde{\boldsymbol{\eta}}^\top & \hat{\boldsymbol{\nu}}^\top \end{bmatrix} \bar{\mathbf{Q}} \begin{bmatrix} \tilde{\boldsymbol{\eta}} \\ \hat{\boldsymbol{\nu}} \end{bmatrix} + \frac{1}{2}\gamma^2 \mathbf{b}^\top \mathbf{b} - \frac{1}{2}\bar{\mathbf{y}}^\top \bar{\mathbf{y}} \tag{5.28}$$

$$\bar{\mathbf{y}} \triangleq \frac{1}{\gamma}\hat{\mathbf{J}}^{-\top} \left[\hat{\mathbf{M}}^{-1}\mathbf{S}^\top \tilde{\boldsymbol{\eta}} + \hat{\boldsymbol{\nu}} \right] \tag{5.29}$$

The input of dissipative mapping is equal to the disturbance $\mathbf{b}$ and the output is given by $\bar{\mathbf{y}}$. The last equation is exactly the $\mathcal{L}_2$ differential dissipation inequality, with the supply rate $\varpi = \frac{1}{2}\gamma^2 \mathbf{b}^\top \mathbf{b} - \frac{1}{2}\bar{\mathbf{y}}^\top \bar{\mathbf{y}}$. Providing the existence of $\mathbf{S}$ as mentioned in section 4.6.2, it follows that the same inequality is necessary and

sufficient condition for $\mathcal{L}_2$ ISS condition. This means that a squared integrally bounded disturbance will only make a squared integrally bounded state distance from the equilibrium point. (See for example [64], p 243). The parameter γ determines how small the disturbance effect will be seen in the output propagation.

5.4   Simulation Results

In this subsection, we present simulations of the underactuated controller design. In the following simulations, the controller that we use has $\mathbf{D}_a$ that does not cancel the Coriolis and natural damping of the vehicle. $\mathbf{D}_a$ is set to be constant to give higher damping effects to make the system more robust. Ocean disturbances are also assumed to be irrational here. The overall design of the controller and navigation unit is shown in figure 5.4.
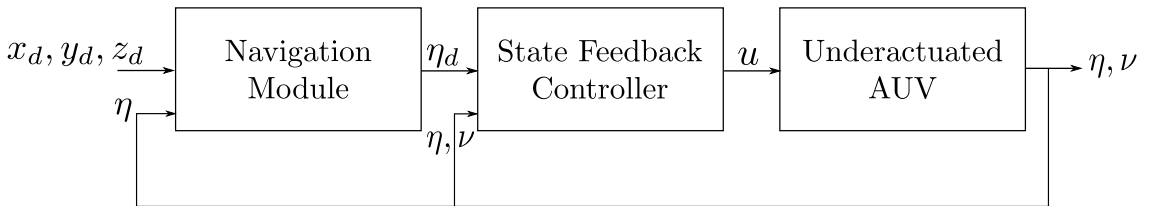

Figure 5.4: Controller and navigation design for underactuated AUV

5.4.1   Horizontal Plane Tracking

For horizontal plane tracking, we make a circlular trajectory with forward velocity increasing from zero to a maximum value and then decreasing again to zero. To give a picture about LOS algorithm work, we place an initial position error. Trial and error shows that the best practice is to set q_{ang} more than ten

times higher than q_{pos} in (5.13). Trajectory simulation result is shown in figure 5.5. As we can see, the vehicle is first driven to the correct attitude at the beginning and then goes to the initial point. Some of disturbance effect can be seen as well, where the trajectory and attitude is a little bit disturbed. When the vehicle nearly reaches the desired trajectory and the surge velocity increases, then the disturbance effect is decreased, as we are expecting from eq. (5.28).

Due to the natural damping in roll body-fixed velocity and restoring force, the roll angle of the vehicle is nearly zero, as seen in figure 5.7d. The depth of the vehicle can also be maintained well at 25 m, as seen in figure 5.7c. The pitch angle is slightly bigger than the roll angle since it is driven by LOS to keep up the vehicle depth as seen also in figure 5.7e. Heading angle is shown in figure 5.7f, where it is more disturbed compared to roll and pitch angle, as it is maintained by LOS to converge to the desired attitude in the presence of disturbance and initial position error.

Thrusters command are shown in figure 5.6. High forces are observed at the starting period for the two thrusters at the rear end of the AUV due to the initial position error. Afterwards the back thrusters force are almost less than 50 N. For the thrusters present on the body, the forces are less compared to the two at the rear. The forces required are less than 10 N, which is mainly to keep the vehicle depth constant at 25 m.

5.4.2   Full Space Tracking

Using the same controller parameters as given in the previous subsection, this simulation shows the ability of the designed controller to drive the MARES in
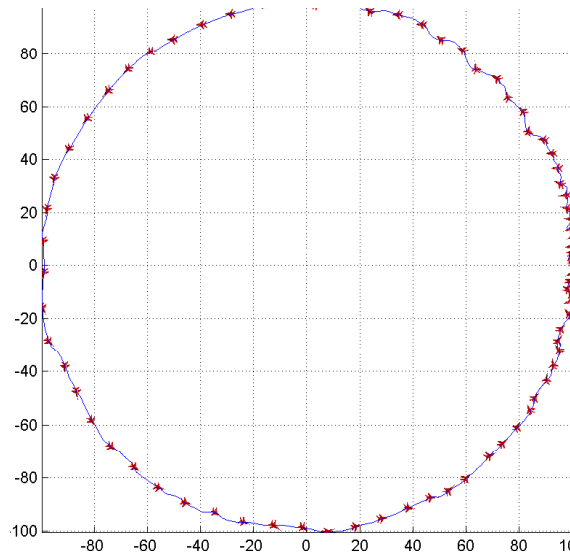
Figure 5.5: Trajectory of underactuated MARES - horizontal tracking

three-dimensional tracks. Here, we require the AUV to follow spiral trajectory which moves from sea surface to sea bottom. Figures 5.9,5.10, 5.12 and 5.11 show the ability of the controller to handle even bigger disturbances, hence the vehicle still tracks the desired trajectory.

Furthermore, as we can see from figure 5.10, the thrust forces nearly are very much similar to the horizontal plane tracking thrust forces mentioned before. The pitch angle almost settles near -0.06 rad as seen in figure 5.11e, whilst roll angle is near zero as seen in figure 5.11d. From these two simulations, we can see that the closed loop AUV is capable of tracking the desired trajectory with satisfactory results, even in the presence of exogenous disturbance. In the following section we shall make a comparison between our results with the result of the back-stepping design technique developed in [2][3].

(a) Thruster command force 1 f_1

(b) Thruster command force 2 f_2

(c) Thruster command force 3 f_3
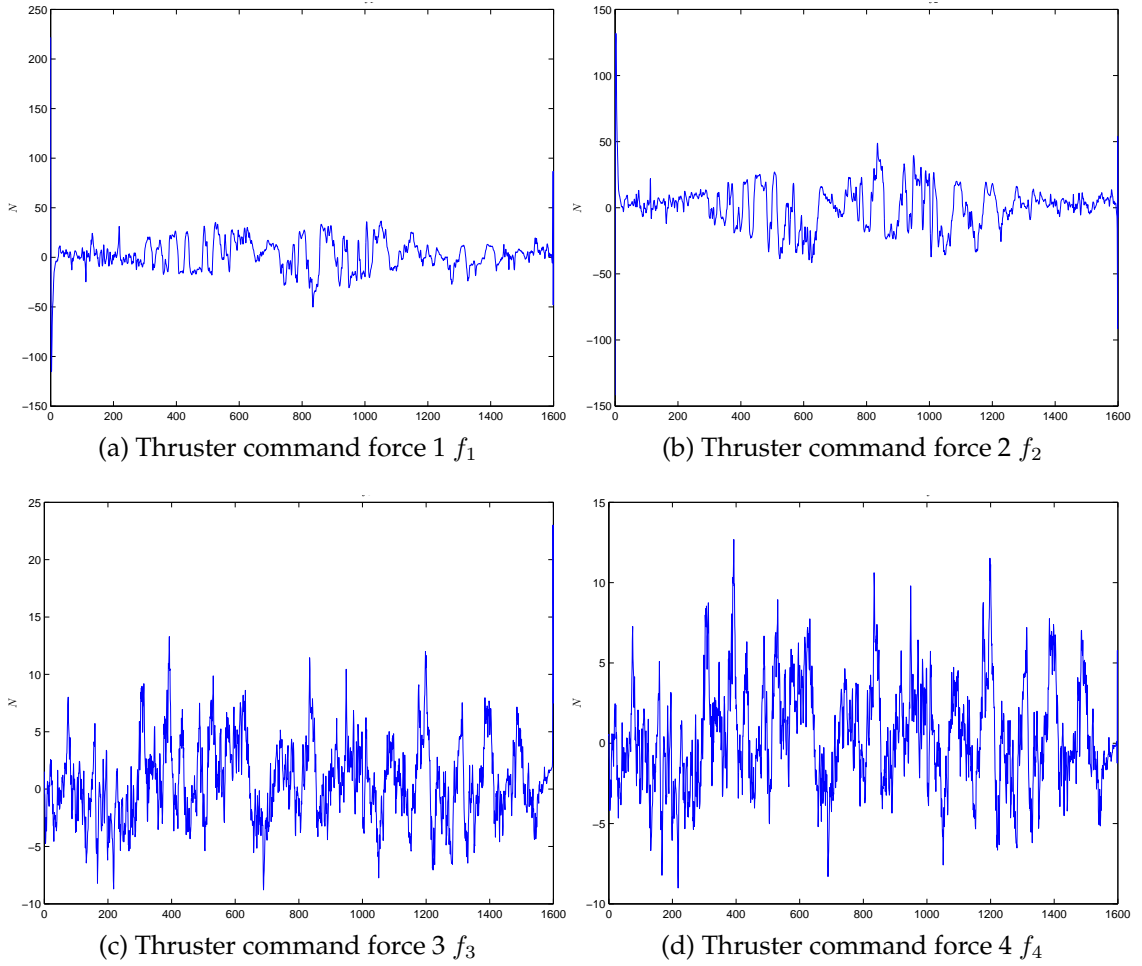
(d) Thruster command force 4 f_4

Figure 5.6: Thruster command force for underactuated MARES - horizontal tracking
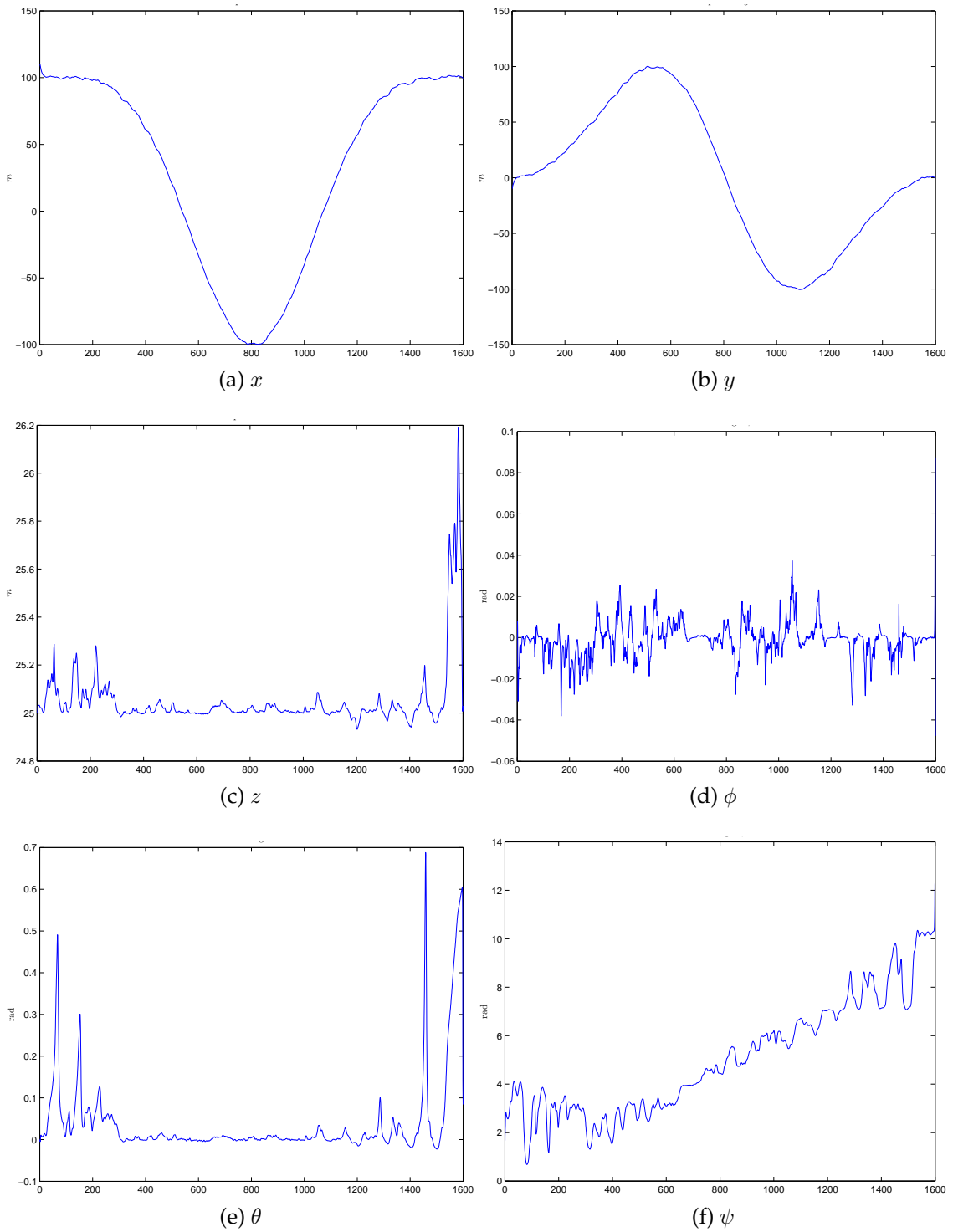
Figure 5.7: Inertial position and angle for underactuated MARES - horizontal tracking

(a) u

(b) v

(c) w

(d) p

(e) q

(f) r

Figure 5.8: Body-fixed velocity for underactuated MARES - horizontal tracking
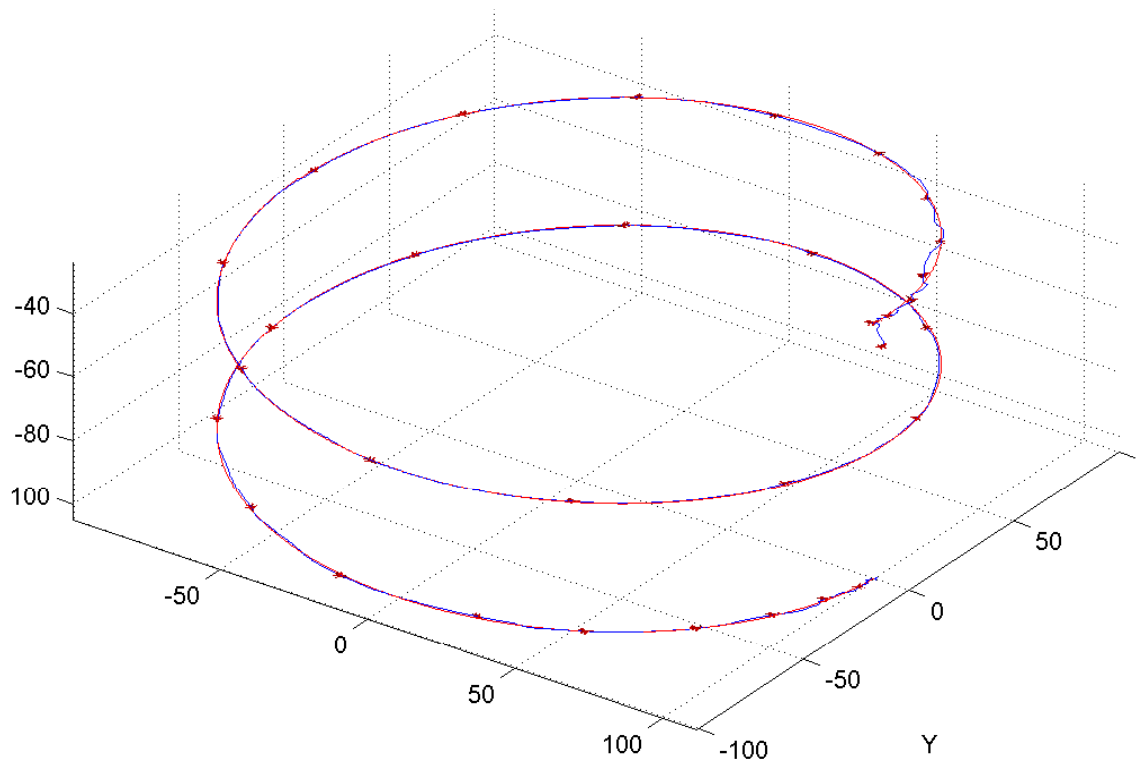
Figure 5.9: Trajectory of underactuated MARES - full space tracking

(a) Thruster command force 1 f_1

(b) Thruster command gorce 2 f_2

(c) Thruster command force 3 f_3

(d) Thruster command force 4 f_4

Figure 5.10: Thruster command force for underactuated MARES - full space tracking
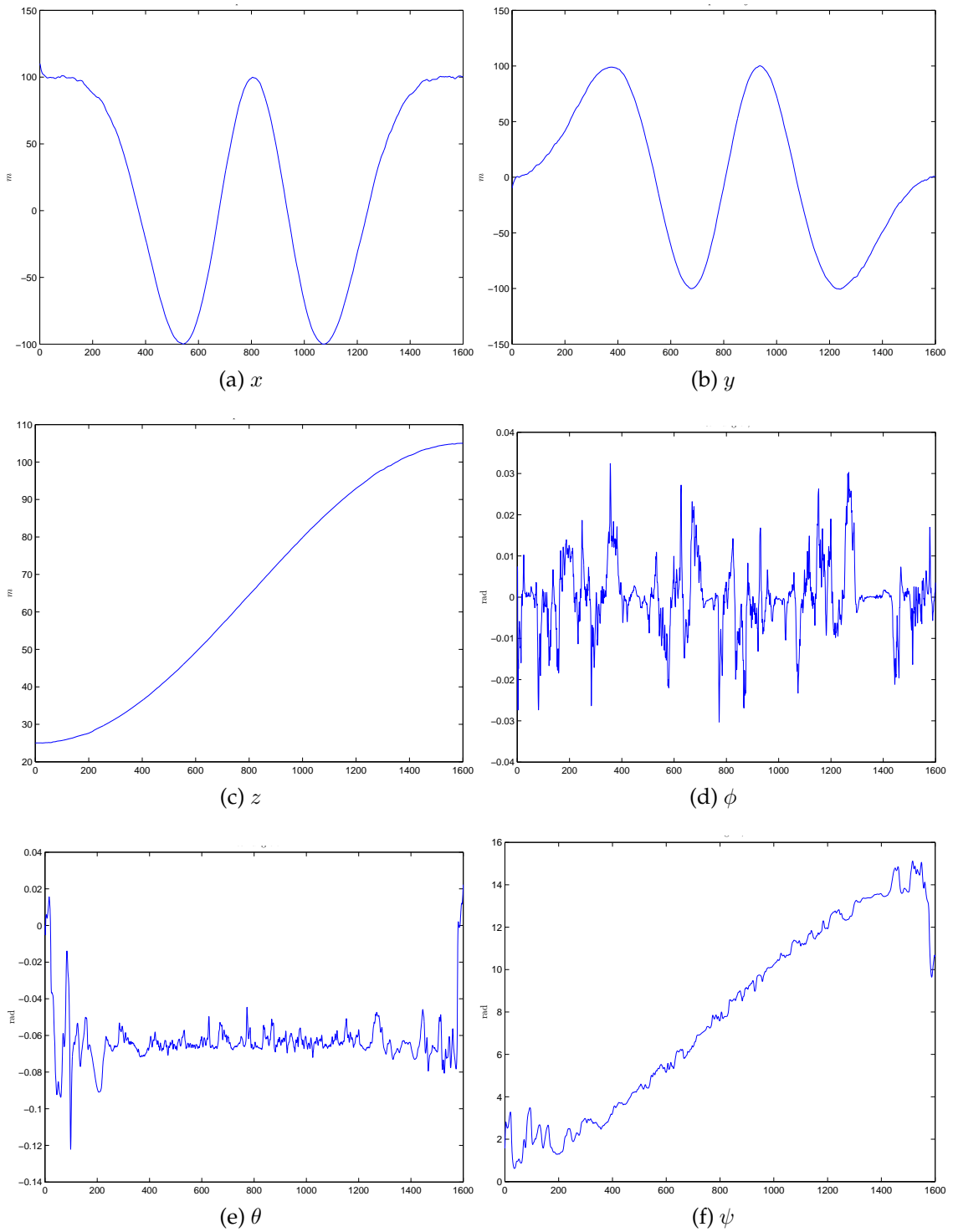
Figure 5.11: Inertial position and angle for underactuated MARES - full space tracking
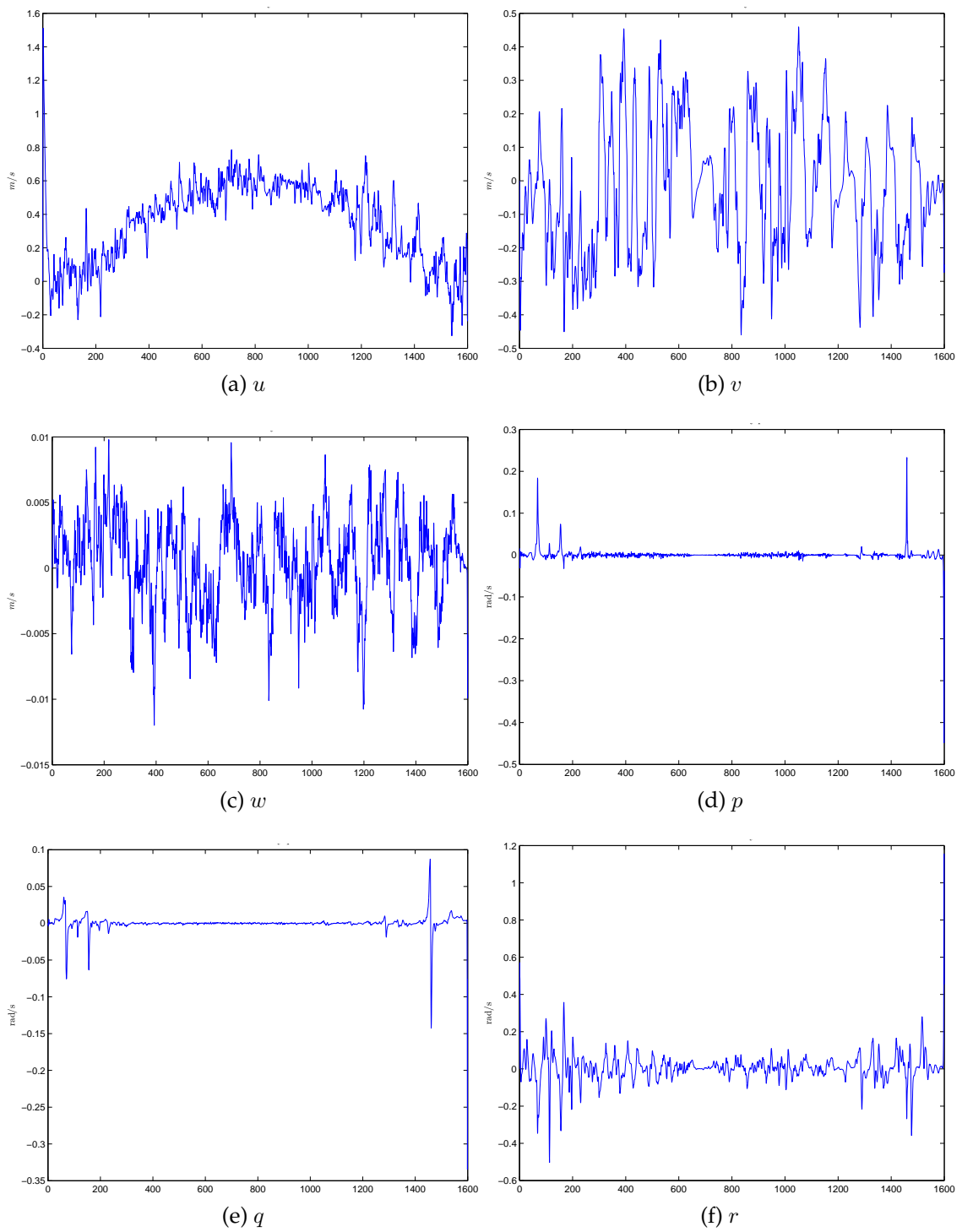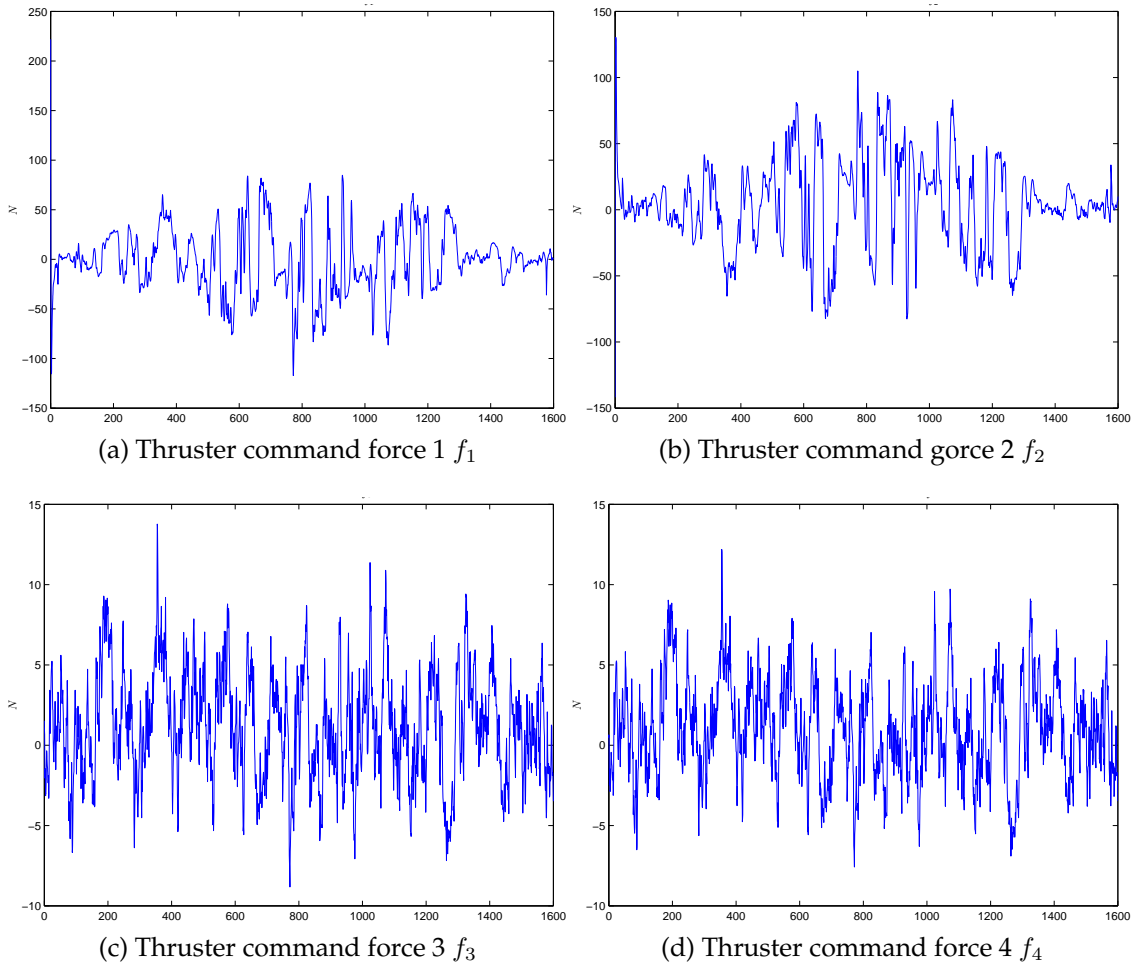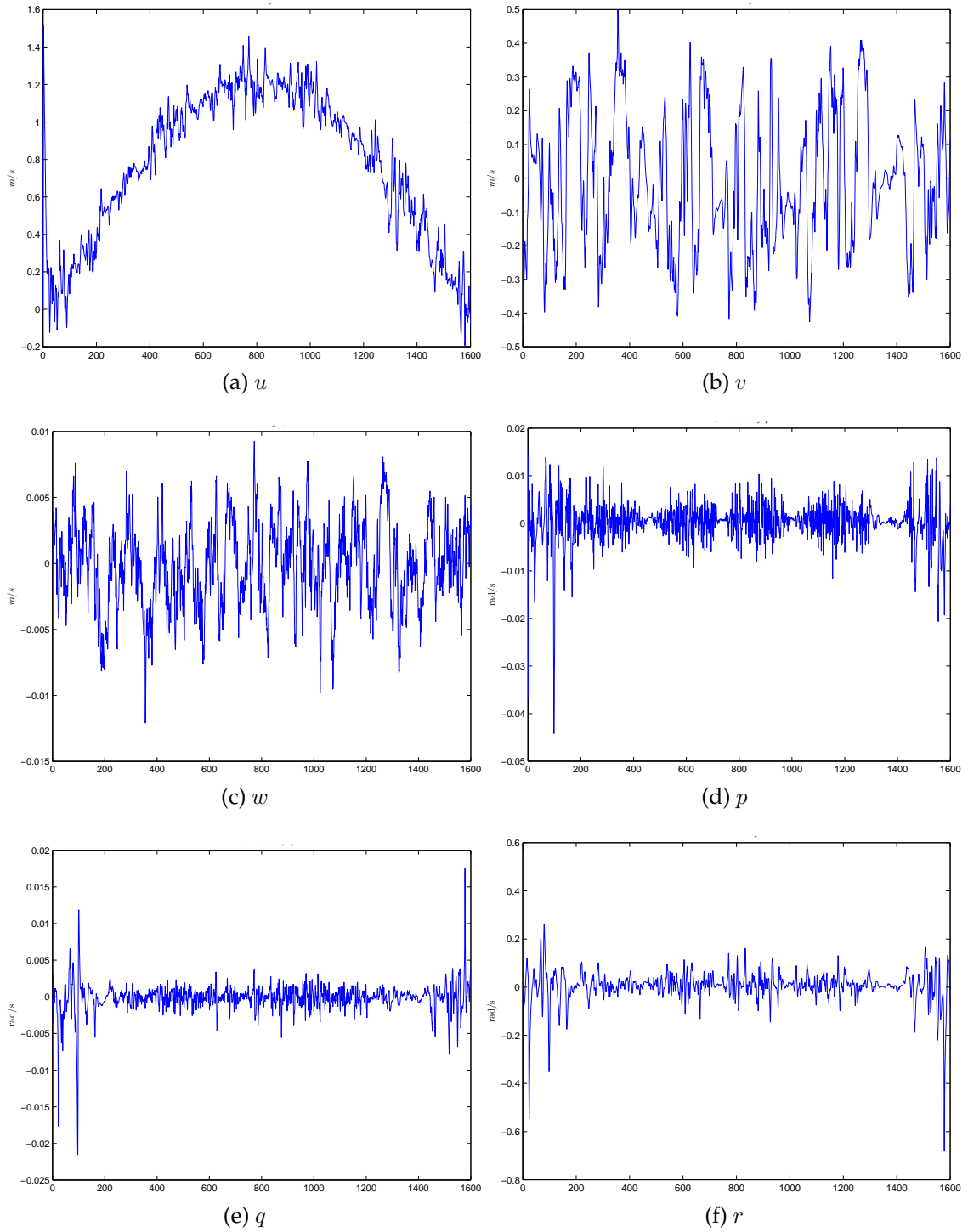
(a) u

(b) v

(c) w

(d) p

(e) q

(f) r

Figure 5.12: Body-fixed velocity for underactuated MARES - full space tracking

5.4.3 Full Space Tracking - Comparison

To show the appealing benefits of the proposed controller design, we present a comparison with back-stepping design of underactuated AUV proposed in [2][3]. To support the fairness of comparison, we shall modify the MARES to three degrees of freedom forces, because the back-stepping design was developed for three DOF underactuated vehicle. Added mass, drag forces, restoring forces and the amount of exogenous disturbances are kept the same as in the previous simulation.

As seen from figure 5.13, although the back-stepping design is not designed to handle exogenous disturbance, coupled quadratic drag and coupled translational-rotational added mass, the closed loop response still gives a good trajectory tracking. However, the trajectory tracking result is inferior when compared to the proposed design. This is explained as given below,

1. Trajectory tracking errors are much higher compared to PCH design. See figure 5.15, blue line for PCH, while red line for back-stepping.

2. The thrust forces are far more higher compared to PCH. Some of them have order 10^5 N. This probably comes from the computation of input signal where the differentiation of α involving third time derivative of the desired inertial position as well as differentiation of quadratic drag which is a function of an absolute value of velocity.

3. The roll, pitch and yaw angle have a large jump. This is probably caused by the same reason mentioned in number 2.
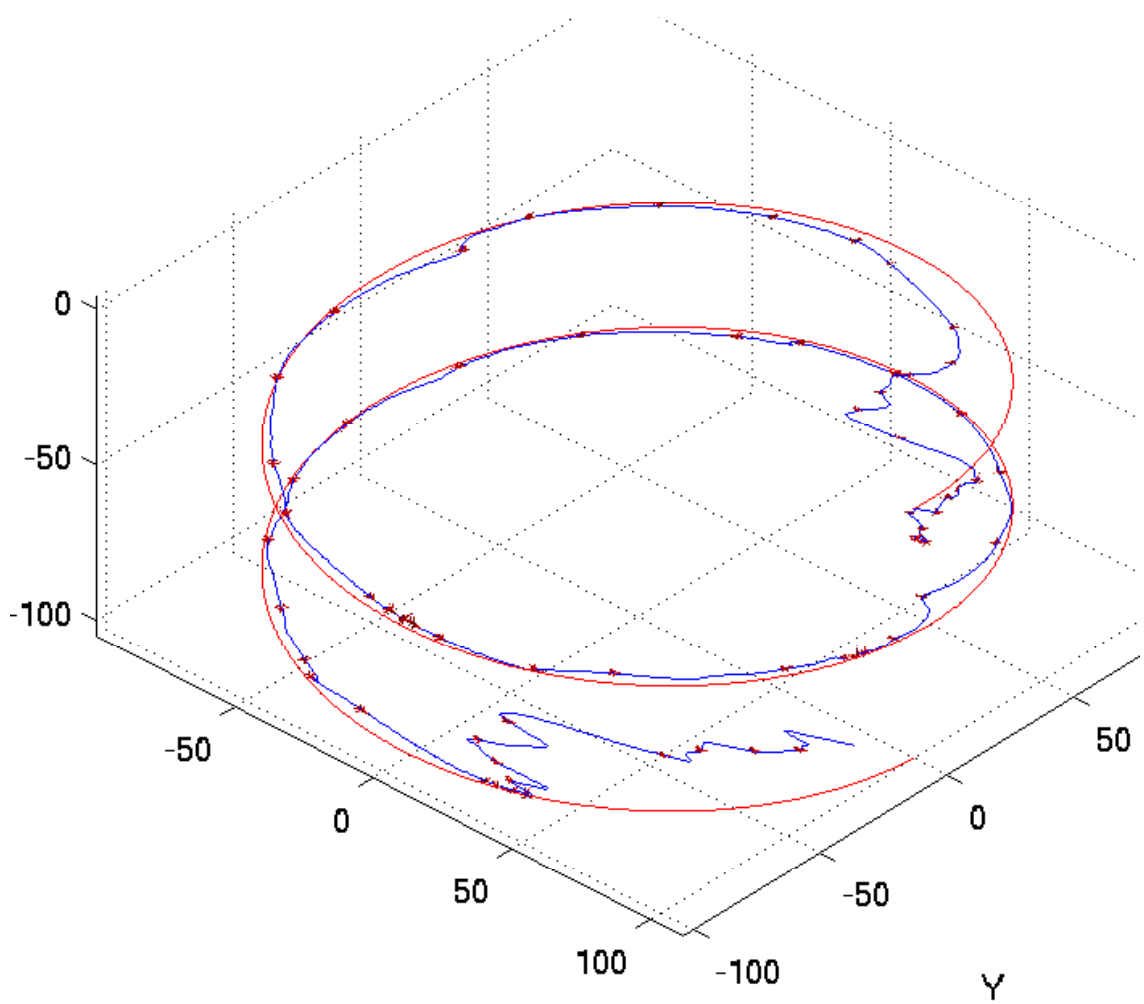
Figure 5.13: Trajectory of underactuated MARES - full space tracking (Back-stepping)

(a) Thruster command force 1 f_1

(b) Thruster command force 2 f_2

(c) Thruster command force 3 f_3
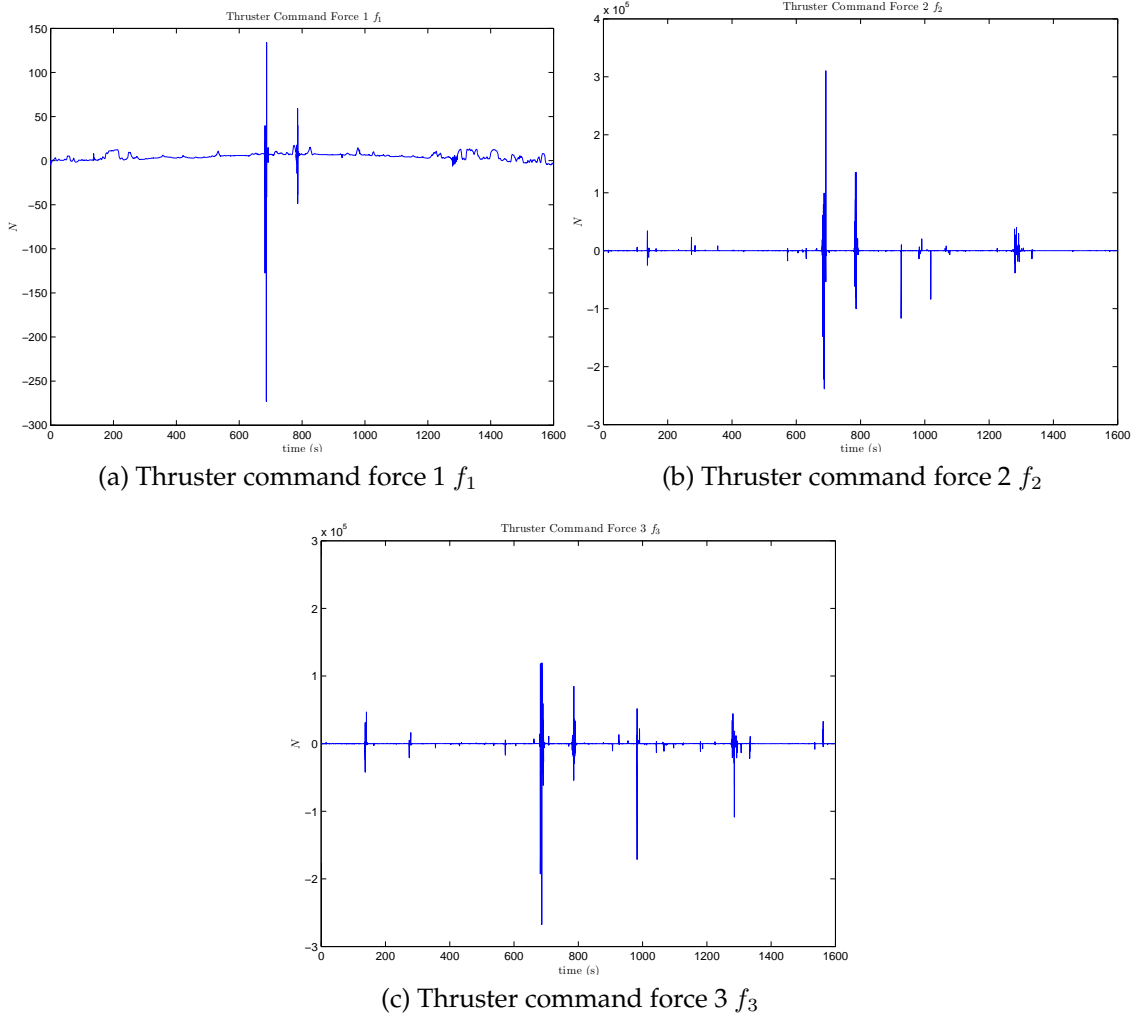
Figure 5.14: Thruster command force for underactuated MARES - full space tracking(Back-stepping)

(a) e_x

(b) e_y

(c) e_z
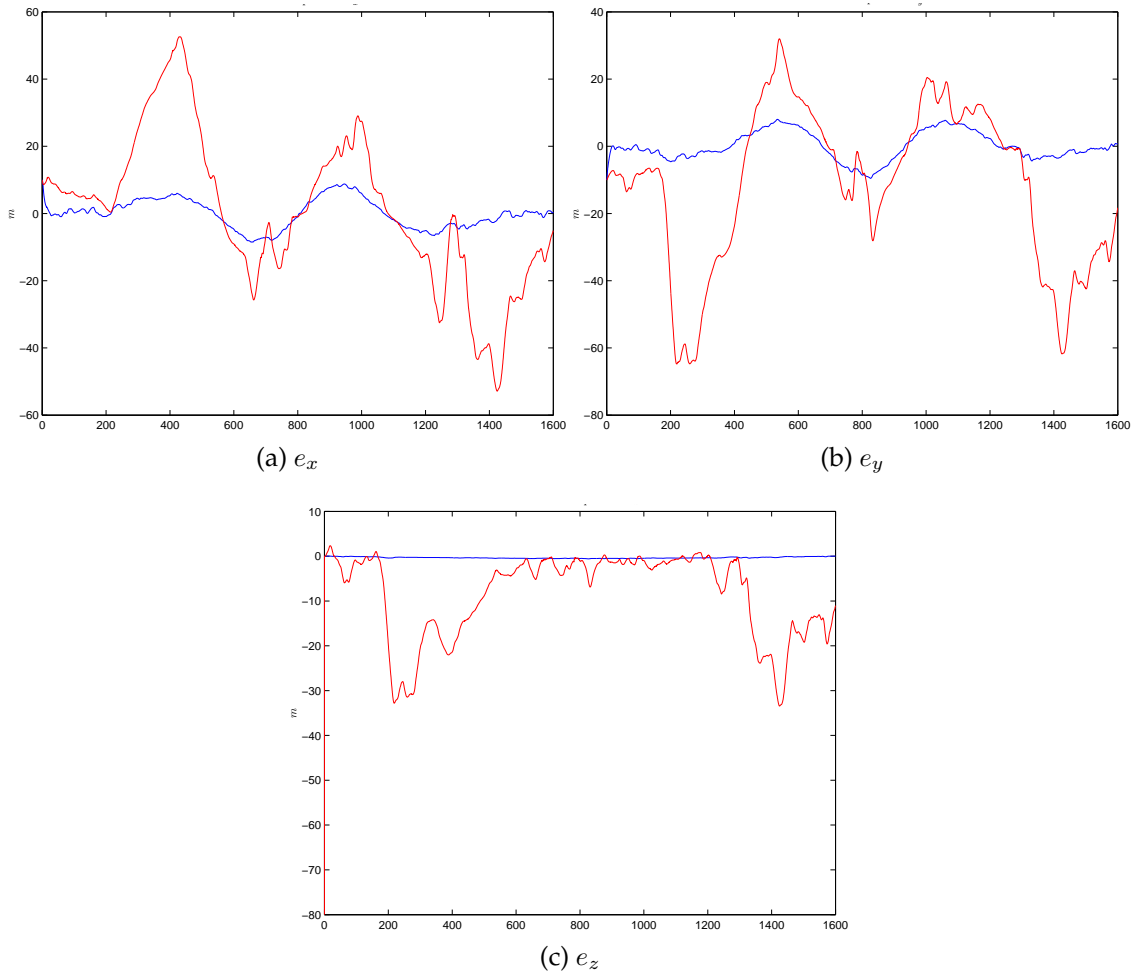
Figure 5.15: Comparison of trajectory tracking error (inertial frame) - Back-stepping and PCH

121
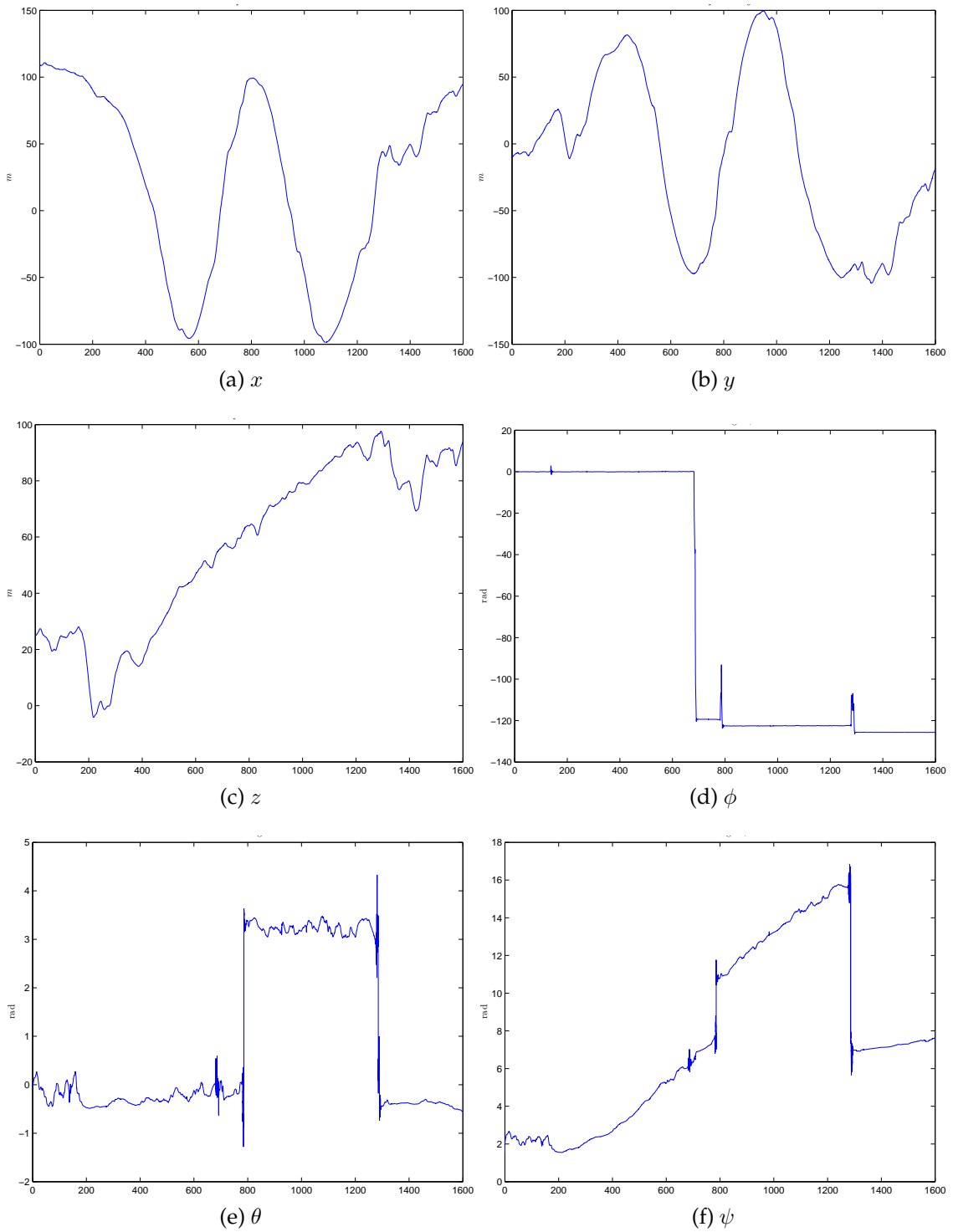
Figure 5.16: Inertial position and angle for underactuated MARES - full space Tracking (Back-stepping)

(a) u

(b) v

(c) w

(d) p

(e) q

(f) r
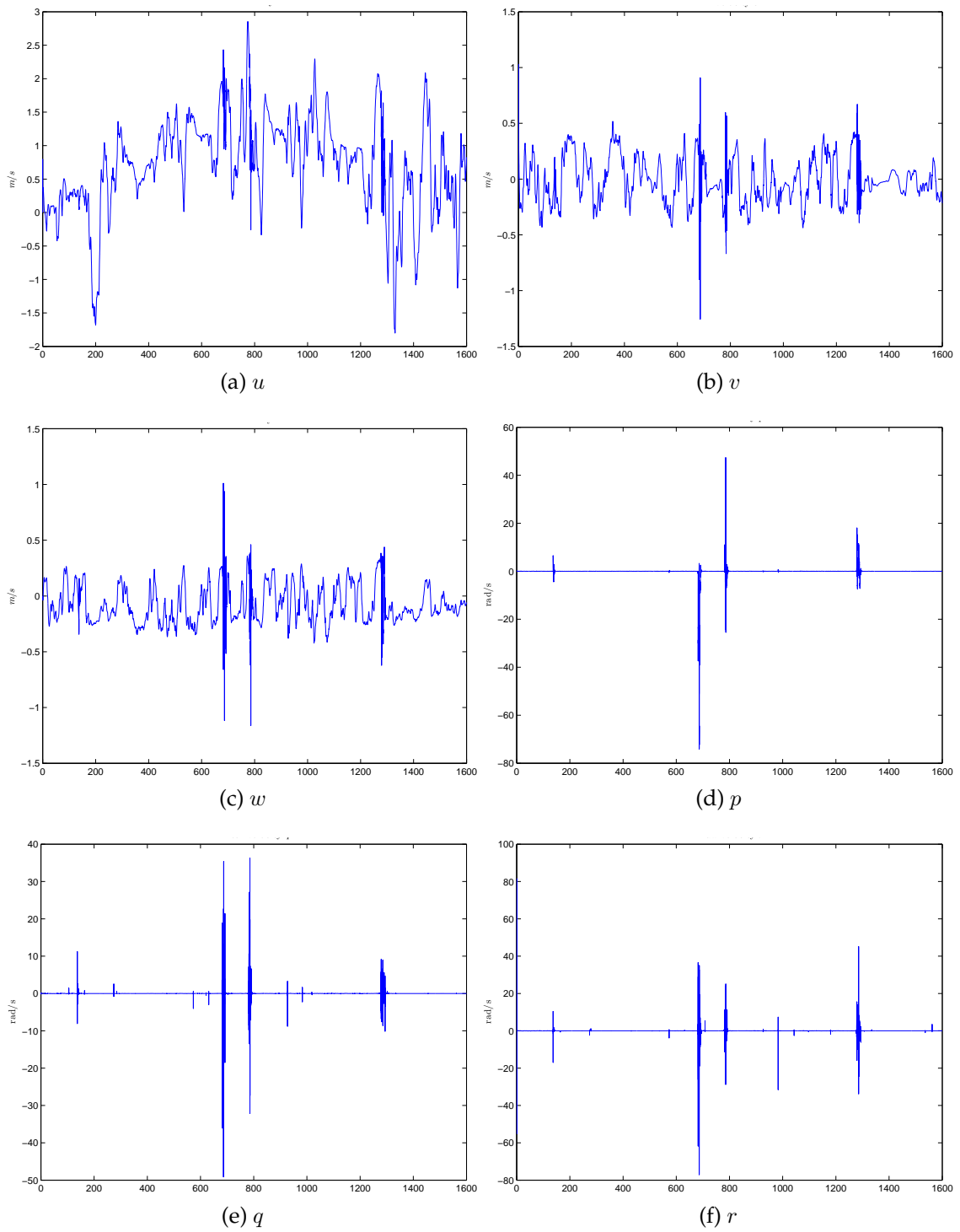
Figure 5.17: Body-fixed velocity for underactuated MARES - full space tracking (Back-stepping)

123

5.5 Conclusions

In this chapter, we have established the extension of the passivity-based PCH control design of AUV to the underactuated condition. Using a proper design of desired attitude and validating the matching condition for the underactuated restriction, we are able to design the controller that can lead the underactuated AUV to track full space trajectory. The benchmark results with the back-stepping design developed in [3],[2] show a definite superiority of the proposed controller design over the back-stepping design.

Chapter 6

Observer Design

6.1 Introductions

The state feedback design requires the availability of the states to produce the control input. While many controller designs are based on the state feedback, it is a fact that in many systems, measuring all states might be not possible or physically not feasible. The observer provides a way to have an image of the system states from measurements of the output. In the framework of Port Controlled Hamiltonian (PCH), we present an approach to design an observer for a specific class of PCH that is well suited to Autonomous Underwater Vehicle (AUV). Since the pioneer work of Luenberger's observer in the mid sixties [61], observer design for dynamic systems has drawn much attention and experienced many remarkable results [95, 34, 78].

The design of an observer for linear system is a mature field. On the other hand, for the non-linear counterpart, the design problem is still challenging. There are

many observer design results available in the literature for specific classes of non-linear systems [47, 48, 104, 40, 72, 6, 79]. For PCH, there have been several ob-server designs for Hamiltonian systems proposed in the literature. Herbert [93], proposed a design method for a class of generalized Hamiltonian systems, in which the output was assumed to be linear and the structure matrix was assumed to be constant. Lohmiller and Slotine [59] proposed an observer design of a class of Hamiltonian systems based on their earlier work on contraction analysis to produce a globally convergent observer. In [103], an observer of PCH systems was designed using what is called 'Augment plus Feedback'. In this method, the observer is designed using not only output error, but also a feedback through the observed system, aiming to create a passivation in the augmented state and state estimate dynamics. In [97], the observer design was proposed using a similar way.

Before we present the observer design in PCH, we need to recall the vanishing perturbation theorem[42] in input to state stability of nonlinear systems and the stability of cascaded nonlinear time varying system [77]. We will use the vanish-ing perturbation lemma to show that the error dynamics have asymptotic stable equilibrium point at origin. The stability of cascaded nonlinear systems will be used to establish the separation principle of PCH observer and controller design.

The contributions of this chapter are

1. New framework of observer design for quadratic Hamiltonian PCH sys-tems.

2. Design of PCH based nonlinear observer for AUV.

3. The separation principle analysis of PCH systems in generals and AUV for

particular cases.

4. Re-design of AUV observer proposed in [83].

6.2 Vanishing Perturbation

Consider the system

$$\dot{\mathbf{x}} = f(t, \mathbf{x}) + g(t, \mathbf{x}) \tag{6.1}$$

where $f : [0, \infty) \times \mathcal{D} \to \mathbb{R}^n$ and $g : [0, \infty) \times \mathcal{D} \to \mathbb{R}^n$ are piecewise continuous in t and locally Lipschitz in $\mathbf{x}$ on $[0, \infty) \times \mathcal{D}$ and $\mathcal{D} \subset \mathbb{R}^n$ is an open connected set that contains the origin $\mathbf{x} = 0$. We consider this system as a perturbation of the nominal system

$$\dot{\mathbf{x}} = f(t, \mathbf{x}) \tag{6.2}$$

The perturbation term $g(t, \mathbf{x})$ could result from errors in modeling the nonlinear dynamics or external forces. In a typical situation we do not know $g(t, \mathbf{x})$, but we know some information about it, like its upper-bound $\|g(t, \mathbf{x})\|$. We will consider the special class of the perturbations, where $g(t, 0) = 0$, known as *Vanishing Perturbation*. In this case, the perturbed system (6.1) has an equilibrium point at the origin.

Suppose that the origin is an exponentially stable equilibrium point of the nomi-

nal system (6.2) and let $V(t, \mathbf{x})$ be a Lyapunov function that satisfies

$$c_1 \|\mathbf{x}\|_2^2 \leq V(t, \mathbf{x}) \leq c_2 \|\mathbf{x}\|_2^2 \tag{6.3}$$

$$\frac{\partial V(t, \mathbf{x})}{\partial t} + \frac{\partial V(t, \mathbf{x})}{\partial \mathbf{x}} f(t, \mathbf{x}) \leq -c_3 \|\mathbf{x}\|_2^2 \tag{6.4}$$

$$\left\| \frac{\partial V(t, \mathbf{x})}{\partial \mathbf{x}} \right\|_2 \leq c_4 \|\mathbf{x}\|_2 \tag{6.5}$$

for all $[0, \infty) \times \mathcal{D}$, for some positive constant c_1, c_2, c_3, c_4. In addition, suppose the perturbation term $g(t, \mathbf{x})$ satisfies the linear growth bound

$$\|g(t, \mathbf{x})\|_2 \leq \gamma(t)\|\mathbf{x}\|_2, \forall t \geq 0, \forall \mathbf{x} \in \mathcal{D} \tag{6.6}$$

where $\gamma : \mathbb{R} \to \mathbb{R}$ is non-negative and piecewise continuous. The derivative of V along the trajectories of (6.1) is given by

$$\dot{V} = \frac{\partial V(t, \mathbf{x})}{\partial t} + \frac{\partial V(t, \mathbf{x})}{\partial \mathbf{x}} f(t, \mathbf{x}) + \frac{\partial V(t, \mathbf{x})}{\partial \mathbf{x}} g(t, \mathbf{x})$$

With growth bound (6.6) as our only information on g, the best we can do is to perform the worst case analysis as given below

$$\dot{V} \leq -c_3 \|\mathbf{x}\|_2^2 + \left\| \frac{\partial V(t, \mathbf{x})}{\partial \mathbf{x}} \right\|_2 \|g(t, \mathbf{x})\|_2$$

$$\dot{V} \leq -c_3 \|\mathbf{x}\|_2^2 + c_4 \gamma(t) \|\mathbf{x}\|_2^2$$

if $\gamma(t)$ is small enough to satisfy the bound

$$\gamma(t) \leq \bar{\gamma} < \frac{c_3}{c_4}, \forall t \geq 0 \tag{6.7}$$

then

$$\dot{V}(t, \mathbf{x}) \le -(c_4 - \bar{\gamma}c_4)\|\mathbf{x}\|_2^2, (c_4 - \bar{\gamma}c_4) > 0$$

Lemma 6.1. *[42] Let* $\mathbf{x} = 0$ *be an exponentially stable Equilibrium point of the nominal system (6.2). Let* $V(t, \mathbf{x})$ *be a Lyapunov function of the nominal system satisfying the (6.3),(6.4),(6.5) inequalities in* $[0, \infty) \times \mathcal{D}$. *Suppose the perturbation term satisfies the growth condition (6.6). Then* $\mathbf{x} = 0$ *is an exponentially stable equilibrium point of the perturbed system (6.1). Moreover, if all assumptions hold globally, then the origin is globally exponentially stable.*

6.3 Stability of Cascaded Nonlinear Time Varying System

In this section, we recall the analysis of stability of cascaded nonlinear time varying system as given in [77], where the detailed proofs may be found. Consider a cascaded system as given below

$$\Sigma_1 : \dot{\mathbf{x}}_1 = f_1(t, \mathbf{x}_1) + g(t, \mathbf{x})\mathbf{x}_2 \tag{6.8}$$

$$\Sigma_2 : \dot{\mathbf{x}}_2 = f_2(t, \mathbf{x}_2) \tag{6.9}$$

where $\mathbf{x} = \begin{bmatrix} \mathbf{x}_1^\top & \mathbf{x}_2^\top \end{bmatrix}^\top$. Consider the following assumptions

Assumption 6.1. The system $\dot{\mathbf{x}}_1 = f_1(t, \mathbf{x}_1)$ is Uniformly Globally Asymptotically Stable (UGAS) with a Lyapunov function $V(t, \mathbf{x}_1) : \mathbb{R}_+ \times \mathbb{R}^n \to \mathbb{R}_+$ positive

definite and radially unbounded which satisfies

$$\left\|\frac{\partial V(t, \mathbf{x}_1)}{\partial \mathbf{x}_1}\right\| \|\mathbf{x}_1\| \le c_1 V(t, \mathbf{x}_1), \forall \|\mathbf{x}_1\| \ge \sigma \tag{6.10}$$

where $c_1, \sigma > 0$ and

$$\left\|\frac{\partial V(t, \mathbf{x}_1)}{\partial \mathbf{x}_1}\right\| \le c_2, \forall \|\mathbf{x}_1\| \ge \sigma \tag{6.11}$$

Assumption 6.2. The function $g(t, \mathbf{x})$ satisfies

$$\|g(t, \mathbf{x})\| \le \varphi_1(\|\mathbf{x}_2\|) + \varphi_2(\|\mathbf{x}_1\|)\|\mathbf{x}_2\| \tag{6.12}$$

where $\varphi_1, \varphi_2 : \mathbb{R}_+ \to \mathbb{R}_+$ are continuous.

Assumption 6.3. Equation $\dot{\mathbf{x}}_2 = f_2(t, \mathbf{x}_2)$ is UGAS and for all $t_0 \ge 0$,

$$\int_{t_0}^{\infty} \|\mathbf{x}_2(t, t_0, \mathbf{x}_2(t_0))\| dt \le \phi(\|\mathbf{x}_2(t_0)\|) \tag{6.13}$$

where ϕ is a class $\mathcal{K}$ function.

Theorem 6.1. *If Assumptions 6.1-6.3 are satisfied and $\dot{\mathbf{x}}_1 = f_1(t, \mathbf{x}_1)$ is Uniformly Globally Stable (UGS), then the cascaded system* (6.8),(6.9) *is UGS*

Theorem 6.2. *If Assumptions 6.1-6.3 are satisfied and $\dot{\mathbf{x}}_1 = f_1(t, \mathbf{x}_1)$ is UGAS with Lyapunov function satisfying inequality* (6.10) *and Assumption 6.2-6.3, then the cascaded system* (6.8),(6.9) *is UGAS*

6.4 Port Controller Hamiltonian Based Observer

In this section, rather than using the augmented approach as in [103, 97], we propose to design an observer that relies only on the output error, which is inspired

by the linear Luenberger observer design. Consider the general PCH system as below

$$\dot{\mathbf{x}} = \left[\mathcal{J}(\mathbf{x}) - \mathcal{R}(\mathbf{x}) \right] \nabla_x \mathcal{H} + \mathbf{Gu}$$

$$\dot{\mathbf{x}} = \mathcal{T}(\mathbf{x}) \nabla_x \mathcal{H} + \mathbf{Gu} \tag{6.14}$$

The measurement of the system does not have to be the output of PCH system. The assumptions that are used in the observer design are given as follows,

Assumption 6.4 (Quadratic Error Hamiltonian). The Hamiltonian of the system is a quadratic function of the systems state, such that, the partial derivative of the Hamiltonian with respect to the system state is linear function of the system states and the difference between the partial derivative of Hamiltonian with respect to the system state and the Hamiltonian with respect to state estimate is linear in error, i.e. $\mathbf{e} = \mathbf{x} - \hat{\mathbf{x}}$ and $\mathcal{H}_e = \frac{1}{2}\mathbf{e}^\top \mathbf{Pe}$. In addition, the shaped Hamiltonian error $\mathcal{H}_{s,e}$ is assumed quadratic.

Assumption 6.5. The PCH interconnection matrix, $\mathcal{J}$, and its associate damping, $\mathcal{R}$, have the following properties,

$$\mathcal{T}(\mathbf{x}) = \mathcal{T}(\hat{\mathbf{x}}) + \Delta\mathcal{T}(\hat{\mathbf{x}}, \mathbf{e}) \tag{6.15}$$

$$\mathcal{J}(\mathbf{x}) = \mathcal{J}(\hat{\mathbf{x}}) + \Delta\mathcal{J}(\hat{\mathbf{x}}, \mathbf{e})$$

$$\mathcal{R}(\mathbf{x}) = \mathcal{R}(\hat{\mathbf{x}}) + \Delta\mathcal{R}(\hat{\mathbf{x}}, \mathbf{e})$$

Assumption 6.6. There exists an observer gain matrix $\mathbf{L}(\hat{\mathbf{x}})$, such that

$$\mathbf{L}(\hat{\mathbf{x}})\tilde{\mathbf{y}} = \left[\mathcal{J}(\hat{\mathbf{x}}) - \mathcal{R}(\hat{\mathbf{x}}) \right] \nabla_e \mathcal{H}_e - \left[\mathcal{J}_s(\hat{\mathbf{x}}) - \mathcal{R}_s(\hat{\mathbf{x}}) \right] \nabla_e \mathcal{H}_{s,e}$$

where $\mathcal{J}_s$ is the desired antisymmetric interconnection matrix and $\mathcal{R}_s$ is the desired damping characteristic.

Using the assumptions above, we develop the following observer design for a class of PCH.

Theorem 6.3. *Consider the system* (6.14), *the following observer equation*

$$\dot{\hat{\mathbf{x}}} = \mathcal{T}(\hat{\mathbf{x}})\nabla_{\hat{x}}\mathcal{H} + \mathbf{G}\mathbf{u} + \mathbf{L}\left(\mathbf{y} - \hat{\mathbf{y}}\right) \tag{6.16}$$

with $\Delta\mathcal{T}$ and $\Delta\mathcal{R}$ having bounded gain. The observer described above has a Lyapunov stable error dynamic, with the shaped Hamiltonian error $\mathcal{H}_{s,e}$, if the following inequalities are satisfied

$$-\nabla_e\mathcal{H}_{s,e}^\top\mathcal{R}_s\nabla_e\mathcal{H}_{s,e} + \nabla_e\mathcal{H}_{s,e}^\top\Delta\mathcal{T}(\hat{\mathbf{x}},\mathbf{e})\nabla_x\mathcal{H} \leq 0 \tag{6.17}$$

Asymptotic stability is given, if the largest invariant set described by the above equation contains only the origin.

Proof. Subtracting the state estimate dynamics from the state dynamics, we have

$$\dot{\mathbf{x}} - \dot{\hat{\mathbf{x}}} = [\mathcal{T}(\mathbf{x})\nabla_x\mathcal{H} - \mathcal{T}(\hat{\mathbf{x}})\nabla_{\hat{x}}\mathcal{H}] - \mathbf{L}(\hat{\mathbf{x}})\tilde{\mathbf{y}}$$

$$\dot{\mathbf{e}} = [\mathcal{T}(\hat{\mathbf{x}})\nabla_e\mathcal{H}_e + \Delta\mathcal{T}(\hat{\mathbf{x}},\mathbf{e})\nabla_x\mathcal{H}] - \mathbf{L}(\hat{\mathbf{x}})\tilde{\mathbf{y}}$$

$$\dot{\mathbf{e}} = [\mathcal{J}_s(\hat{\mathbf{x}}) - \mathcal{R}_s]\nabla_e\mathcal{H}_{s,e} + \Delta\mathcal{T}(\hat{\mathbf{x}},\mathbf{e})\nabla_x\mathcal{H} \tag{6.18}$$

Evaluating the error Hamiltonian time derivative along the trajectory, the following results are obtained

$$\dot{\mathcal{H}}_{s,e} = -\nabla_e\mathcal{H}_{s,e}^\top\mathcal{R}_s\nabla_e\mathcal{H}_{s,e} + \nabla_e\mathcal{H}_{s,e}^\top\Delta\mathcal{T}(\hat{\mathbf{x}},\mathbf{e})\nabla_x\mathcal{H}$$

Since we require

$$-\nabla_e \mathcal{H}_{s,e}^\top \mathcal{R}_s \nabla_e \mathcal{H}_{s,e} + \nabla_e \mathcal{H}_{s,e}^\top \Delta \mathcal{T}(\hat{\mathbf{x}}, \mathbf{e}) \nabla_x \mathcal{H} \le 0,$$

The error dynamics is Lyapunov stable, with respect to the Hamiltonian of the error. The asymptotic stability properties are provided if the largest invariant set in $\{e : \dot{\mathcal{H}}_{s,e} = 0\}$ is the origin. $\qquad\square$

Remark 6.1. In the case that $\mathcal{R}_s$ is full rank matrix and positive definite, we can use Lemma 6.1 to prove the exponential stability of the origin in error dynamic. Consider now the states in the perturbed system (6.1) and the nominal system (6.2) as the errors between the true state values and the estimates respectively. From eq. (6.18), f will be equal to $[\mathcal{J}_s(\hat{\mathbf{x}}) - \mathcal{R}_s] \nabla_e \mathcal{H}_e$ and g will be $\Delta \mathcal{T}(\hat{\mathbf{x}}, \mathbf{e}) \nabla_x \mathcal{H}$. g is equal to zero if $\mathbf{e} = 0$, which implies the perturbations will vanish at the origin. If there is an upper bound value $\bar{\gamma}$ such that, $g \le \bar{\gamma} \|\mathbf{e}\|$ and $\|\nabla_e \mathcal{H}_e\| \le c_4 \|\mathbf{e}\|$ -which can easily be found, since we assume in the beginning that $\nabla_e \mathcal{H}_e$ is linear in e-, then following lemma 6.1, the error dynamics may shown to be exponentially stable.

6.5 Separation Principle

In this section, we investigate the stability of the observer based feedback systems of PCH. It is well known from Luenberger linear observer that the observer design can be done separately without affecting the closed loop system stability, or in simple terms, the observer gain $\mathbf{L}$ can be chosen independently from the feedback gain $\mathbf{K}$. While general separation principle is guaranteed in linear

systems, this is not valid in the nonlinear systems. So, it can happen that using asymptotic stable state estimation, the asymptotically stable closed loop system under state feedback control produces unstable closed loop dynamics.

Recall the general equation of the PCH system (6.14), where the feedback is a function of the state estimate,

$$\dot{\mathbf{x}} = \mathcal{T}(\mathbf{x})\nabla_x\mathcal{H} + \mathbf{G}\mathbf{u}(\hat{\mathbf{x}}) \tag{6.19}$$

$\mathbf{u}(\hat{\mathbf{x}})$ is the feedback signal which is a function of the state estimate. To analyze the stability of (6.19), we need the following assumption

Assumption 6.7. The feedback signal $\mathbf{u}(\hat{\mathbf{x}})$ can be selected such that

$$\mathbf{u}(\hat{\mathbf{x}}) = \mathbf{u}_{es}(\hat{\mathbf{x}}) + \mathbf{u}_{ad}(\hat{\mathbf{x}})$$
$$\dot{\mathbf{x}} = \mathcal{T}(\mathbf{x})\nabla_x\mathcal{H}_s + \mathbf{G}\mathbf{u}_{ad}(\hat{\mathbf{x}})$$

We state the stability of the controlled system (6.19) as follows

Theorem 6.4. *Consider the system* (6.19), *the closed loop system is Lyapunov stable if the following inequality is satisfied*

$$- \nabla_x\mathcal{H}_s^\top \left[\mathcal{R}_s(\mathbf{x}) - \Delta\mathcal{R}_a(\hat{\mathbf{x}}, \mathbf{e}) \right] \nabla_x\mathcal{H}_s + \nabla_x\mathcal{H}_s^\top \mathcal{R}_a(\hat{\mathbf{x}})\nabla_e\mathcal{H}_{s,e} \leq 0 \tag{6.20}$$

Asymptotic stability is given, if the largest invariant set contains only the origin.

Proof. Select $\mathbf{u}_{ad} = -\mathcal{R}_a(\hat{\mathbf{x}})\nabla_{\hat{x}}\mathcal{H}_s$ and substitute it into the dynamics of the PCH

system in (6.14). Doing this, we obtain

$$\dot{\mathbf{x}} = \mathcal{T}(\mathbf{x})\nabla_x\mathcal{H}_s + \mathbf{G}\mathbf{u}_{ad}(\hat{\mathbf{x}})$$

$$\dot{\mathbf{x}} = \mathcal{T}(\mathbf{x})\nabla_x\mathcal{H} - \mathcal{R}_a(\hat{\mathbf{x}})\left[\nabla_x\mathcal{H}_s - \nabla_e\mathcal{H}_{s,e}\right]$$

$$\dot{\mathbf{x}} = \left[\mathcal{J}(\mathbf{x}) - (\mathcal{R}(\mathbf{x}) + \mathcal{R}_a(\mathbf{x}))\right]\nabla_x\mathcal{H}_s + \Delta\mathcal{R}_a(\hat{\mathbf{x}}, \mathbf{e})\nabla_x\mathcal{H}_s + \mathcal{R}_a(\hat{\mathbf{x}})\nabla_e\mathcal{H}_{s,e}$$

$$\dot{\mathbf{x}} = \left[\mathcal{J}(\mathbf{x}) - \mathcal{R}_s(\mathbf{x})\right]\nabla_x\mathcal{H}_s + \Delta\mathcal{R}_a(\hat{\mathbf{x}}, \mathbf{e})\nabla_x\mathcal{H}_s + \mathcal{R}_a(\hat{\mathbf{x}})\nabla_e\mathcal{H}_{s,e} \qquad (6.21)$$

Evaluating the time derivative of the Hamiltonian along the trajectory, we obtain

$$\dot{\mathcal{H}} = -\nabla_x\mathcal{H}_s^\top\left[\mathcal{R}_s(\mathbf{x}) - \Delta\mathcal{R}_a(\hat{\mathbf{x}}, \mathbf{e})\right]\nabla_x\mathcal{H}_s + \nabla_x\mathcal{H}_s^\top\mathcal{R}_a(\hat{\mathbf{x}})\nabla_e\mathcal{H}_{s,e} \qquad (6.22)$$

Since we require

$$-\nabla_x\mathcal{H}_s^\top\left[\mathcal{R}_s(\mathbf{x}) - \Delta\mathcal{R}_a(\hat{\mathbf{x}}, \mathbf{e})\right]\nabla_x\mathcal{H}_s + \nabla_x\mathcal{H}_s^\top\mathcal{R}_a(\hat{\mathbf{x}})\nabla_e\mathcal{H}_{s,e} \leq 0$$

the closed loop system is Lyapunov stable with respect to the Hamiltonian. The asymptotic stability property is provided if the largest invariant set in $\{x : \dot{\mathcal{H}}_s = 0\}$ is only the origin. □

Remark 6.2. In some applications, evaluating the condition of $\dot{\mathcal{H}}_s \leq 0$ along the trajectory is difficult. However, we can use theorem 6.1 or 6.2, to show that the closed loop system is UGS or UGAS. If the error dynamics of the constructed observer has UGAS behaviour, then by invoking theorem 6.1 or 6.2, we can conclude about the observer based closed loop system stability, provided that the assumptions of the theorems are satisfied. This is related to the bound on Lyapunov function, the growth rate on the perturbations and the integrable condition of the error dynamics.

Remark 6.3. If the additional damping $\mathcal{R}_a$ is a constant matrix, the problem becomes simplified since $\Delta\mathcal{R}_a$ will be equal to zero. In the AUV case, as we have seen in the previous chapter, because of the antisymmetric properties of the Coriolis matrix and the dissipativity of the natural AUV damping, we can have $\mathcal{R}_a$ as a constant matrix to impose stronger dissipativity.

6.6 AUV applications

To have fully autonomous operation, AUV is typically equipped with on-board set of sensors. These sensors usually contain Inertial Navigation System (INS)(usually strap-down type), Global Positioning Systems (GPS) for at surface earth position sensors and depth sensors. In addition, AUV can also be equipped with Doppler sensors if the AUV travels near sea bed. Beacon type sensors are also commonly used for AUV navigations. One of the main difficulties, is how to estimate the inertial horizontal plane position of AUV , without using the beacon based measurements. It is challenging since although the INS can have very high measurement data rate, its position reading has divergent error characteristic due to two folded integration of acceleration measurement. In the vertical axis (depth), the position of the vehicle can be corrected continuously by a pressure sensor inside the AUV. For the X,Y axis, the problem is more complicated. Indeed, there are many approaches available in the literature dealing with the corrections (aiding) of the INS inertial position measurements. The main approaches make use of the kinematic equation of the vehicle and Extended Kalman Filter (EKF), mentioned as follows:

1. Beacon based: This is the oldest way for aiding INS, [52]. The difficulties

usually come from the slow rate of beacon based measurement, inherent delay, high noise and high loss of data measurement.

2. Doppler Velocity : From the initial results available in the literature [44][36], aiding INS with Doppler Velocity Log (DVL) provides means such that the horizontal position estimation from INS can be tuned to have 0.01 % error through the traveled path. This method faces difficulty in case the AUV is not near the sea bed, or touching the trench shaped region.

3. Model Aided: This technique originally appeared for Unmanned Aerial Vehicle (UAV) [46]. The idea is to reduce the propagation error of INS using a model that most likely contains uncertainties. After the seminal paper introduced for UAV came with outstanding simulation results[46], the idea has been used in AUV with kinematic model [69], which subtracts the position measurements of INS from the position estimate computed from the model. The errors are then propagated by EKF using perturbation technique. The real experimental results published recently in [33], show the benefit of such method. This technique although it is considered cheap and promising like the DVL aiding technique,it only reduces the horizontal position error propagation and does not make it convergent to zero.

In general, the aiding techniques are used in AUV navigation to have a longer below-surface time operation until next surfacing. When the vehicle appears at the sea surface, the position estimation of INS is corrected by the GPS. Aiding technique by DVL and model does not replace the need for surfacing, since it only reduces the error propagation. Readers are referred to [52] for a detailed survey on this technique. In the next section, we study the possibility of using the PCH based observer method.

6.6.1 PCH based Observer Design

With all tools described in the previous section, we address the observer design problem for AUV. For the observer development, we assume that, depth, attitude, linear velocity and angular velocity are measured. Since the initial Hamiltonian is chosen equal to kinetic energy of the vehicle, the Hamiltonian of error will be

$$\mathcal{H}_e = \frac{1}{2}\mathbf{e}_p^\top \mathbf{M}^{-1}\mathbf{e}_p \tag{6.23}$$

and the observer error equation becomes

$$\dot{\mathbf{e}} = \left(\mathcal{J}(\hat{\mathbf{x}}) - \mathcal{R}(\hat{\mathbf{x}})\right)\nabla_e\mathcal{H}_e + \Delta\Psi(\hat{\mathbf{x}}, \mathbf{e}) + \mathbf{L}\tilde{\mathbf{y}} \tag{6.24}$$

$$\Delta\Psi(\hat{\mathbf{x}}, \mathbf{e}) = \Delta\mathcal{J}(\hat{\mathbf{x}}, \mathbf{e})\nabla_x\mathcal{H} + \Delta\mathcal{R}(\hat{\mathbf{x}}, \mathbf{e})\nabla_x\mathcal{H} \tag{6.25}$$

Next, we choose the shaped Hamiltonian error as below

$$\mathcal{H}_{s,e} = \frac{1}{2}\left[\mathbf{e}_p^\top \mathbf{M}^{-1}\mathbf{e}_p + \mathbf{e}_{\eta_1}^\top \Lambda_1\mathbf{e}_{\eta_1} + \mathbf{e}_{\eta_2}^\top \Lambda_2\mathbf{e}_{\eta_2}\right] \tag{6.26}$$

Evaluating the matching condition, we have

$$\left(\mathcal{J}(\hat{\mathbf{x}}) - \mathcal{R}(\hat{\mathbf{x}})\right)\nabla_e\mathcal{H}_e + \Delta\Psi(\hat{\mathbf{x}}, \mathbf{e}) + \mathbf{L}\tilde{\mathbf{y}} = \left(\mathcal{J}(\hat{\mathbf{x}}) - \mathcal{R}_o\right)\nabla_e\mathcal{H}_{s,e} + \Delta\Psi(\hat{\mathbf{x}}, \mathbf{e})$$

If we select

$$\mathcal{R}_o = \begin{bmatrix} \mathbf{D}_{o_1} & & \\ & \mathbf{D}_{o_2} & \\ & & \mathbf{D}_{o_2} \end{bmatrix}$$

138

Where, $\mathbf{D}_{o_1}, \mathbf{D}_{o_2} \in \mathbb{R}^{3\times3}$ and $\mathbf{D}_{o_3} \in \mathbb{R}^{6\times6}$, then we have

$$\mathbf{L}\tilde{\mathbf{y}} = \begin{bmatrix} -\mathbf{D}_{o_1}\mathbf{\Lambda}_1\mathbf{e}_{\eta_1} \\ -\mathbf{D}_{o_2}\mathbf{\Lambda}_2\mathbf{e}_{\eta_2} \\ -\mathbf{J}_1^\top\mathbf{\Lambda}_1\mathbf{e}_{\eta_1} - \mathbf{J}_2^\top\mathbf{\Lambda}_2\mathbf{e}_{\eta_2} - (\mathbf{D}_{o_3} - \bar{\mathbf{D}})\mathbf{e}_\nu \end{bmatrix} \tag{6.27}$$

However, since two elements in the $\mathbf{e}_{\eta_1}$ are inaccessible (X,Y of inertial position are not measured), then $\mathbf{\Lambda}_1$ has to be chosen as $diag\{0\ 0\ \lambda_z\}$. This implies that, the error on X,Y of inertial position cannot be made convergent to zero, since $\mathcal{H}_{s,e}$ will have non-unique minima. However, one can have a rough estimate of $\mathbf{e}_{\eta_1}$ value by integrating $\mathbf{J}(\boldsymbol{\eta}_2)\mathbf{e}_{\nu_1}$, but this does not guarantee that the observer will have an asymptotic error behaviour.

6.6.2 AUV Observer Alternative

In this subsection, we present an alternative observer design for AUV type with the inertial position measured directly by beacon measurements. The proposed AUV observer is closely related to the one proposed in [83]. However we analyze and derive the error dynamics of the AUV observer without using a filtered error dynamics as used in [83], so the derivation is clearer and shorter. In addition, as we will elaborate more later on this subsection, the use of yet simpler notation can lead to stronger stability results than the one mentioned in [83]. Let us define $\mathbf{x}_1 = \boldsymbol{\eta}, \mathbf{x}_2 = \mathbf{J}(\mathbf{y})\boldsymbol{\nu}, \mathbf{x}_2^b = \boldsymbol{\nu}, \mathbf{x}_3 = \mathbf{b}$ and $\tilde{\mathbf{x}} = \hat{\mathbf{x}} - \mathbf{x}$.

Since the only measurement available is η, the observer is constructed as below

$$\dot{\hat{\mathbf{x}}}_1 = \hat{\mathbf{x}}_2 + \mathbf{L}_1 \tilde{\mathbf{x}}_1$$

$$\dot{\hat{\mathbf{x}}}_2 = \mathbf{M}^{*-1}(\mathbf{y}) \left[\mathbf{J}^{-1}(\mathbf{y})\boldsymbol{\tau} + \hat{\mathbf{x}}_3 - g(\mathbf{y}) - \mathbf{C}^*(\hat{\mathbf{x}}_2^b, \mathbf{y})\hat{\mathbf{x}}_2 - \mathbf{D}^*(\hat{\mathbf{x}}_2^b, \mathbf{y})\hat{\mathbf{x}}_2 \right] + \mathbf{L}_2 \tilde{\mathbf{x}}_1$$

$$\dot{\hat{\mathbf{x}}}_3 = -\mathbf{T}^{-1}\hat{\mathbf{x}}_3 + \mathbf{L}_3 \tilde{\mathbf{x}}_1$$

The plant equations are rewritten as follows,

$$\dot{\mathbf{x}}_1 = \mathbf{x}_2$$

$$\dot{\mathbf{x}}_2 = \mathbf{M}^{*-1}(\mathbf{y}) \left[\mathbf{J}^{-1}(\mathbf{y})\boldsymbol{\tau} + \mathbf{x}_3 - g(\mathbf{y}) - \mathbf{C}^*(\mathbf{x}_2^b, \mathbf{y})\mathbf{x}_2 - \mathbf{D}^*(\mathbf{x}_2^b, \mathbf{y})\mathbf{x}_2 \right]$$

$$\dot{\mathbf{x}}_3 = -\mathbf{T}^{-1}\mathbf{x}_3$$

where we make use of assumptions 2.4 and 2.3. Using the preceding assumptions and properties, the error dynamics are given by

$$\dot{\tilde{\mathbf{x}}}_1 = \tilde{\mathbf{x}}_2 + \mathbf{L}_1 \tilde{\mathbf{x}}_1 \tag{6.28}$$

$$\dot{\tilde{\mathbf{x}}}_2 = \mathbf{M}^{*-1}(\mathbf{y}) \left[\tilde{\mathbf{x}}_3 - \left[\mathbf{C}^*(\hat{\mathbf{x}}_2^b, \mathbf{y})\hat{\mathbf{x}}_2 - \mathbf{C}^*(\mathbf{x}_2^b, \mathbf{y})\mathbf{x}_2 + \mathbf{D}^*(\hat{\mathbf{x}}_2^b, \mathbf{y})\hat{\mathbf{x}}_2 - \mathbf{D}^*(\mathbf{x}_2^b, \mathbf{y})\mathbf{x}_2 \right] \right]$$

$$+ \mathbf{L}_2 \tilde{\mathbf{x}}_1 \tag{6.29}$$

$$\dot{\tilde{\mathbf{x}}}_3 = -\mathbf{T}^{-1}\tilde{\mathbf{x}}_3 + \mathbf{L}_3 \tilde{\mathbf{x}}_1 \tag{6.30}$$

using property 2.2

$$\mathbf{C}^*(\hat{\mathbf{x}}_2^b, \mathbf{y})\hat{\mathbf{x}}_2 = \mathbf{C}^*(\mathbf{x}_2^b, \mathbf{y})\mathbf{x}_2 + \mathbf{C}^*(\mathbf{x}_2^b, \mathbf{y})\tilde{\mathbf{x}}_2 + \mathbf{C}^*(\tilde{\mathbf{x}}_2^b, \mathbf{y})\hat{\mathbf{x}}_2$$

Hence ,

$$\mathbf{C}^*(\hat{\mathbf{x}}_2^b, \mathbf{y})\hat{\mathbf{x}}_2 - \mathbf{C}^*(\mathbf{x}_2^b, \mathbf{y})\mathbf{x}_2 = \mathbf{C}^*(\mathbf{x}_2^b, \mathbf{y})\tilde{\mathbf{x}}_2 + \mathbf{C}^*(\tilde{\mathbf{x}}_2^b, \mathbf{y})\hat{\mathbf{x}}_2$$

For the drag term, using properties 2.3 and 2.2, we have $\mathbf{D}^*(\hat{\mathbf{x}}_2^b, \mathbf{y})\hat{\mathbf{x}}_2 - \mathbf{D}^*(\mathbf{x}_2^b, \mathbf{y})\mathbf{x}_2$

$$= \mathbf{D}_l^*(\mathbf{y})\tilde{\mathbf{x}}_2 + \mathbf{D}_{nl}^*(\mathbf{x}_2^b, \mathbf{y})\mathbf{x}_2 - \mathbf{D}_{nl}^*(\mathbf{x}_2^b, \mathbf{y})\mathbf{x}_2$$

$$= \mathbf{D}_l^*(\mathbf{y})\tilde{\mathbf{x}}_2 + \mathbf{D}_{nl}^*(\mathbf{x}_2^b, \mathbf{y})\tilde{\mathbf{x}}_2 + \mathbf{D}_{nl}^*(\tilde{\mathbf{x}}_2^b, \mathbf{y})\hat{\mathbf{x}}_2$$

Arranging similar terms, we can have the error dynamics for the second state written as

$$\dot{\tilde{\mathbf{x}}}_2 = \mathbf{M}^{*-1}(\mathbf{y}) \left[\tilde{\mathbf{x}}_3 - \boldsymbol{\Psi}_1(\mathbf{x}_2^b, \mathbf{y})\tilde{\mathbf{x}}_2 - \boldsymbol{\Psi}_2^{**}(\tilde{\mathbf{x}}_2^b, \mathbf{y})\hat{\mathbf{x}}_2\right] + \mathbf{L}_2\tilde{\mathbf{x}}_1 \tag{6.31}$$

$$\boldsymbol{\Psi}_1(\mathbf{x}_2^b, \mathbf{y}) \triangleq \mathbf{C}^*(\mathbf{x}_2^b, \mathbf{y}) + \mathbf{D}_l^*(\mathbf{y}) + \mathbf{D}_{nl}^*(\mathbf{x}_2^b, \mathbf{y}) \tag{6.32}$$

$$\boldsymbol{\Psi}_2^{**}(\tilde{\mathbf{x}}_2^b, \mathbf{y}) \triangleq \mathbf{C}^*(\tilde{\mathbf{x}}_2^b, \mathbf{y}) + \mathbf{D}_{nl}^*(\tilde{\mathbf{x}}_2^b, \mathbf{y}) \tag{6.33}$$

From properties 2.2 and 2.3, $\mathbf{C}^*(\tilde{\mathbf{x}}_2^b, \mathbf{y})$ and $\mathbf{D}_{nl}^*(\tilde{\mathbf{x}}_2^b, \mathbf{y})$ depend linearly on $\tilde{\mathbf{x}}_2^b$. Hence,

$$\frac{\partial \boldsymbol{\Psi}_2^{**}(\tilde{\mathbf{x}}_2^b, \mathbf{y})\hat{\mathbf{x}}_2}{\partial \tilde{\mathbf{x}}_2^b}\tilde{\mathbf{x}}_2^b = \boldsymbol{\Psi}_2^*(\hat{\mathbf{x}}_2^b, \mathbf{y})\mathbf{J}(\mathbf{y})\tilde{\mathbf{x}}_2^b$$

$$= \boldsymbol{\Psi}_2(\hat{\mathbf{x}}_2^b, \mathbf{y})\tilde{\mathbf{x}}_2$$

Finally, we have

$$\dot{\tilde{\mathbf{x}}}_2 = \mathbf{M}^{*-1}(\mathbf{y}) \left[\tilde{\mathbf{x}}_3 - \left[\boldsymbol{\Psi}_1(\mathbf{x}_2^b, \mathbf{y}) + \boldsymbol{\Psi}_2(\hat{\mathbf{x}}_2^b, \mathbf{y})\right] \tilde{\mathbf{x}}_2\right] + \mathbf{L}_2\tilde{\mathbf{x}}_1 \tag{6.34}$$

Having this, we select the following Lyapunov candidate function

$$V(\tilde{\mathbf{x}}, \mathbf{y}) = \frac{1}{2} \left[\tilde{\mathbf{x}}_1^\top \boldsymbol{\Lambda}_1 \tilde{\mathbf{x}}_1 + \tilde{\mathbf{x}}_2^\top \mathbf{M}^*(\mathbf{y}) \tilde{\mathbf{x}}_2 + \tilde{\mathbf{x}}_3^\top \boldsymbol{\Lambda}_3 \tilde{\mathbf{x}}_3\right] \tag{6.35}$$

where $\boldsymbol{\Lambda}_1$ and $\boldsymbol{\Lambda}_3$ are symmetric positive definite matrices. Evaluating the time

derivative of V along the trajectory, we have

$$\dot{V} = \tilde{\mathbf{x}}_1^\top \mathbf{\Lambda}_1 \tilde{\mathbf{x}}_2 + \tilde{\mathbf{x}}_1^\top \mathbf{\Lambda}_1 \mathbf{L}_1 \tilde{\mathbf{x}}_1 + \tilde{\mathbf{x}}_2^\top \tilde{\mathbf{x}}_3 - \tilde{\mathbf{x}}_2^\top \mathbf{\Psi}_\top (\hat{\mathbf{x}}_2, \mathbf{x}_2, \mathbf{y}) \tilde{\mathbf{x}}_2$$
$$- \tilde{\mathbf{x}}_3^\top \mathbf{\Lambda}_3 \mathbf{T}^{-1} \tilde{\mathbf{x}}_3 + \tilde{\mathbf{x}}_3^\top \mathbf{\Lambda}_3 \mathbf{L}_3 \tilde{\mathbf{x}}_1 + \tilde{\mathbf{x}}_2^\top \mathbf{\Lambda}_2 \mathbf{L}_2 \tilde{\mathbf{x}}_1 + \frac{1}{2} \tilde{\mathbf{x}}_2^\top \dot{\mathbf{M}}^*(\mathbf{y}) \tilde{\mathbf{x}}_2$$

$$\mathbf{\Psi}_\top (\hat{\mathbf{x}}_2, \mathbf{x}_2, \mathbf{y}) \triangleq \mathbf{\Psi}_1(\mathbf{x}_2^b, \mathbf{y}) + \mathbf{\Psi}_2(\hat{\mathbf{x}}_2^b, \mathbf{y})$$

Deploying the skew symmetric property of $(\dot{\mathbf{M}}^* - 2\mathbf{C}^*)$, property 2.1,the term having $\dot{\mathbf{M}}^*$ can be removed from the equation. Further, we elaborate more on the last equation as below

$$\dot{V} = - \tilde{\mathbf{x}}_1^\top \mathbf{P}_1 \tilde{\mathbf{x}}_1 - \tilde{\mathbf{x}}_3^\top (1 - \gamma^2) \mathbf{P}_3 \tilde{\mathbf{x}}_3 + 2\tilde{\mathbf{x}}_3^\top \mathbf{\Lambda}_3 \mathbf{L}_3 \tilde{\mathbf{x}}_1$$
$$- \tilde{\mathbf{x}}_2^\top \mathbf{P}_2 \tilde{\mathbf{x}}_2 - \tilde{\mathbf{x}}_3^\top (\gamma^2) \mathbf{P}_3 \tilde{\mathbf{x}}_3 + \tilde{\mathbf{x}}_3^\top \tilde{\mathbf{x}}_2$$

$$\mathbf{P}_1 \triangleq \sqrt{\mathbf{\Lambda}_1 \mathbf{L}_1}$$

$$\mathbf{P}_2 \triangleq \sqrt{\mathbf{\Psi}_\top}$$

$$\mathbf{P}_3 \triangleq \sqrt{\mathbf{\Lambda}_3 \mathbf{T}^{-1}}$$

$$\|\gamma\| < 1$$

where we select $\mathbf{L}_2 = -\mathbf{M}^{*-1} \mathbf{\Lambda}_1$. From properties 2.3 and 2.2, as well as the bounded velocity assumption 2.2, $\mathbf{\Psi}_\top$ will be positive definite with non-zero lower bound. Hence, it is possible to design the observer that has $\dot{V}$ always negative along the trajectory by designing proper observer gains, $\mathbf{L}_i$. The time derivative of the Lyapunov as described in the above equation, can be made neg-

ative definite by selecting the $\mathbf{L}_1$ negative definite and ,$\mathbf{L}_3$, $\mathbf{\Lambda}_3$ as follows

$$\mathbf{\Lambda}_3 > \frac{1}{4\gamma^2} \mathbf{\Psi}_{\top\min}^{-1} \mathbf{T} \tag{6.36}$$

$$\mathbf{L}_3 = 2\sqrt{1-\gamma^2}\mathbf{\Lambda}_3^{-1}\sqrt{\mathbf{\Lambda}_3\mathbf{T}^{-1}\mathbf{\Lambda}_1\mathbf{L}_1} \tag{6.37}$$

$$\mathbf{\Psi}_{\top\min} \leq \mathbf{\Psi}_\top \tag{6.38}$$

Finally we state the following proposition

Proposition 6.1. *For the AUV system satisfying all assumptions and properties mentioned in section 2.4, for a given Lyapunov function (6.35) there will be a set of $\mathbf{L}_i, i = 1, 2, 3$,*

$$\mathbf{\Lambda}_3 > \frac{1}{4\gamma^2} \mathbf{\Psi}_{\top\min}^{-1} \mathbf{T} \tag{6.39}$$

$$\mathbf{L}_1 < 0 \tag{6.40}$$

$$\mathbf{L}_2 = -\mathbf{M}^{*-1}\mathbf{\Lambda}_1 \tag{6.41}$$

$$\mathbf{L}_3 = 2\sqrt{1-\gamma^2}\mathbf{\Lambda}_3^{-1}\sqrt{\mathbf{\Lambda}_3\mathbf{T}^{-1}\mathbf{\Lambda}_1\mathbf{L}_1} \tag{6.42}$$

that render the system Uniformly Globally Exponentially Stable (UGES).

6.6.3   Separation Principle

As mentioned in remark 6.2, we have to show that the output feedback closed loop system satisfies the required assumption of the theorem. The nominal system of the AUV state dynamics has UGAS properties. Based on the discussion in the previous chapter, we showed that there is an associated quadratic Lyapunov function which proves that the desired equilibrium point is Uniformly Locally

Exponentially Stable (ULES). As mentioned in [77], the growth condition of the Lyapunov function mentioned in assumption 6.1 is satisfied by all functions of the form $V(t, x) = k\|x\|^p, \forall p \in (1, \infty), k > 0$, which is satisfied by the Lyapunov function of the AUV as mentioned in the previous chapter.

We have the following equation for the AUV dynamics,

$$\dot{\mathbf{x}} = \mathcal{T}(\mathbf{x})\nabla_x \mathcal{H}_s + \mathbf{G}\left(-\Delta \mathbf{u}_{es}(\hat{\mathbf{x}}, \mathbf{e}) + \mathbf{u}_{ad}(\hat{\mathbf{x}}) - \Delta g(\hat{\mathbf{x}}, \mathbf{e})\right) \quad (6.43)$$

Since $\mathbf{G}\mathbf{u}_{ad}(\hat{\mathbf{x}}) = -\mathcal{R}_a(\hat{\mathbf{x}})\nabla_{\hat{x}}\mathcal{H}_s$

$$\dot{\mathbf{x}} = \left[\mathcal{J}(\mathbf{x}) - \mathcal{R}_s(\mathbf{x})\right]\nabla_x \mathcal{H}_s - \Delta \mathcal{R}(\hat{\mathbf{x}}, \mathbf{e})\nabla_x \mathcal{H}_s$$
$$+ \mathbf{G}\left(-\Delta \mathbf{u}_{es}(\hat{\mathbf{x}}, \mathbf{e}) - \Delta g(\hat{\mathbf{x}}, \mathbf{e}) + \mathcal{R}_a(\hat{\mathbf{x}})\nabla_e \mathcal{H}_{s,e}\right) \quad (6.44)$$

Next, we separate the state dynamics into the following two terms

$$\mathbf{f}(\mathbf{x}) = \left[\mathcal{J}(\mathbf{x}) - (\mathcal{R}_s(\mathbf{x}) - \Delta \mathcal{R}_a(\hat{\mathbf{x}}, \mathbf{e}))\right]\nabla_x \mathcal{H}_s \quad (6.45)$$

$$\varrho(\hat{\mathbf{x}}, \mathbf{e}) = -\mathbf{G}\left(\Delta \mathbf{u}_{es}(\hat{\mathbf{x}}, \mathbf{e}) + \Delta g(\hat{\mathbf{x}}, \mathbf{e}) + \mathcal{R}_a(\hat{\mathbf{x}})\nabla_e \mathcal{H}_{s,e}\right) \quad (6.46)$$

Using proper selection, the nominal value of state dynamic $\dot{\mathbf{x}} = \mathbf{f}(\mathbf{x})$ is UGAS. This can be achieved by selecting $\mathcal{R}_s > \sup_{\hat{x}} \Delta R_a$ and this will lead to negative definite shaped Hamiltonian time derivative. In addition, as pointed out in remark 6.3, for most AUV types, we can always select $\mathcal{R}_a$ as a constant. Next, we show that the assumption 6.2 and 6.3 are satisfied as well, which is related to the growth bound of the perturbations. ϱ will be treated separately in relationship with cascaded system analysis as given in section 6.3.

Perturbation growth of ϱ

This section is intended to discuss the perturbation growth of ϱ and its relation with the total stability of the system. We will elaborate more using the cascaded theorem, with $\mathbf{x}_1 = \mathbf{x}$ and $\mathbf{x}_2 = \mathbf{e}$. $\Delta \mathbf{u}_{es}(\hat{\mathbf{x}}, \mathbf{e})$ is given by

$$
\begin{aligned}
\Delta \mathbf{u}_{es}(\hat{\mathbf{x}}, \mathbf{e}) &= \mathbf{u}_{es}(\mathbf{x}) - \mathbf{u}_{es}(\hat{\mathbf{x}}) \\
&= -\mathbf{J}^\top(\hat{\boldsymbol{\eta}}_2)\hat{\mathbf{Q}}\mathbf{e}_\eta - \Delta \mathbf{J}^\top \hat{\mathbf{Q}}\tilde{\boldsymbol{\eta}}
\end{aligned}
$$

Recall that in the state dynamics, ϱ can be given by

$$
\begin{aligned}
\varrho(\hat{\mathbf{x}}, \mathbf{e}) &= + \mathbf{G}\left(-\Delta \mathbf{u}_{es}(\hat{\mathbf{x}}, \mathbf{e}) - \Delta g(\hat{\mathbf{x}}, \mathbf{e}) + \mathbf{R}_a(\hat{\mathbf{x}})\nabla_e \mathcal{H}_{s,e}\right) \\
&= \mathbf{J}^\top(\hat{\boldsymbol{\eta}}_2)\hat{\mathbf{Q}}\mathbf{e}_\eta + \Delta \mathbf{J}^\top \hat{\mathbf{Q}}\tilde{\boldsymbol{\eta}} + \mathbf{R}_a(\hat{\boldsymbol{\nu}})\mathbf{e}_\nu - \Delta g(\hat{\mathbf{x}}, \mathbf{e})
\end{aligned}
$$

Using the mean value theorem there will be $\mathbf{x}_r$ on the line joining $\mathbf{x}$ and $\hat{\mathbf{x}}$, such that

$$
\mathcal{X}(\mathbf{x}) - \mathcal{X}(\hat{\mathbf{x}}) = \left.\frac{\partial \mathcal{X}}{\partial \mathbf{x}}\right|_{\mathbf{x}=\mathbf{x}_r} \mathbf{e} \tag{6.47}
$$

Furthermore, if $\mathcal{X}$ is *Lipschitz* continuous in $\mathbf{x}$, there will be a constant ς, such that

$$
|\mathcal{X}(\mathbf{x}) - \mathcal{X}(\hat{\mathbf{x}})| \leq \sup_x \left\|\frac{\partial \mathcal{X}}{\partial \mathbf{x}}\right\| \|\mathbf{e}\| = \varsigma \|\mathbf{e}\| \tag{6.48}
$$

Using the mean value theorem, we get the following results

$$\|\varrho\| \le \lambda_{JQ}\|\mathbf{e}_\eta\| + (\lambda_{\Delta JQ} + \lambda_g)\|\mathbf{e}_{\eta_2}\| + \lambda_{D_a}\|\mathbf{e}_\nu\|$$

$$\lambda_{JQ} \triangleq \sup_{\eta_2} \left\|\mathbf{J}^\top(\boldsymbol{\eta}_2)\hat{\mathbf{Q}}\right\|$$

$$\lambda_{\Delta JQ} \triangleq \sup_{\eta_2} \left\|\frac{\partial \mathbf{J}^\top(\boldsymbol{\eta}_2)\hat{\mathbf{Q}}}{\partial \boldsymbol{\eta_2}}\right\| \|\tilde{\boldsymbol{\eta}}\|$$

$$\lambda_g \triangleq \sup_{\eta_2} \left\|\frac{\partial g(\boldsymbol{\eta}_2)}{\partial \boldsymbol{\eta}_2}\right\|$$

$$\lambda_{D_a} \triangleq \sup_{\nu} \mathbf{D}_a(\boldsymbol{\nu})$$

From the above equation, using angle restriction assumption 2.1, bounded $\mathbf{J}$ property 2.5 and bounded velocities assumption 2.2, the condition in assumption 6.2 of cascaded theorem is satisfied. Assumption 6.3 is satisfied by the fact that the estimation error $\mathbf{e}$ dynamic is UGES.

6.7 Simulation Results

The PCH observer and the alternative observer simulation results are presented here. The simulations are carried in the presence of ocean current as external disturbance which are assumed to be irrotional. The measurements are also assumed to be corrupted with white noise. We present two cases of simulation. The first set of simulation is carried out with the controller input signals computed using the true value of the state. This has to be taken first to show the convergence of the estimation, since the system is open loop unstable. The second simulation set is carried out with the controller signals computed using the estimated states to show observer-controller closed loop responses.
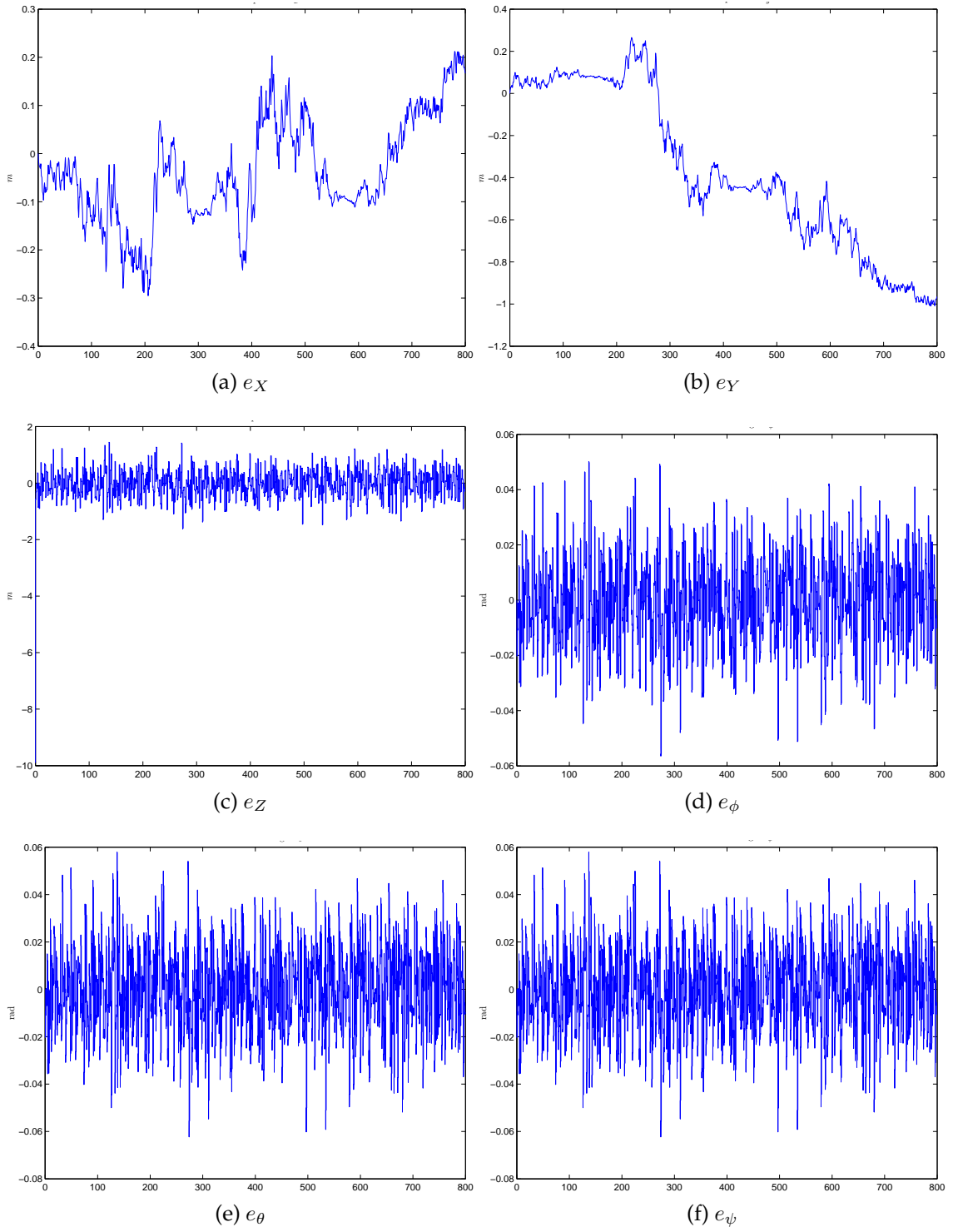
(a) e_X

(b) e_Y

(c) e_Z

(d) e_ϕ

(e) e_θ

(f) e_ψ

Figure 6.1: Error on inertial position estimation - case 1

147

(a) e_u

(b) e_v

(c) e_w

(d) e_p

(e) e_q

(f) e_r
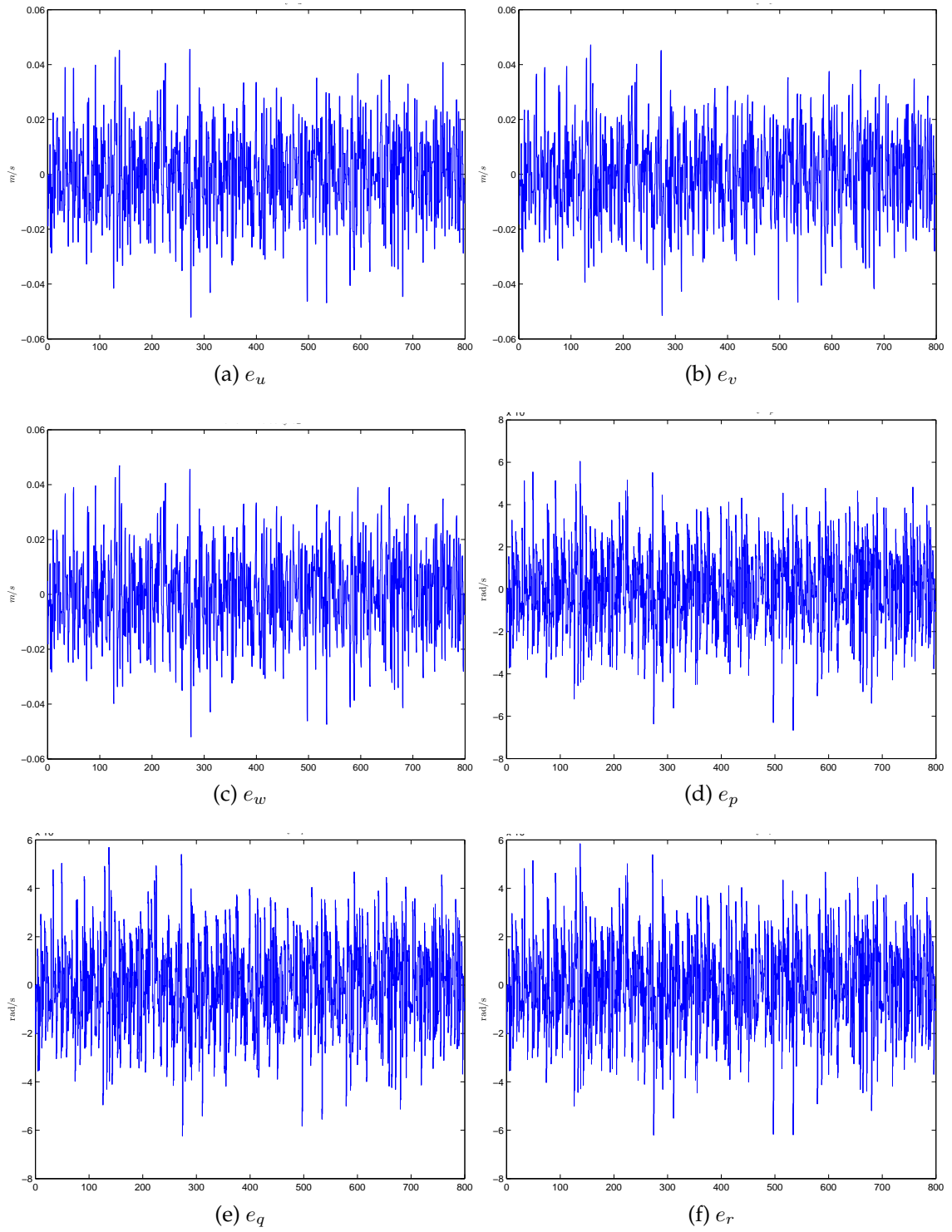
Figure 6.2: Error on body-fixed velocity estimation - case 1

(a) e_X

(b) e_Y

(c) e_Z

(d) e_ϕ

(e) e_θ

(f) e_ψ

Figure 6.3: Error on inertial position estimation - case 2

(a) e_u

(b) e_v

(c) e_w

(d) e_p

(e) e_q

(f) e_r
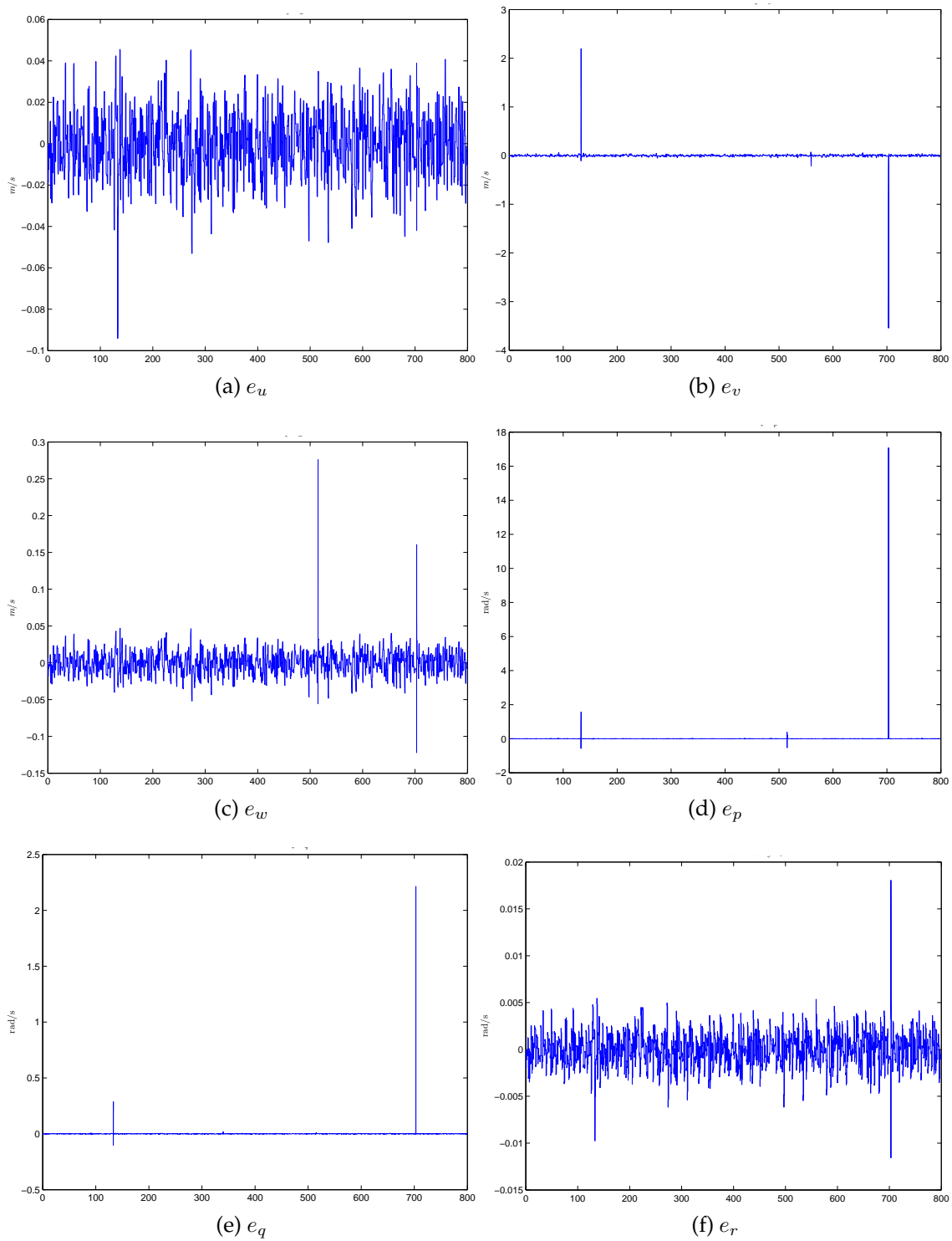
Figure 6.4: Error on body-fixed velocity estimation - case 2

(a) u

(b) v

(c) w

(d) p

(e) q

(f) r

Figure 6.5: Body-fixed frame velocity - case 1

(a) u

(b) v

(c) w

(d) p

(e) q

(f) r
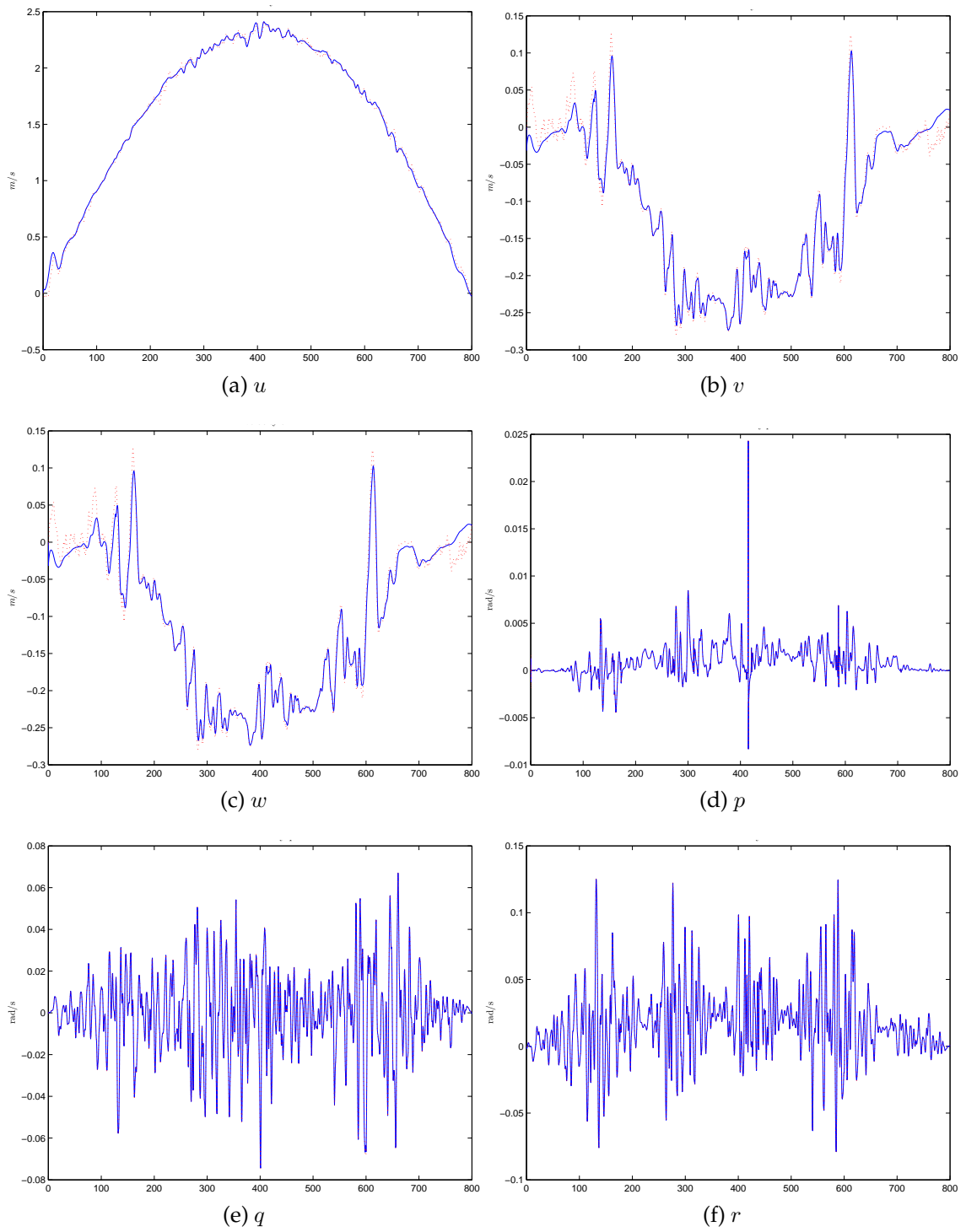
Figure 6.6: Body-fixed frame velocity - case 2

(a) e_X

(b) e_Y

(c) e_Z

(d) e_ϕ

(e) e_θ

(f) e_ψ
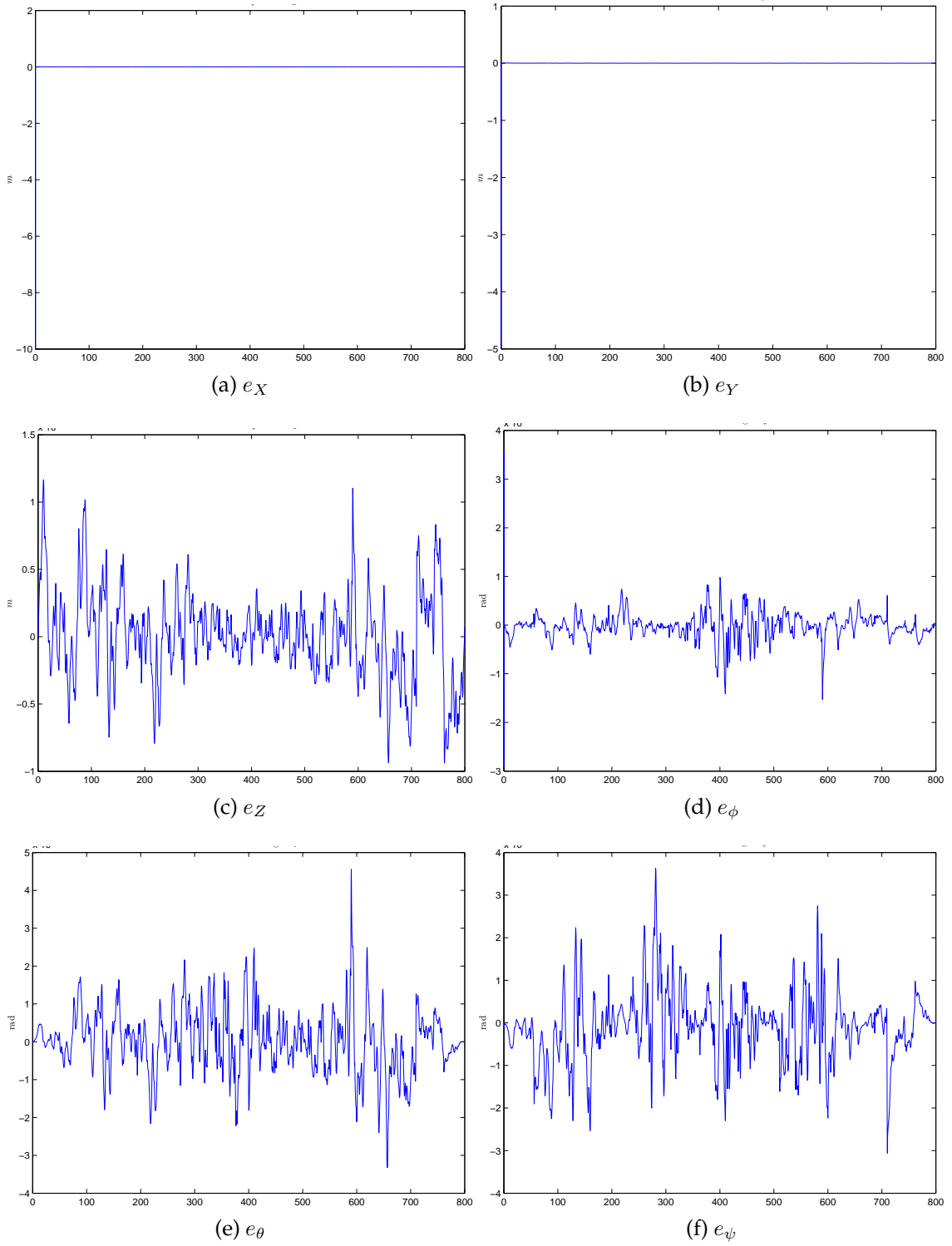
Figure 6.7: Error on inertial position estimation - case 1

153
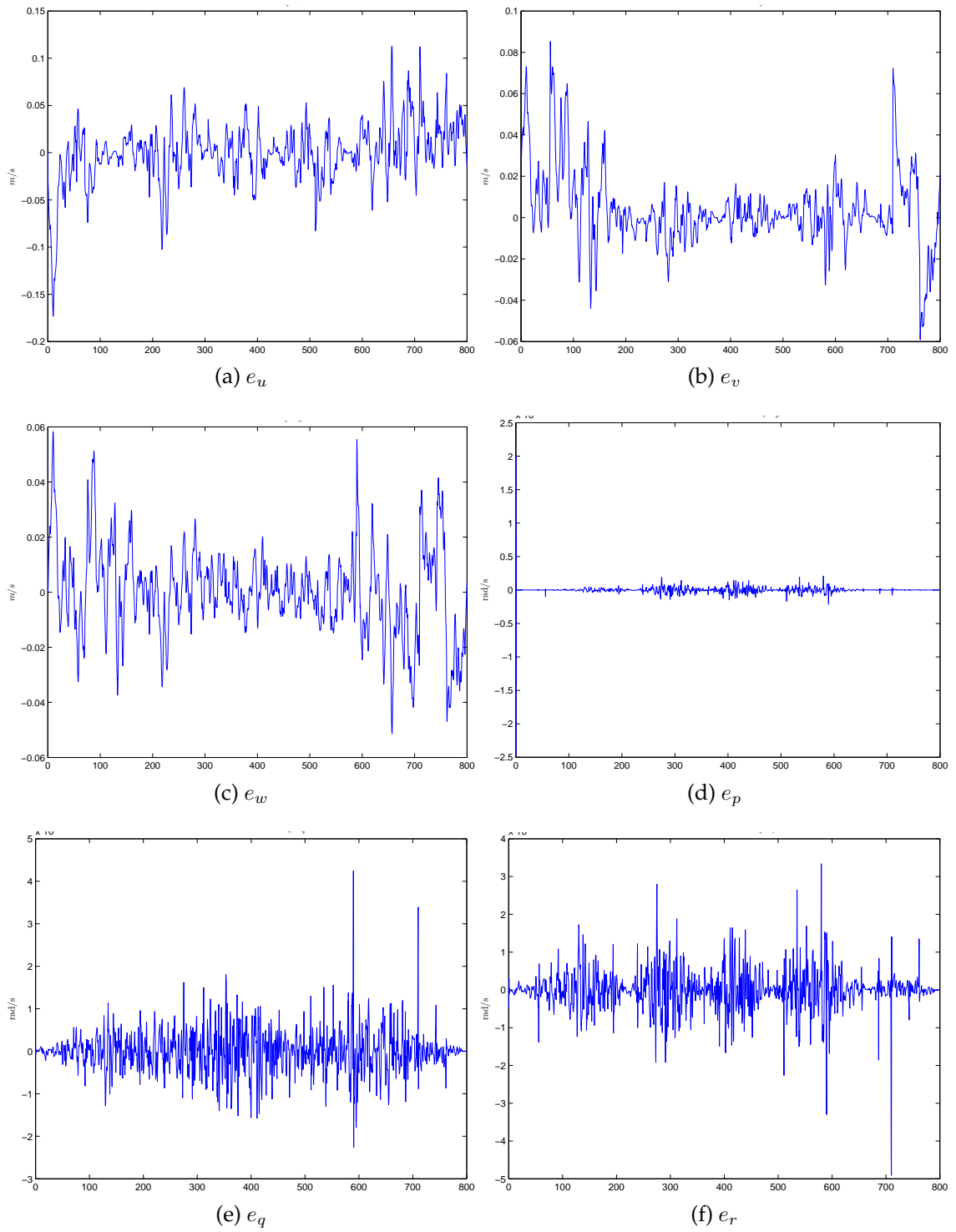
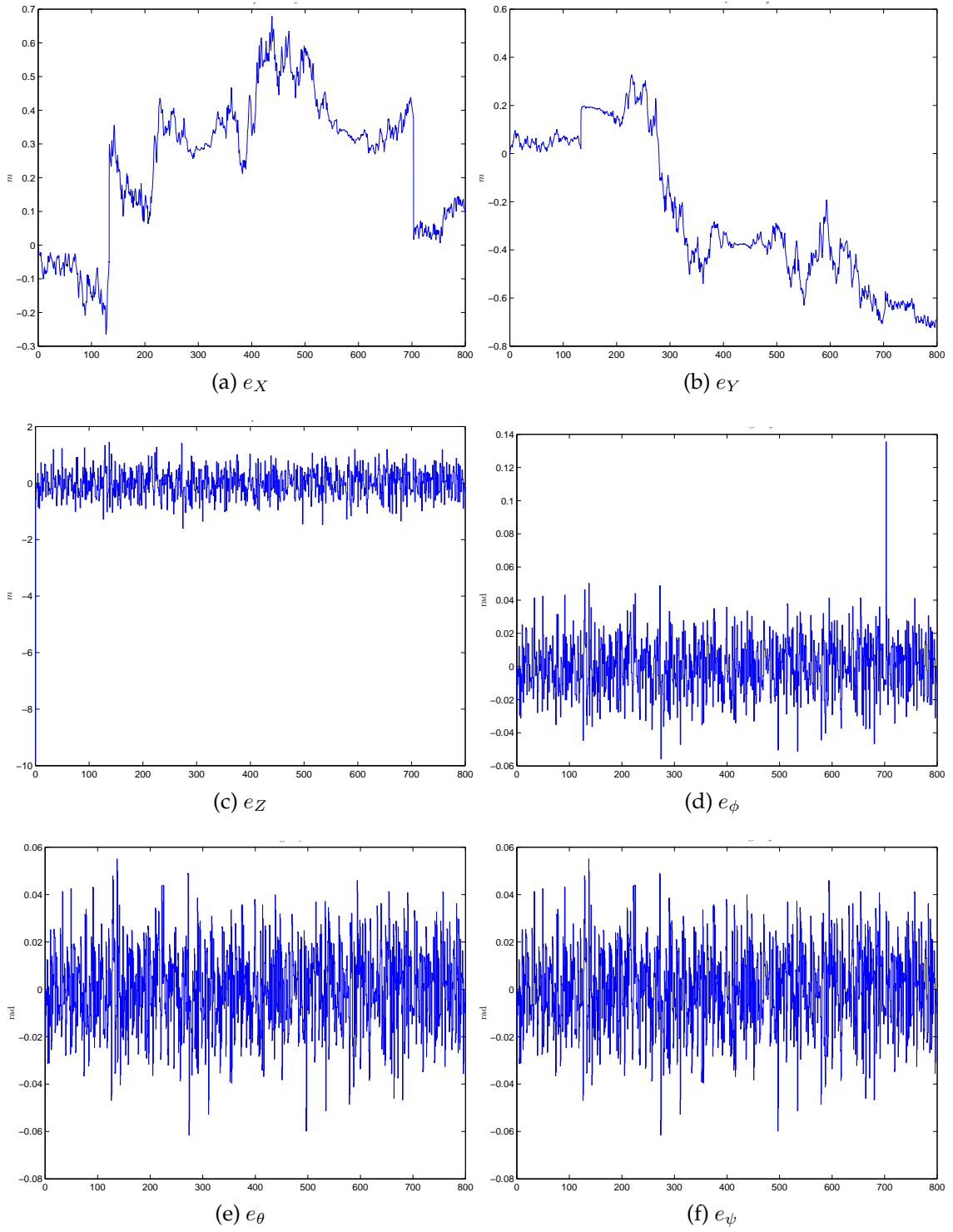Figure 6.8: Error on body-fixed velocity estimation - case 1

(a) e_X (b) e_Y
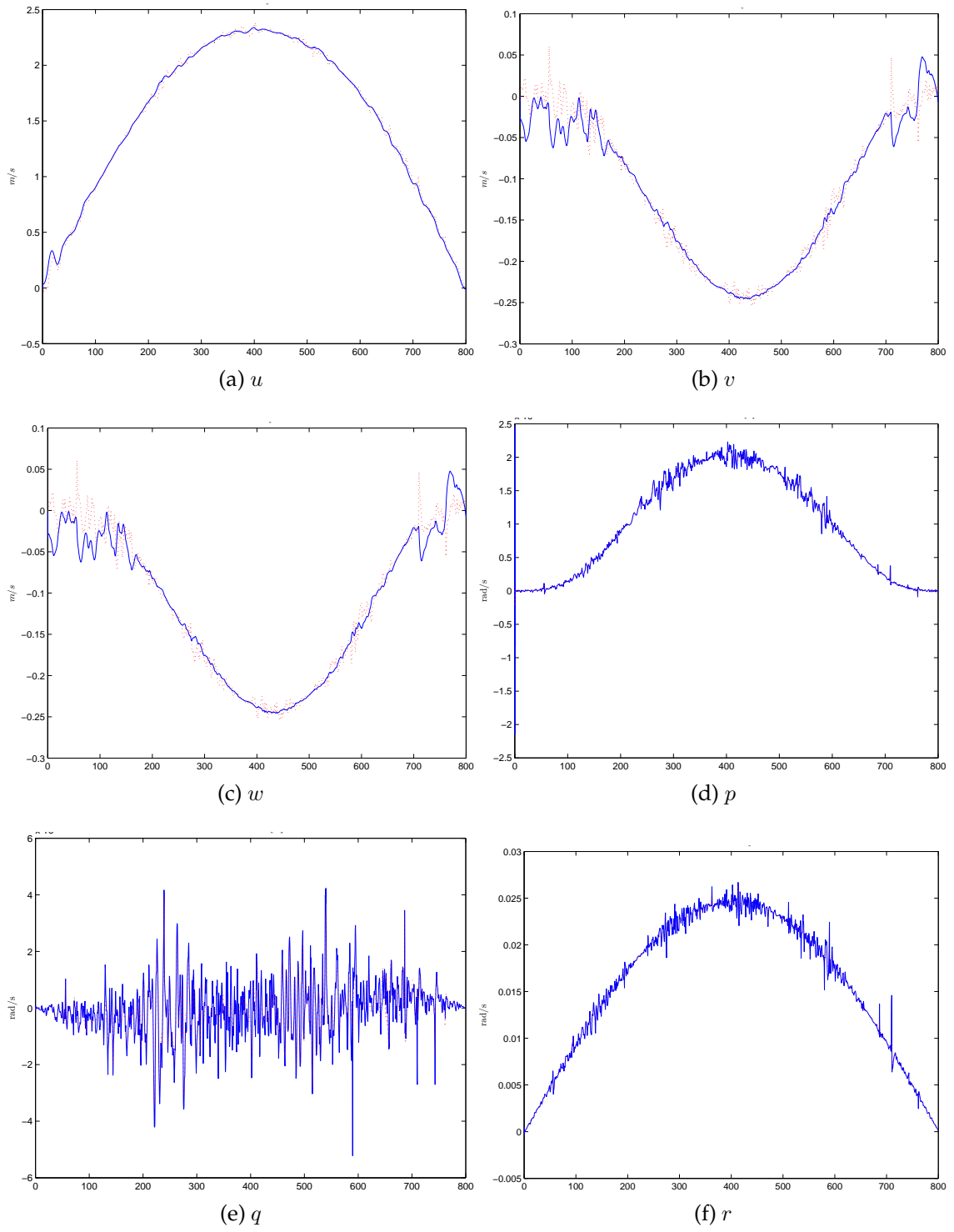
(c) e_Z (d) e_ϕ

(e) e_θ (f) e_ψ
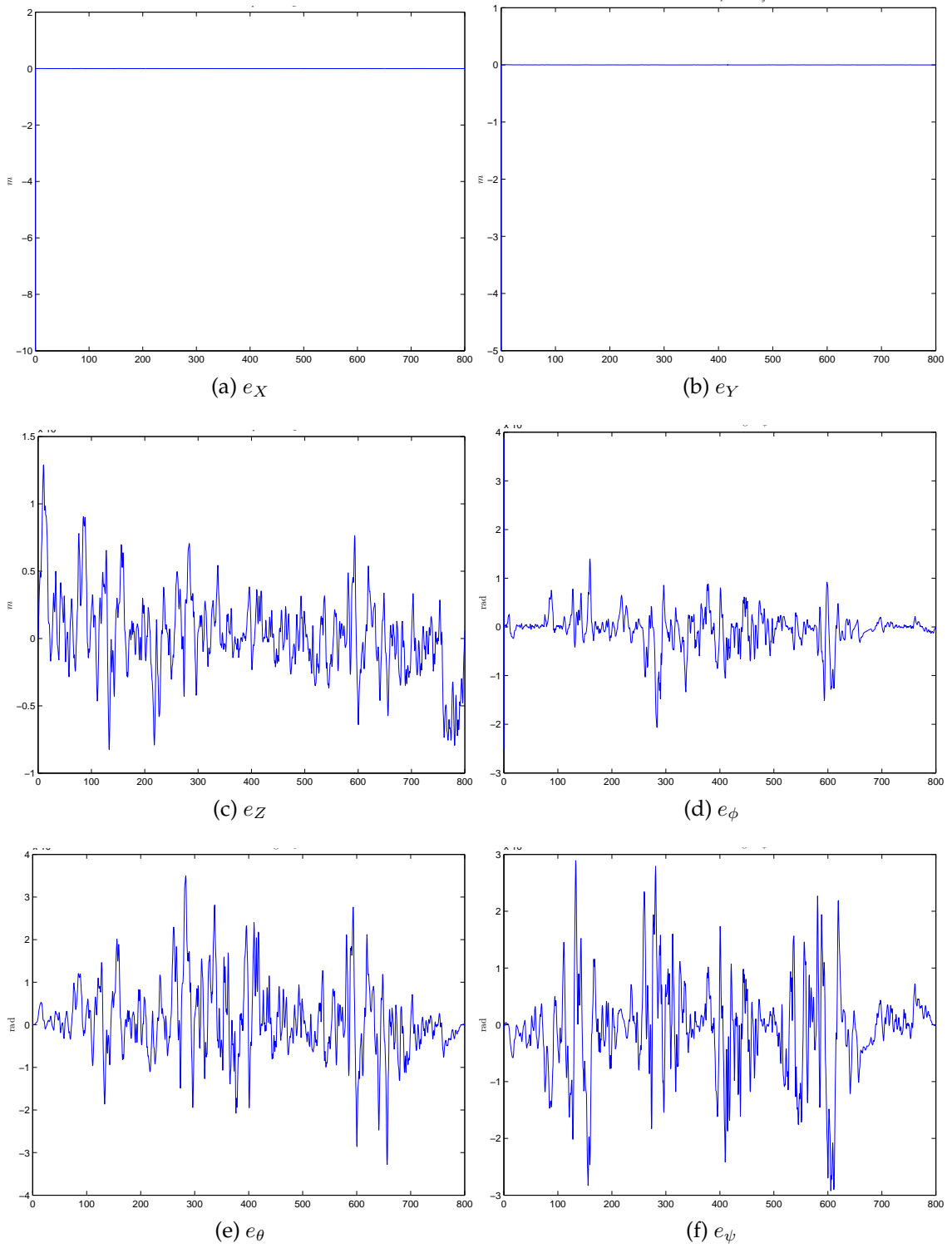
Figure 6.9: Error on inertial position estimation - case 2

(a) e_u

(b) e_v

(c) e_w

(d) e_p

(e) e_q

(f) e_r

Figure 6.10: Error on body-fixed velocity estimation - case 2

6.7.1 PCH Observer

The simulation results for the first case are shown in figures 6.1 and 6.2, whilst the results of the second case are shown in figures 6.3 and 6.4. From the simulation case 1 as shown in figures 6.1 and 6.2, we can see that the observer is able to produce good estimations in body-fixed velocity, angle and depth. The depth actually has an initial value error, as can be seen in figure 6.1c, but 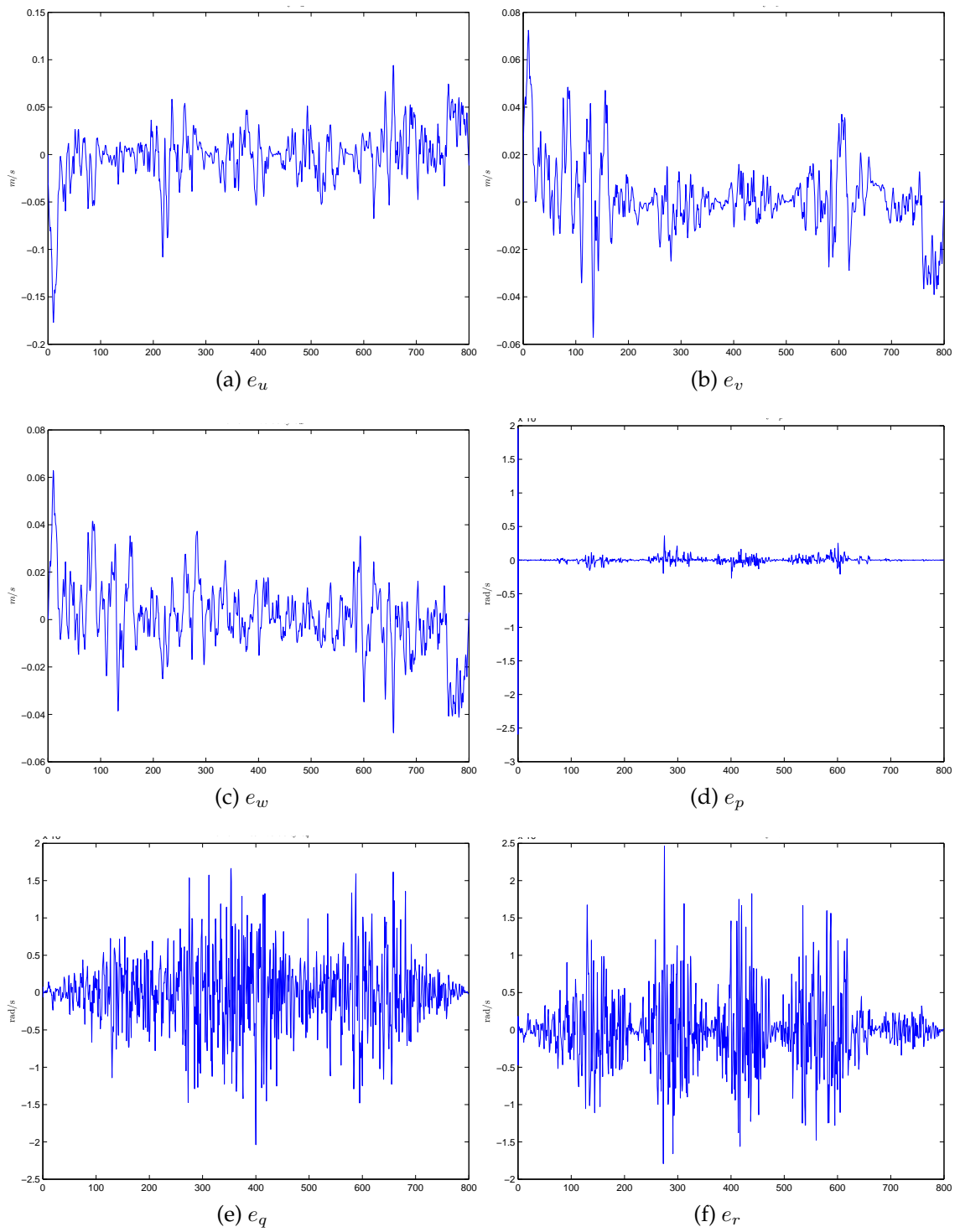it reduces very fast to the white noise. The fact that the horizontal inertial position errors are not converging can also be seen in figure 6.1a and 6.1b. As we already predicted before, the horizontal inertial position estimation cannot converge. The drifts in horizontal position are also propagated as the vehicle moves in the horizontal plane. Fortunately, from 800 seconds simulation, the error of the inertial horizontal plane is less than one meter. The combination of the controller and observer is also able to track the desired path, nearly the same with the direct feedback.

6.7.2 Alternative Observer

The estimation errors in the first case are shown in figures 6.7 and 6.8, whilst the results of the second case are shown in figures 6.9 and 6.10. From figures 6.7 and 6.2, we can see that the observer is able to produce good estimations for body-fixed velocities and inertial positions. The X and Y positions have an initial error. The errors reduce very fast as seen in 6.7a and 6.7b. The results of body-fixed velocity estimation are also considerably good, even for angular velocities u, v, w. The estimations are smoother than the measurement as seen in figure 6.5. Inertial position and angle comparison between the estimated and the true value are not presented here, since they closely coincide each other. The observer-controller

output feedback simulations also give a satisfactory trajectory tracking result, but with the trajectory errors becoming slightly bigger than direct state feedback. (See figures 6.9, 6.10 and 6.6)

6.8 Conclusions

In this chapter, we have presented a new observer design for a class of PCH that has a quadratic Hamiltonian function. The separation principle is also described for the class of PCH. However, when we use the designed PCH observer for AUV where horizontal position is not measured, the estimation errors are still converging to zero. Fortunately, as shown in the simulation results, the horizontal estimation drifts are considerably small compared to the travelled trajectory. The simulations show that the output-feedback design using the proposed PCH observer is able to track the desired trajectory with small drifts.

We also redesigned an observer for an AUV type with inertial position measurements. The proposed AUV observer is closely related to the one proposed in [83]. Using nearly the same assumptions and properties, we can meet a stronger stability condition on observer estimation error dynamics.

Chapter 7

Conclusions

7.1 Contributions

In this thesis, the following problems have been carefully presented through rigorous mathematical analysis

- Chapter 4,

    1. PCH formulation of AUV dynamics.

    2. Design of nonlinear passivity-based controller for AUV based on PCH formalism.

    3. Extension of the work in [91] in $\mathcal{L}_2$ disturbance attenuation for PCH. In our work,we relaxed the input gain matrix $\mathbf{G}(\mathbf{x})$ restriction, where we allow the disturbance have different input gain matrix $\mathbf{G}_2$.

    4. Extension to the work in [57] in adaptive $\mathcal{L}_2$ disturbance attenuation for PCH. We relaxed the $\mathbf{G}(\mathbf{x})$ restriction, where we allow the input

and disturbance matrix gain to have some uncertainties.

5. Convergence rate analysis of closed loop AUV systems.

6. Stability analysis of the designed closed loop AUV system in the presence of parameter uncertainty and exogenous disturbance.

7. Application of the $\mathcal{L}_2$ and adaptive $\mathcal{L}_2$ attenuation for PCH system into the AUV.

- Chapter 5,

    1. Robust $\mathcal{L}_2$ Input to State Stable (ISS) trajectory tracking design with respect to the ocean currents.

    2. Relaxation of a smooth time differentiable desired trajectory constraint as in [2, 3].

- Chapter 6,

    1. New framework of observer design for quadratic Hamiltonian PCH system.

    2. Design of PCH based nonlinear observer for AUV.

    3. The separation principle analysis of PCH system in general and AUV for particular case.

    4. Re-design of AUV observer proposed in [83].

7.2 Concluding Remarks

Based on the work presented here, we can have the following conclusions

1. PCH based nonlinear controller and observer design find an easy application for wide mechanical systems. In our development, we look that by means of PCH formulation, we can meet both simplicity of the design as well as the robustness against parameter uncertainty and exogenous disturbance. Using the PCH formulation, design of $\mathcal{L}_2$ disturbance attenuation control as well as its adaptive scheme found a straight forward extension and easy application in AUV.

2. The extension of the passivity-based PCH control design of AUV for underactuated condition has been established here. Using a proper design of desired attitude and validating the matching condition for the underactuated restriction, we are able to design the controller that can lead the underactuated AUV to track full-space desired trajectory.

3. The designed PCH observer for AUV still does not able to meet the convergence condition on horizontal position estimation. However, from the simulation results, the drift of the horizontal estimation is considerably small when compared to the travelled trajectory. The simulations also show that the closed loop of the observer based feedback is able to track the desired trajectory with small drift in the horizontal inertial position.

7.3   Future Work

1. Controller design that we presented is restricted to the affine controlled type of AUV. However, for AUV with a fin surface as a controller, the dynamics equation is not input affine. An extension of this work to non affine conditions will be a good contribution.

2. The actuator dynamics and saturation restrictions are not considered here. However, for real implementation, this factor has to be carefully considered. Extension of this work with actuators restrictions will be also an interesting problem to examine.

Bibliography

[1] O. Aamo, M. Arcak, T. Fossen, and P. Kokotovic. Global output tracking control of a class of Euler-Lagrange systems. In *Decision and Control, 2000. Proceedings of the 39th IEEE Conference on*, volume 3, pages 2478–2483. IEEE, 2000.

[2] A. Aguiar, L. Cremean, and J. Hespanha. Position tracking for a nonlinear underactuated hovercraft: controller design and experimental results. In *Decision and Control, 2003. Proceedings. 42nd IEEE Conference on*, volume 4, pages 3858 – 3863 vol.4, dec. 2003.

[3] A. Aguiar and J. Hespanha. Trajectory-tracking and path-following of underactuated autonomous vehicles with parametric modeling uncertainty. *Automatic Control, IEEE Transactions on*, 52(8):1362–1379, 2007.

[4] A. Alessandri, M. Caccia, G. Indiveri, and G. Veruggio. Application of LS and EKF techniques to the identification of underwater vehicles. In *Control Applications, 1998. Proceedings of the 1998 IEEE International Conference on*, volume 2, pages 1084–1088. IEEE, 1998.

[5] F. Alonge, F. D'Ippolito, and F. Raimondi. Trajectory tracking of underactuated underwater vehicles. In *Decision and Control, 2001. Proceedings of the*

40th IEEE Conference on, volume 5, pages 4421 –4426 vol.5, 2001.

[6] M. Arcak and P. Kokotovi. Nonlinear observers: a circle criterion design and robustness analysis. *Automatica*, 37(12):1923–1930, 2001.

[7] A. Astolfi, D. Chhabra, and R. Ortega. Asymptotic stabilization of some equilibria of an underactuated underwater vehicle. *Systems & control letters*, 45(3):193–206, 2002.

[8] A. Astolfi, D. Karagiannis, and R. Ortega. *Nonlinear and adaptive control with applications*. Springer Verlag, 2008.

[9] D. Auckly, L. Kapitanski, and W. White. Control of nonlinear underactuated systems. *Arxiv preprint math/9901140*, 1999.

[10] P. Batista, C. Silvestre, and P. Oliveira. A quaternion sensor based controller for homing of underactuated AUVs. In *Decision and Control, 2006 45th IEEE Conference on*, pages 51 –56, dec. 2006.

[11] G. Besancon, S. Battilotti, and L. Lanari. On output feedback tracking control with disturbance attenuation for Euler-Lagrange systems. In *Decision and Control, 1998. Proceedings of the 37th IEEE Conference on*, volume 3, pages 3139 –3143 vol.3, 1998.

[12] A. Bloch, D. Chang, N. Leonard, and J. Marsden. Potential and kinetic shaping for control of underactuated mechanical systems. In *American Control Conference, 2000. Proceedings of the 2000*, volume 6, pages 3913–3917. IEEE, 2000.

[13] A. Bloch, N. Leonard, and J. Marsden. Controlled Lagrangians and the stabilization of mechanical systems. I. The first matching theorem. *Automatic*

Control, IEEE Transactions on, 45(12):2253–2270, 2000.

[14] M. Breivik. Nonlinear maneuvering control of underactuated ship. Master's thesis, Norwegian University of Science and Technology, 2003.

[15] B. Brogliato, R. Lozano, B. Maschke, and O. Egeland. *Dissipative Systems Analysis and Control: Theory and Applications*. Communications and Control Engineering. Springer, 2010.

[16] D. Cheng, T. Shen, and T. Tarn. Pseudo-Hamiltonian realization and its application. *Communications in Information and Systems*, 2(2):91–120, 2002.

[17] R. Cristi, F. A. Papoulias, and A. J. Healey. Adaptive sliding mode control of autonomous underwater vehicles in the dive plane. *IEEE Journal of Oceanic Engineering*, 15:152–160, 1990.

[18] Z. Dong, J. Feng, and X. Huang. Nonlinear observer-based feedback dissipation load-following control for nuclear reactors. *Nuclear Science, IEEE Transactions on*, 56(1):272 –285, feb. 2009.

[19] Z. Dong, X. Huang, and J. Feng. Water-level control for the U-tube steam generator of nuclear power plants based on output feedback dissipation. *Nuclear Science, IEEE Transactions on*, 56(3):1600 –1612, june 2009.

[20] P. Encarnaçao and A. Pascoal. 3d path following for autonomous underwater vehicle. In *Decision and Control, 2000. Proceedings of the 39th IEEE Conference on*, volume 3, pages 2977–2982. IEEE, 2000.

[21] B. Ferreira, M. Pinto, A. Matos, and N. Cruz. Control of the MARES autonomous underwater vehicle. In *OCEANS 2009, MTS/IEEE Biloxi - Marine Technology for Our Future: Global and Local Challenges*, pages 1 –10, oct. 2009.

[22] B. Ferreira, M. Pinto, A. Matos, and N. Cruz. Hydrodynamic modeling and motion limits of AUV MARES. In *Industrial Electronics, 2009. IECON'09. 35th Annual Conference of IEEE*, pages 2241–2246. IEEE, 2009.

[23] B. Ferreira, M. Pinto, A. Matos, and N. Cruz. Modeling and motion analysis of the MARES autonomous underwater vehicle. In *OCEANS 2009, MTS/IEEE Biloxi-Marine Technology for Our Future: Global and Local Challenges*, pages 1–10. IEEE, 2009.

[24] T. Fossen. *Guidance and control of ocean vehicles*. Wiley (Chichester and New York), 1994.

[25] T. Fossen. *Handbook of Marine Craft Hydrodynamics and Motion Control*. John Wiley & Sons, 2011.

[26] T. Fossen and O. Fjellstad. Robust adaptive control of underwater vehicles: A comparative study. In *Proc. of the 3rd IFAC Workshop on Control Applications in Marine Systems (CAMS'95*. Citeseer, 1995.

[27] T. Fossen and A. Grøvlen. Nonlinear output feedback control of dynamically positioned ships using vectorial observer backstepping. *Control Systems Technology, IEEE Transactions on*, 6(1):121 –128, jan 1998.

[28] T. Fossen and J. Strand. Passive nonlinear observer design for ships using lyapunov methods: full-scale experiments with a supply vessel. *AUTOMATICA-OXFORD-*, 35:3–16, 1999.

[29] L. Gentili and A. van der Schaft. Regulation and input disturbance suppression for port-controlled Hamiltonian systems. In *Lagrangian and Hamil-*

tonian methods for nonlinear control 2003: a proceedings volume from the 2nd IFAC Workshop, Seville, Spain, 3-5 April, 2003, page 205. Pergamon, 2003.

[30] F. Gomez-Estern, R. Ortega, F. Rubio, and J. Aracil. Stabilization of a class of underactuated mechanical systems via total energy shaping. In *Decision and Control, 2001. Proceedings of the 40th IEEE Conference on*, volume 2, pages 1137–1143. IEEE, 2001.

[31] W. Haddad and V. Chellaboina. *Nonlinear dynamical systems and control: a Lyapunov-based approach*. Princeton Univ Pr, 2008.

[32] A. J. Healey and D. Lienard. Multivariable sliding mode control for autonomous diving and steering of unmanned underwater vehicles. *IEEE Journal of Oceanic Engineering*, 18:327–339, 1993.

[33] O. Hegrenaes and O. Hallingstad. Model-aided INS with sea current estimation for robust underwater navigation. *Oceanic Engineering, IEEE Journal of*, 36(2):316–337, 2011.

[34] L. Hunt and M. Verma. Observers for nonlinear systems in steady state. *Automatic Control, IEEE Transactions on*, 39(10):2113–2118, 1994.

[35] T. I. Fossen and J. Strand. Nonlinear passive weather optimal positioning control (WOPC) system for ships and rigs: experimental results. *Automatica*, 37(5):701–715, 2001.

[36] B. Jalving, K. Gade, K. Svartveit, A. Willumsen, R. Sorhagen, and K. Maritime. DVL velocity aiding in the HUGIN 1000 integrated inertial navigation system. *Modeling Identification and Control*, 25(4):223–236, 2004.

[37] J. Jouffroy and J. Lottin. On the use of contraction theory for the design of nonlinear observers for ocean vehicles. In *American Control Conference, 2002. Proceedings of the 2002*, volume 4, pages 2647 – 2652 vol.4, 2002.

[38] J. Jouffroy and J. Opderbecke. Underwater vehicle trajectory estimation using contracting pde-based observers. In *American Control Conference, 2004. Proceedings of the 2004*, volume 5, pages 4108–4113. IEEE, 2004.

[39] G. Karras, S. Loizou, and K. Kyriakopoulos. On-line state and parameter estimation of an under-actuated underwater vehicle using a modified Dual Unscented Kalman Filter. In *Intelligent Robots and Systems (IROS), 2010 IEEE/RSJ International Conference on*, pages 4868–4873. IEEE, 2010.

[40] N. Kazantzis and C. Kravaris. Nonlinear observer design using Lyapunov's auxiliary theorem. *Systems & Control Letters*, 34(5):241–247, 1998.

[41] A. Kebairi, S. Cai, M. Becherif, and M. El Bagdouri. Modeling and passivity-based control of the Pierburg mechatronic actuator. In *Control and Fault-Tolerant Systems (SysTol), 2010 Conference on*, pages 287 –292, oct. 2010.

[42] H. K. Khalil. *Nonlinear Systems*. Macmillan Publishing, 1992.

[43] J. Kinsey. Preliminary field experience with the DVLNAV integrated navigation system for oceanographic submersibles. *Control Engineering Practice*, 12:1541–1549, 2004.

[44] J. Kinsey, R. Eustice, and L. Whitcomb. A survey of underwater vehicle navigation: Recent advances and new challenges. In *Proceedings of the 7th*

Conference on Maneuvering and Control of Marine Craft (MCMC'2006). IFAC, Lisbon. Citeseer, 2006.

[45] J. C. Kinsey and L. L. Whitcomb. Model-based nonlinear observers for underwater vehicle navigation: Theory and preliminary experiments. In *Proc. IEEE Int Robotics and Automation Conf*, pages 4251–4256, 2007.

[46] M. Koifman and I. Bar-Itzhack. Inertial navigation system aided by aircraft dynamics. *Control Systems Technology, IEEE Transactions on*, 7(4):487–493, 1999.

[47] A. Krener and A. Isidori. Linearization by output injection and nonlinear observers. *Systems & Control Letters*, 3(1):47–52, 1983.

[48] A. Krener and W. Respondek. Nonlinear observers with linearizable error dynamics. *SIAM Journal on Control and Optimization*, 23(2):197–216, 1985.

[49] M. Krstic, I. Kanellakopoulos, P. Kokotović, et al. *Nonlinear and adaptive control design*, volume 222. Wiley New York, 1995.

[50] L. Lapierre, D. Soetanto, and A. Pascoal. Nonlinear path following with applications to the control of autonomous underwater vehicles. In *Decision and Control, 2003. Proceedings. 42nd IEEE Conference on*, volume 2, pages 1256–1261. IEEE, 2003.

[51] P. D. Lax. *Functional Analysis*. Wiley Interscience, 2002.

[52] J. Leonard, A. Bennett, C. Smith, and H. Feder. Autonomous underwater vehicle navigation. In *IEEE ICRA Workshop on Navigation of Outdoor Autonomous Vehicles*, 1998.

[53] N. Leonard. Control synthesis and adaptation for an underactuated autonomous underwater vehicle. *Oceanic Engineering, IEEE Journal of*, 20(3):211–220, 1995.

[54] N. Leonard. Periodic forcing, dynamics and control of underactuated spacecraft and underwater vehicles. In *Decision and Control, 1995., Proceedings of the 34th IEEE Conference on*, volume 4, pages 3980–3985. IEEE, 1995.

[55] N. Leonard. Stability of a bottom-heavy underwater vehicle. *Automatica*, 33(3):331–346, 1997.

[56] N. Leonard. Mechanics and nonlinear control: Making underwater vehicles ride and glide. In *Proc. 4th IFAC Nonlinear Control Design Symp*, pages 1–6, 1998.

[57] S. Li and Y. Wang. Adaptive $\mathcal{H}_\infty$ control of synchronous generators with steam valve via Hamiltonian function method. *Journal of Control Theory and Applications*, 4(2):105–110, 2006.

[58] K.-P. W. Lindegaard. *Acceleration Feedback in Dynamic Positioning*. PhD thesis, Norwegian University of Science and Technology, Department of Engineering Cybernetics Norwegian University of Science and Technology NO-7491 Trondheim, NORWAY, September 2003 2003.

[59] W. Lohmiller and J. Slotine. Simple observers for hamiltonian systems. In *American Control Conference, 1997. Proceedings of the 1997*, volume 5, pages 2748–2753. IEEE, 1997.

[60] A. Loria, T. I. Fossen, and E. Panteley. A separation principle for dynamic

positioning of ships: theoretical and experimental results. *IEEE Transactions on Control Systems Technology*, 8:332–343, 2000.

[61] D. Luenberger. Observers for multivariable systems. *Automatic Control, IEEE Transactions on*, 11(2):190–197, 1966.

[62] A. Macchelli, A. van der Schaft, and C. Melchiorri. Port hamiltonian formulation of infinite dimensional systems I. Modeling. In *Decision and Control, 2004. CDC. 43rd IEEE Conference on*, volume 4, pages 3762 – 3767 Vol.4, dec. 2004.

[63] D. B. Marco and A. J. Healey. Command, control, and navigation experimental results with the NPS ARIES AUV. *IEEE Journal of Oceanic Engineering*, 26:466–476, 2001.

[64] H. J. Marquez. *Nonlinear Control System Analysis and Design*. John Wiley & Sons, 2003.

[65] S. Mei, T. Shen, W. Hu, Q. Lu, and L. Sun. Robust $\mathcal{H}_\infty$; control of a Hamiltonian system with uncertainty and its application to a multi-machine power system. *Control Theory and Applications, IEE Proceedings -*, 152(2):202 – 210, march 2005.

[66] R. Meise and D. Vogt. *Introduction to functional analysis*, volume 2. Oxford University Press, USA, 1997.

[67] K. Miller. On the inverse of the sum of matrices. *Mathematics Magazine*, 54(2):67–72, 1981.

[68] S. Mohan and A. Thondiyath. A non-linear tracking control scheme for an under-actuated autonomous underwater robotic vehicle. *International*

Journal of Ocean System Engineering, 1:120–135, 2011.

[69] M. Morgado, P. Oliveira, C. Silvestre, and J. Vasconcelos. Vehicle dynamics aiding technique for USBL/INS underwater navigation system. In *Control Applications in Marine Systems*, 2007.

[70] S. Muhammad and A. Dòria Cerezo. Output feedback passivity based controllers for dynamic positioning of ships. In *DYNAMIC POSITIONING CONFERENCE*. Dynamic Positioning Comitee, October 2010.

[71] J. Newman. *Marine hydrodynamics*. The MIT press, 1977.

[72] H. Nijmeijer and T. Fossen. *New directions in nonlinear observer design*. Number 244 in Lecture notes in control and information sciences. Springer, 1999.

[73] J. Oden and L. Demkowicz. *Applied functional analysis*. CRC press, 2009.

[74] R. Ortega and E. Garcia-Canseco. Interconnection and damping assignment passivity-based control: A survey. *European Journal of Control*, 10(5):432–450, 2004.

[75] R. Ortega, M. Spong, F. Gomez-Estern, and G. Blankenstein. Stabilization of a class of underactuated mechanical systems via interconnection and damping assignment. *Automatic Control, IEEE Transactions on*, 47(8):1218 – 1233, aug 2002.

[76] R. Ortega, A. Van Der Schaft, B. Maschke, and G. Escobar. Interconnection and damping assignment passivity-based control of port-controlled Hamiltonian systems* 1. *Automatica*, 38(4):585–596, 2002.

[77] E. Panteley and A. Loria. On global uniform asymptotic stability of nonlinear time-varying systems in cascade. *Systems & Control Letters*, 33:131–138,

1998.

[78] J. Park, D. Shin, and T. Chung. Dynamic observers for linear time-invariant systems. *Automatica*, 38(6):1083–1087, 2002.

[79] A. Pertew, H. Marquez, and Q. Zhao. $\mathcal{H}_\infty$ observer design for Lipschitz nonlinear systems. *Automatic Control, IEEE Transactions on*, 51(7):1211–1216, 2006.

[80] K. Pettersen and O. Egeland. Exponential stabilization of an underactuated surface vessel. In *Decision and Control, 1996., Proceedings of the 35th IEEE*, volume 1, pages 967–972. IEEE, 1996.

[81] K. Pettersen and O. Egeland. Position and attitude control of an underactuated autonomous underwater vehicle. In *Decision and Control, 1996., Proceedings of the 35th IEEE*, volume 1, pages 987–991. IEEE, 1996.

[82] J. Refsnes, K. Pettersen, and A. Sørensen. Observer design for underwater vehicles with position and angle measurement. In *7th IFAC Conference on Manoeuvring and Control of Marine Craft*, 2006.

[83] J. Refsnes, A. Sorensen, and K. Pettersen. Design of output-feedback control system for high speed maneuvering of an underwater vehicle. In *OCEANS, 2005. Proceedings of MTS/IEEE*, pages 1167–1174. IEEE, 2005.

[84] J. Refsnes, A. Sorensen, and K. Pettersen. Output feedback control of an AUV with experimental results. In *Control Automation, 2007. MED '07. Mediterranean Conference on*, pages 1 –8, june 2007.

[85] J. Refsnes, A. Sorensen, and K. Pettersen. Model-based output feedback control of slender-body underactuated AUVs: Theory and experiments.

Control Systems Technology, IEEE Transactions on, 16(5):930 –946, sept. 2008.

[86] J. E. Refsnes, A. J. Sørensen, and K. Y. Pettersen. Output feedback control of slender body underwater vehicles with current estimation. *International Journal of Control*, 80:1136–1150, 2007.

[87] D. Ribas, P. Ridao, M. Carreras, and X. Cufi. An EKF vision-based navigation of an UUV in a structured environment. In *Manoeuvring and control of marine craft 2003 (MCMC 2003): a proceedings volume from the 6th IFAC Conference, Girona, Spain, 17-19 September 2003*. Elsevier Science, 2004.

[88] S. Sagatun and T. Fossen. Lagrangian formulation of underwater vehicles dynamics. In *Systems, Man, and Cybernetics, 1991.'Decision Aiding for Complex Systems, Conference Proceedings., 1991 IEEE International Conference on*, pages 1029–1034. IEEE, 1991.

[89] R. Sepulchre, M. Janković, and P. Kokotović. *Constructive nonlinear control*. Communications and control engineering. Springer, 1997.

[90] T. Shen, R. Ortega, Q. Lu, S. Mei, and K. Tamura. Adaptive $\mathcal{L}_2$ disturbance attenuation of Hamiltonian systems with parametric perturbation and application to power systems. In *Decision and Control, 2000. Proceedings of the 39th IEEE Conference on*, volume 5, pages 4939 –4944 vol.5, 2000.

[91] T. Shen, R. Ortega, Q. Lu, S. Mei, and K. Tamura. Adaptive $\mathcal{L}_2$ disturbance attenuation of Hamiltonian systems with parametric perturbation and application to power systems. *Asian Journal of Control*, 5(1):143–152, 2003.

[92] G. Siouris. *Missile Guidance and Control Systems*. Springer, 2004.

[93] H. Sira-Ramirez and C. Cruz-Hernandez. Synchronizaton of chaotic systems: a generalized Hamiltonian systems approach. In *American Control Conference, 2000. Proceedings of the 2000*, volume 2, pages 769–773. IEEE, 2000.

[94] R. Skjetne and H. Shim. A systematic nonlinear observer design for a class of Euler-Lagrange systems. In *Proc. 9th Mediterranean Conf. on Control and Automation, Dubrovnik, Croatia*, 2001.

[95] J. Slotine, J. Hedrick, and E. Misawa. On sliding observers for nonlinear systems. In *American Control Conference, 1986*, pages 1794–1800. IEEE, 1986.

[96] D. A. Smallwood and L. L. Whitcomb. Model-based dynamic positioning of underwater robotic vehicles: Theory and experiment. *IEEE Journal of Oceanic Engineering*, 29:169–186, 2004.

[97] A. Venkatraman. *Control of Port-Hamiltonian Systems: Observer Design and Alternate Passive Input-Output Pairs*. PhD thesis, University of Groningen, 2010.

[98] Y. Wang, G. Feng, D. Cheng, and Y. Liu. Adaptive disturbance attenuation control of multi-machine power systems with SMES units. *Automatica*, 42(7):1121 – 1132, 2006.

[99] Y. Wang, C. Li, and D. Cheng. Generalized Hamiltonian realization of time-invariant nonlinear systems. *Automatica*, 39(8):1437 – 1443, 2003.

[100] M. Wondergem. Output feedback tracking of a fully actuated ship. Master's thesis, Technische Universiteit Eindhoven, 2005.

[101] C. Woolsey and N. Leonard. Underwater vehicle stabilization by internal rotors. In *American Control Conference, 1999. Proceedings of the 1999*, volume 5, pages 3417–3421. IEEE, 1999.

[102] Z. Xi and D. Cheng. Passivity-based stabilization and $\mathcal{H}_\infty$ control of the Hamiltonian control systems with dissipation and its applications to power systems. *International Journal of Control*, 73(18):1686–1691, 2000.

[103] W. Yuzhen, G. SS, and C. Daizhan. Observer and observer-based $\mathcal{H}_\infty$ control of generalized Hamiltonian systems. *SCIENCE IN CHINA SERIES F (INFORMATION SCIENCES)*, 48(2), 2005.

[104] M. Zeitz. The extended Luenberger observer for nonlinear systems. *Systems & Control Letters*, 9(2):149–156, 1987.

[105] S. Zhao and J. Yuh. Experimental study on advanced underwater robot control. *IEEE Transactions on Robotics*, 21:695–703, 2005.

Appendix A

Selected Contributions

1. Muhammad Fuady Emzir and Sami El Ferik. Nonlinear trajectory tracking control design for underactuated autonomous underwater vehicle. under preparation

2. Sami El Ferik and Muhammad Fuady Emzir. PCH-based $\mathcal{L}_2$ disturbance attenuation and control of autonomous underwater vehicle. In *Navigation Guidance and Control of Underwater Vehicle, IFAC Conference 2012 Portugal*, 2012.

3. Sami El Ferik and Muhammad Fuady Emzir. A port-controlled hamiltonian approach for $\mathcal{L}_2$-based trajectory tracking control of autonomous underwater vehicle. Submitted to Taylor & Francis International Journal of Control, January 2012.

CURRICULUM VITAE

Name	Muhammad Fuady Emzir
Nationality	Indonesian
Email	puat133@gmail.com
Address	KFUPM - Bldg 803-303. (K.S.A) ; Jl. Pepaya 2 No 77 Perumnas 1 Bekasi, West Java Indonesia. (Indonesia)
Phone	+966-550909125
Education	

M.S., **System Engineering** (April 2012), *King Fahd University of Petroleum and Minerals*, Saudi Arabia

B.S., **Engineering Physics** (June 2006), *Bandung Institute of Technology*, Indonesia